ABSTRACT

Title of Document: MODELING GERMLINE BRCA2 MUTATIONS IN ZEBRAFISH

Heather R. Shive, DVM, Dipl. ACVP

Directed By: Professor Siba K. Samal, Department of Veterinary Medical Science, and Dennis D. Hickstein, MD, Experimental Transplantation and Immunology Branch, National Cancer Institute, National Institutes of Health

Human ovarian cancer is a leading cause of morbidity and mortality in women, but the pathophysiology of this disease is not well-defined. Humans with inherited mutations in the breast cancer 2 gene (*BRCA2*) are at increased risk for developing breast and ovarian cancer; however, the relationship between *BRCA2* mutation and these cancers is not understood. Studies of *Brca2* mutation by gene targeting in mice are limited, as homozygous *Brca2* mutation typically leads to early embryonic lethality. We established a zebrafish line with a nonsense mutation in *brca2* exon 11 (*brca2*^{Q658X}), a mutation similar in location and type to *BRCA2* mutations found in humans with hereditary breast and ovarian cancer. *brca2*^{Q658X} homozygous zebrafish were viable and survived to adulthood; however, juvenile homozygotes failed to develop ovaries during sexual differentiation. Instead, *brca2*^{Q658X} homozygotes developed as infertile males with meiotic arrest in spermatocytes. Germ cell

migration to the embryonic gonadal ridge was unimpaired in *brca2*^{Q658X} homozygotes; thus, failure of ovarian development is not due to defects in early establishment of the embryonic gonad. Homozygous *tp53* mutation rescued ovarian development in *brca2*^{Q658X} homozygous zebrafish, reflecting the importance of germ cell apoptosis in gonad morphogenesis. In adulthood, *brca2*^{Q658X} homozygous zebrafish were predisposed to testicular neoplasias. Additionally, tumorigenesis in multiple tissues was significantly accelerated in combination with homozygous *tp53* mutation in both *brca2*^{Q658X} homozygous and *brca2*^{Q658X} heterozygous zebrafish. These studies reveal a critical role for *brca2* in zebrafish ovarian development, demonstrate a conserved association for *brca2* mutation in reproductive tumorigenesis in zebrafish, and indicate that *tp53* mutation is an important contributor to *brca2*-associated carcinogenesis. The *brca2*^{Q658X}-mutant zebrafish line is an important resource for studying both gonadogenesis and *brca2*-associated carcinogenesis.

MODELING GERMLINE BRCA2 MUTATIONS IN ZEBRAFISH

By

Heather R. Shive, DVM

Dissertation submitted to the Faculty of the Graduate School of the
University of Maryland, College Park, in partial fulfillment
of the requirements for the degree of
Doctor of Philosophy
2010

Advisory Committee:
Professor Siba K. Samal, Chair
Dennis D. Hickstein, MD
P. Paul Liu, MD, PhD
R. Mark Simpson, DVM, PhD
Associate Professor Xiaoping Zhu
Professor Liangli Yu (Dean's Representative)

Acknowledgements

I gratefully acknowledge the following individuals for their contributions to this work, and for their support throughout the duration of my graduate training.

My advisor, Dennis Hickstein, and my colleagues on the zebrafish project:

Mizuki Azuma
Lisa Embree
Robert West
Gagan Raju

The members of my graduate committee:

Siba Samal
Paul Liu
R. Mark Simpson
Liangli Yu
Xiaoping Zhu

In Mark Simpson's group, Shelley Hoover, Jennifer Edwards, and Josh Webster.

In Paul Liu's group, Raman Sood and Kevin Bishop.

The Fellows in the Molecular Pathology GPP.

I would also like to thank my friends and family for the inexhaustible support they have provided me through these years.

Research funding support was provided through the Intramural Research Program, Center for Cancer Research, National Cancer Institute, Bethesda, MD. I received a Cancer Research Training Award and was a Molecular Pathology Graduate Fellow in the NCI Molecular Pathology Graduate Partnership Program with the University of Maryland, College Park.

Table of Contents

List of Tables

List of Figures

Chapter 1: Introduction

Introduction

Ovarian cancer is a major cause of morbidity and mortality in women. In the United States, it is the 5th-leading cause of cancer-related death in women and is 8th among the most common female cancers (1). Moreover, the mortality rate among women with ovarian cancer has remained largely unchanged over the last two decades (1, 2), despite numerous advances in diagnostic technologies and therapeutic modalities. This is largely attributable to the difficulty in detecting ovarian cancer at early stages (3-5). Women who are diagnosed in advanced stages of disease have a substantially lower 5-year survival rate than women who are diagnosed before regional or distant metastases have occurred (2, 5). Unfortunately, the majority of women who receive a diagnosis of ovarian cancer have already developed metastatic foci by the time that disease is detected (5, 6).

An overview of ovarian carcinogenesis

The pathophysiology of ovarian carcinogenesis is poorly understood. The majority of ovarian tumors are carcinomas, and serous carcinoma is both the most common and the most malignant type (7). Historically, these tumors are thought to arise from the ovarian surface epithelium, a thin, mesodermally-derived epithelial layer that covers the ovary and is contiguous with the peritoneum (8). Neoplastic cells are believed to arise from clefts or microscopic inclusion cysts that develop in the ovarian surface epithelium with increasing age (8, 9). While small to microscopic carcinomas have

been detected infrequently in the ovarian surface epithelium as incidental findings, reliable precursor lesions in the ovarian surface epithelium have been difficult to define (9).

Proposed mechanisms for development of ovarian cancer from the ovarian surface epithelium have included both physical damage and hormonal signaling. The incessant ovulation hypothesis suggests that ongoing cycles of damage, proliferation, and repair to the ovarian surface epithelium during reproductive years may lead to neoplastic transformation (3, 4). Alterations in gonadotropin and steroid hormone signaling that occur with aging, pregnancy, and premature ovarian failure are also thought to influence ovarian surface epithelial proliferation and transformation (3, 4).

In recent years, several studies have suggested that the fallopian tubular epithelium may be an alternative site for the origin of ovarian cancer (5). In this model, pre-neoplastic or neoplastic cells originate from tubular epithelia and transfer to the ovarian surface (10). This alternate theory of ovarian cancer pathogenesis has arisen from histologic examinations of fallopian tissue from women who have undergone salpingo-oophorectomy, either after a diagnosis of ovarian cancer, as a risk-reducing procedure in women from high-risk families, or for other therapeutic reasons (9, 11). Studies of these tissues have, in some cases, demonstrated microscopic foci of cells that range from dysplastic to overtly neoplastic (10). Serous intraepithelial carcinomas (STICs) found in tubular epithelium are often highly proliferative secretory cells with marked cytologic atypia and one or more genetic aberrations,

similar to ovarian cancer cells (10, 11). The most common genetic alterations detected in STICs are mutations in *p53* (10).

Known risk factors for ovarian cancer are few; non-genetic factors associated with ovarian cancer susceptibility include age, reproductive history, and hormonal therapy (4). In general, the majority of women who develop ovarian cancer are in the 6^{th} decade of life (4). With regard to reproductive history, parity is the strongest predictor for ovarian cancer risk. One or more full-term pregnancies decreases the risk for ovarian cancer, while risk is increased in nulliparous women (3, 4). Some studies have indicated that long-term use of oral contraceptives also decreases ovarian cancer risk (3, 4), although this correlation has not been substantiated in all study populations. The effects of fertility drugs and post-menopausal hormone replacement therapy on ovarian cancer risk remain controversial, but both have been suggested to increase risk (3, 4).

Genetics of ovarian cancer

Multiple genetic aberrations have been associated with ovarian carcinogenesis, although many uncertainties remain about the sequence of events leading to neoplastic transformation (12). The majority of ovarian cancer cases are considered sporadic, with no known relevant family history to suggest a heritable component to the disease (4). However, some somatically acquired genetic changes have been associated with development of sporadic ovarian cancer (7, 13, 14). Interestingly, specific genetic alterations have been linked to certain histologic subtypes of ovarian

cancer (Table 1.1). These observations have led to a classification scheme based on histologic type, genetic alterations, and cancer progression (13). In this scheme, type I tumors include low-grade serous carcinoma, mucinous carcinoma, endometrioid carcinoma, clear cell carcinoma, and malignant Brenner (transitional) tumor (13, 14). Type I tumors, for which defined precursor lesions have been identified, are slow growing and often restricted to the ovary at diagnosis (13, 14). Type II tumors are typically high-grade serous or undifferentiated carcinomas (13, 14). In contrast to type I tumors, type II tumors are not associated with any known precursor lesions, are highly aggressive, and frequently have metastasized at the time of diagnosis (13, 14).

Hereditary forms of ovarian cancer account for approximately 10% of all cases (15-17). Over 90% of hereditary ovarian cancers are associated with pathologic mutations in the breast cancer associated genes *BRCA1* and *BRCA2* (3, 18). A small number of hereditary ovarian cancer cases are associated with mutations in mismatch repair genes, most commonly *MLH1* and *MSH2* (12, 15). In these instances, ovarian cancer predisposition is a component of the hereditary nonpolyposis colorectal cancer (HNPCC) syndrome (12, 15).

The type I/II ovarian cancer designation described above has not been formally applied to hereditary ovarian cancers, perhaps because these represent a small fraction of total ovarian cancer cases. Most women with hereditary forms of the disease develop high-grade serous carcinomas, although other histologic subtypes have been observed in low numbers of individuals (15, 19). *BRCA*-associated ovarian cancers

Histologic subtype	Incidence	Type	Precursor lesion	Associated genetic alterations
Serous carcinoma	50%	High grade (Type II)	None known (STICs)?	*p53* mutation *HER2/neu* amplification or overexpression *AKT* amplification or overexpression *p16* inactivation
		Low grade (Type I)	Serous cystadenoma/adenofibroma Atypical proliferative serous tumor Noninvasive micropapillary serous carcinoma	*BRAF* mutation *KRAS* mutation
Endometrioid carcinoma	20%	Type I (low grade) or Type II (high grade)	Endometriosis Endometriod adenofibrooma Atypical proliferative clear cell tumor Intraepithelial carcinoma	*PTEN* mutation *PTEN* loss of heterozygosity *B-catenin* mutation *KRAS* mutation Microsatellite instability
Mucinous carcinoma	10%	Type I	Mucinous cystadenoma Atypical proliferative mucinous tumor Intraepithelial carcinoma	*KRAS* mutation
Clear cell carcinoma	5%	Type I (low grade) or Type II (high grade)	Endometriosis Clear cell adenofibroma Atypical proliferative clear cell tumor Intraepithelial carcinoma	*KRAS* mutation Microsatellite instability *TGF-β* RII mutation
Other	15%	Transitional tumor (Type I)	Brenner tumor Atypical proliferative Brenner tumor	Undetermined
		Undifferentiated carcinoma (Type II)	None known	Undetermined
		Malignant mixed mesodermal tumor /carcinosarcoma (Type I)	None known	*p53* mutation

Table 1.1 Sporadic (nonhereditary) forms of human ovarian cancer. Sporadic ovarian cancers can be classified by histologic type, precursor lesion, and associated genetic alterations. Adapted from Shih 2004, Willner 2007, Cho 2008, Edson 2009. Type I tumors, low grade; Type II tumors, high grade; STIC, serous intratubular carcinomas (see text).

are thought to originate from the tubular or fimbrial epithelium at a frequency equal to or above that of sporadic ovarian cancers (20).

In familial cases, ovarian cancer susceptibility occurs in women who are heterozygous carriers of pathologic *BRCA* mutations, and cancer cells frequently have loss of heterozygosity (21). Loss of the wildtype *BRCA* allele is considered to be an important step in carcinogenesis, but the timing of this event in disease pathogenesis is unclear (15, 20). Mutations in *p53* are the most common and perhaps most significant additional genetic change that occur in *BRCA*-associated ovarian cancer (19, 20). A recently proposed model for hereditary ovarian cancer originating from the tubular epithelium suggests that *p53* mutation is an early event in *BRCA*-associated ovarian cancer, with loss of heterozygosity leading to overt neoplastic transformation (20).

BRCA2 mutation and ovarian cancer risk

Without a known relevant family history of breast or ovarian cancer, a woman's lifetime risk for developing ovarian cancer is less than 2% (18, 22). In contrast, women carrying deleterious mutations in *BRCA2* have a lifetime risk for developing ovarian cancer of 20 – 30% (15, 23). Families with mutations in *BRCA2* demonstrate an autosomal dominant inheritance pattern for breast and ovarian cancer susceptibility (15, 18). Female carriers of pathologic *BRCA2* mutations are at risk for either breast or ovarian cancer, which includes the possibility that both cancers may occur in the same individual (18). *BRCA2* mutations are additionally associated with increased

risk for other types of cancer, including a particularly high risk for male breast cancer (24, 25).

The majority of known deleterious *BRCA2* mutations are frameshift mutations resulting in premature termination of the protein coding sequence (3, 15, 26). A lesser number of deleterious nonsense and missense mutations have been described (26). While a small number of defined mutations occur at high frequency in certain ethnic groups, most reported *BRCA2* mutations arise in single cases or small numbers of families (18, 26, 27).

Inherited mutations in *BRCA2* are a well-established risk factor for developing ovarian cancer (18, 22, 28), but the link between *BRCA2* mutation and ovarian cancer is not understood. However, the site of the mutation within the *BRCA2* gene may give some indication of ovarian cancer risk. Epidemiologic evidence shows that mutations in the "ovarian cancer cluster region" in *BRCA2* exon 11 are associated with an increased incidence of ovarian cancer relative to breast cancer in affected families (16, 29). These findings suggest that mutations in this portion of the gene may increase an individual's risk for ovarian cancer.

BRCA2 structure and function

The human *BRCA2* gene is 11,387 base pairs with 27 exons, and encodes a 3,418 residue protein with no significant similarity to any known protein (Fig. 1.1) (30). BRCA2 participates in the repair of double-strand DNA breaks (DSB) by

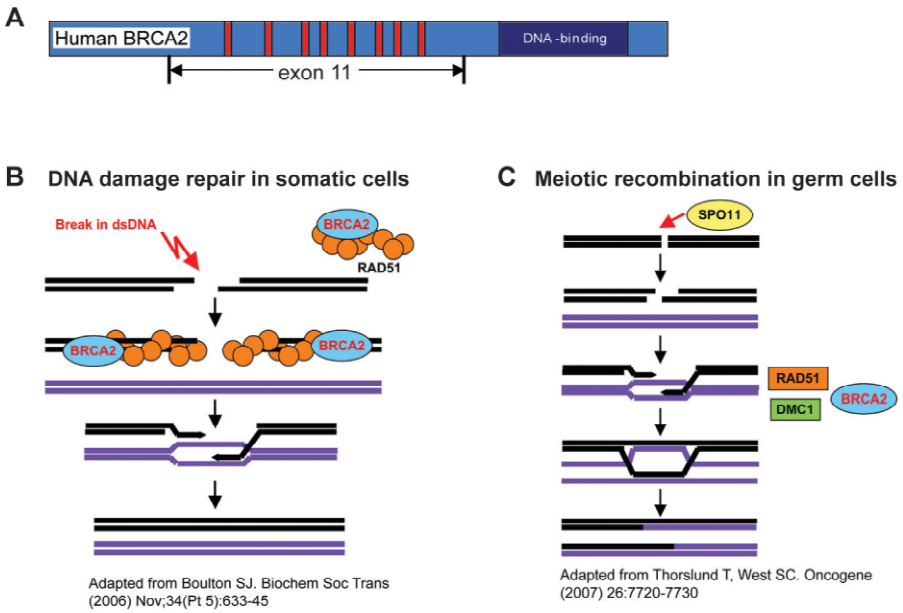

Fig. 1.1 BRCA2 structure and function. (A) The human *BRCA2* gene (NC_0000.1310) is 11,387 base pairs with 27 exons, and encodes a 3,418 amino acid protein (NP_000050.2). Red bars represent the BRC repeats required for binding to RAD51. Multiple conserved DNA binding domains are represented by the dark blue box. (B) Following a dsDNA break, BRCA2 binds to RAD51 and facilitates the interaction between RAD51 and the DNA strands. RAD51 mediates error-free repair through recombination with a region of homology. (C) dsDNA breaks induced by SPO11 are necessary for meiotic recombination in germ cells. BRCA2 is required for localization of RAD51 and DMC1 to SPO11-induced DNA breaks. RAD51 and DMC1 mediate recombination between sister chromatids.

homologous recombination (Fig. 1.1) (30-34). BRCA2 participates in this repair process through physical interaction with RAD51, a recombinase that initiates chromosomal strand invasion and recombination during DNA break repair (30, 33, 34). BRCA2 and RAD51 colocalize at sites of DNA damage (30, 34, 35). The BRCA2-RAD51 interaction occurs via binding of RAD51 to a series of approximately 30-40 amino acid motifs, referred to as the BRC repeats, that are encoded in exon 11 of the human BRCA2 gene (30, 33, 34).

In addition to its role in mediating homology-directed repair of DNA damage, BRCA2 also mediates homologous recombination during meiosis (Fig. 1.1) (34). In meiotically active germ cells, the cellular enzyme SPO11 induces DSB in chromosomes in early prophase I (34). Some DSB are repaired by homologous recombination, requiring the activity of BRCA2 (34). Similar to its role in DNA damage repair, BRCA2 is required for the localization of recombinases to DSB sites (34, 36). Meiotic recombination requires two recombinases: RAD51 and the meiosis-specific recombinase DMC1 (34). The process of homologous recombination and crossover between regions of homology within chromatids allows for genetic reassortment in gametes (34).

Studies in *BRCA2*-deficient cell lines have revealed that a variety of chromosomal changes can arise in the absence of BRCA2. These spontaneous chromosomal changes include DSB, aneuploidy, tri-radial and quadri-radial chromosomes, and gross chromosomal rearrangements (30, 31, 34). *BRCA2*-deficient cells exhibit

increased sensitivity to ionizing radiation, mitomycin C, and other DNA-damaging agents (31, 35). These aberrations are presumably attributable to impaired DSB repair; *BRCA2* deficient cells exhibit diminished formation of RAD51 nuclear foci (30, 31, 35). *In vitro* assays for DSB repair demonstrate that repair processes mediated by homologous recombination are deficient in these cells (32, 37). Deficiencies in DNA repair have been exploited in the treatment of patients with *BRCA*-associated cancers, which are exquisitely sensitive to DNA damaging agents, such as cisplatin, and to agents that block alternate DNA repair mechanisms, such as poly(ADP-ribose) polymerase (PARP) inhibitors (38, 39). Interestingly, chemotherapeutic resistance in neoplastic cells has been associated with reversion of the *BRCA* mutation (38, 40).

BRCA2 mutation and Fanconi anemia

Surprisingly, *BRCA2* mutations are associated with a separate human disease entity, Fanconi anemia, that appears unrelated to breast and ovarian cancer susceptibility. Fanconi anemia (FA) is a multifaceted syndrome characterized by congenital abnormalities, aplastic anemia, leukemia, and solid tumor formation (41). Mutations in a number of genes are associated with this syndrome; these genes are united by their roles in the Fanconi anemia DNA damage response and repair pathway (42). BRCA2, also known as FANCD1, was identified as a member of the FA complex in 2002, and mutations in *BRCA2* were causally linked to the FA syndrome (43).

In contrast to individuals at risk for hereditary breast and ovarian cancer, who are heterozygous carriers for *BRCA2* mutation, individuals with *BRCA2*-associated FA carry biallelic mutations in *BRCA2* (44). Mutations in *BRCA2* that are associated with FA include both missense and nonsense mutations (43, 44). The majority of these mutations are considered deleterious; however, no studies have identified patients who are homozygous for the same null mutation, suggesting that such a situation would prevent viability (44). Interestingly, many missense mutations in *BRCA2* that have been identified in FA patients are localized in a tight cluster within the carboxy-terminal region (44).

While the spectrum of syndromes that occur in FA patients can be quite diverse, FA in individuals with *BRCA2* mutations is phenotypically distinct (44). This is particularly evident in *BRCA2*-associated cancer susceptibility. The incidence of childhood cancers in patients with *BRCA2*-associated FA is remarkably high in comparison to patients with mutations in other FA genes, with a 97% risk for developing a malignancy by the age of 5.2 years (44). These human studies demonstrate a clear association between *BRCA2* mutations and cancer risk in both heterozygotic and homozygotic individuals.

Animal models of ovarian cancer

Spontaneous epithelial ovarian cancer in animal species is uncommon, with the exception of aged hens kept under intensive laying conditions (4, 45). Various approaches for initiating ovarian epithelial carcinogenesis have been instituted.

Xenograft models employ subcutaneous, intraperitoneal, or sub-bursal injection of ovarian cancer cells [reviewed in (46, 47)]. These models are limited by several factors: the necessary use of immunodeficient animals, use of cell lines derived from late-stage ovarian cancer, and, in subcutaneous and intra-peritoneal models, failure to recapitulate pre-metastatic stages of disease (46, 47).

Development of transgenic mouse models for ovarian cancer has been hindered by the lack of promoters specific for the ovarian surface epithelium (OSE) (4, 45-47). Connolly et al. describe successful generation of a transgenic model for epithelial ovarian cancer by targeting expression of the early region of SV40 to the OSE via the promoter for the Müllerian Inhibiting Substance type II Receptor (MISIIR) (48). In this model, ovarian tumors were detectable in some newborn mice. Transgenic female mice developed poorly differentiated ovarian carcinomas as early as 6 weeks of age and were infertile, preventing the establishment of a transgenic line (48). An alternative approach for targeting the OSE utilizes the Cre-lox system to locally inactivate tumor suppressor genes or activate oncogenes via injection of a recombinant adenoviral vector expressing Cre recombinase under the ovarian bursa (46). This system successfully generates epithelial ovarian tumors, but is labor-intensive, costly, and the results are variable (46).

Animal models of *BRCA2* mutation

Brca2-mutant mouse models have proven equally difficult to generate. Mouse models for *Brca2* mutation generated by gene targeting, which have resulted in partial

or complete deletion of *Brca2* exon 11, are typically characterized by early embryonic lethality in homozygotes (Table 1.2). Homozygous mutant embryos exhibit impaired embryonic development, developmental arrest, and decreased cellular proliferation (49-53). Two *Brca2*-mutant mouse models that were generated by targeting exon 11 have produced low numbers of homozygous mutants that survive to adulthood (54, 55). In these studies, homozygous *Brca2*-mutant mice exhibited various developmental defects, gonadal dysgenesis and hypoplasia, infertility, and a predisposition for thymic lymphoma (54, 55).

Several *Brca2*-mutant mouse models with partial or complete loss of exon 27 have also been described (52, 56). In these models, homozygous mutant mice generally did not experience high levels of early embryonic lethality, and were fertile (Table 1.2). However, homozygous *Brca2*-mutant mice exhibited a higher incidence and an earlier onset of a variety of solid tumors in comparison to control animals (52, 56). Irradiation of *Brca2*-mutant mice with loss of exon 27 increased the incidence of some tumor types in both homozygotes and heterozygotes (57).

One mouse model was described in which a Bacterial Artificial Chromosome (BAC) containing human *BRCA2* was used to rescue embryonic lethality from homozygous *Brca2* mutation (58). While viability was restored, the transgene was poorly expressed in the gonads, and homozygous *Brca2*-mutant mice were infertile (58). Male homozygotes exhibited incomplete spermatogenesis, meiotic arrest before pachynema, reduced numbers of RAD51 foci, and increased apoptosis (58). These

Homozygous *Brca2*-mutant mouse models exhibiting embryonic lethality					
Brca2 mutation	Position	Transcript	Embryonic lethality	Embryonic phenotype	Reference
Brca2$^{10\text{-}11}$	Exon 10	Exon 1 – 5' part of exon 10	ED 8.5 – 10.5	Developmental arrest after ED 6.5 Cellular hypoproliferation Increased p21 expression	Suzuki et al., 1997
Brca2^{Brdm1}	Exon 11	Exon 1 – 10	ED 7.5	Developmental arrest after ED 6.5 Hypersensitivity to γ-irradiation	Sharan et al., 1997
Brca2^{ex11}	Exon 11	Exon 1 – 5' part of exon 11	ED 8.5	Developmental arrest after ED 6.5 Cellular hypoproliferation	Ludwig et al., 1997
Brca2^{Tm1Mhun}	Exon 11	Exon 1 – 5' part of exon 11	ED 8.5 – 9.5	ND	Yan et al., 2004
Brca2^{F11}	Exon 11	Exon 1 – 10 and 12 – 27 (Δ11)	ED 8.5	Developmental arrest after ED 6.5	Jonkers et al., 2001
Brca2^{Lex2}	Exon 26	Exon 1 – 5' part of exon 26	ED ~8.5	Developmental arrest ~ ED 6	Donoho et al., 2003
Homozygous *Brca2*-mutant mouse models exhibiting partial or full viability					
Brca2 mutation	Position	Transcript	Viability	Phenotype	Reference
Brca2^{Tm1Cam}	Exon 11	Exon 1 – 5' part of exon 11	10%	Axial skeletal defects Lack of germ cells (male and female) and infertility Thymic lymphoma	Friedman et al., 1998
Brca2^{Tr2014}	Exon 11	Exon 1 – 5' part of exon 11	1.6 – 7.4%	Axial skeletal deformation and growth retardation Gonadal hypoplasia Failure of spermatogenesis and oogenesis Thymic lymphoma MEFs hypersensitive to UV irradiation, overexpress p21 and p53, and have DNA repair defects	Connor et al., 1997
Brca2^{Lex1}	Exon 27	Exon 1 – exon 26	100%	Fertile Decreased lifespan compared to controls Early onset of solid tumors and sepsis compared to controls	Donoho et al., 2003
Brca2^{F27}	Exon 27	Exon 1 – 26 (Δ27)	~67%	Fertile Reduced tubular branching in mammary glands Solid tumor incidence > 2-fold higher than controls	McAllister et al., 2002

Table 1.2 Conventional and conditional *Brca2*-mutant mouse models. Most homozygotes exhibit embryonic lethality or severely reduced viability. Surviving homozygous *Brca2*-mutant mice generally exhibit various developmental defects, reduced lifespan, and increased incidence of various solid tumors. *Brca2*-mutant mouse models with tissue-specific disruption or loss of *Brca2* are not included. ED, embryonic day; ND, not described; MEF, mouse embryonic fibroblast.

findings indicated that spermatocytes lacking Brca2 were arrested in early prophase I and did not complete meiotic recombination (58). Female homozygotes exhibited progressive oocyte loss and subsequent follicular degeneration; interestingly, some oocytes were capable of completing meiosis I (58). Some oocytes were fertile, but frequently exhibited abnormal chromosomal segregation (58).

One rat model for *Brca2* mutation has been described with a nonsense mutation in *Brca2* exon 11 that was derived by Ethylnitrosourea (ENU) mutagenesis (59). Homozygous *Brca2*-mutant rats were fully viable (59), in contrast to what has been observed in mouse models (Table 1.2). This finding suggests that targeted deletions of portions of *Brca2* are significantly more deleterious than point mutations. Both male and female homozygous *Brca2*-mutant rats were infertile (59). Homozygous *Brca2*-mutant male rats exhibited incomplete spermatogenesis and meiotic arrest (59), similar to findings in *Brca2*-mutant mice described by Sharan et al. (58). Ovaries from homozygous *Brca2*-mutant female rats were not described (59). *Brca2* homozygotes experienced decreased survival and increased tumor incidence in comparison to *Brca2* heterozygous and wildtype cohorts (59). *Brca2* homozygotes developed a variety of tumor types, including ovarian thecomas and granulosa cell tumors in female *Brca2* homozygotes (59).

The introduction of *p53* mutation in *Brca2*-mutant mouse models has produced variable results. Loss of *p53* in homozygous *Brca2*-mutant mice with the mutation targeted to exon 11 reduced the severity of embryonic defects, but did not rescue

survival (51). In homozygous *Brca2*-mutant mice with the mutation targeted to exon 27, *p53* mutation increased tumorigenesis and reduced survival (57).

Some conditional mouse models with tissue-specific deletion of *Brca2* have been developed that target *Brca2* mutation to mammary epithelium, skin, salivary gland, thymocytes, and peripheral T-cells [(60) and reviewed in (61, 62)]. In some models that targeted mammary epithelium, an increase in mammary tumorigenesis was reported (60-62). Concurrent *p53* mutation enhanced mammary tumorigenesis in both homozygous and heterozygous *Brca2*-mutant mice, including increased tumor incidence and reduced latency of tumor formation (61, 62). Targeting *Brca2* mutation to the thymus resulted in thymic lymphoma in 25% of homozygotes (60).

These studies of *Brca2* mutation in murine models indicate that *Brca2* is important for embryonic survival. Viable *Brca2*-mutant models have demonstrated that homozygous *Brca2* mutation is associated with tumorigenesis in multiple tissues, and tumorigenesis can be enhanced by *p53* mutation (52, 54-57). Homozygous *Brca2* mutation is additionally associated with defects in spermatogenesis and meiotic arrest (58, 59). Some of the variations in phenotypes among different *Brca2*-mutant rodent models are likely to reflect the effects of strain background and the methods used to introduce mutations in *Brca2* (62). No significant phenotype has been observed thus far in heterozygous *Brca2*-mutant mice in the majority of studies (59, 61, 62).

Zebrafish as a cancer model

The zebrafish (*Danio rerio*) emerged as a vertebrate model system for research in the 1930's, with initial work focusing on embryological development (63). This model offers certain advantages over traditional vertebrate models, including rapid generation time, high stocking density in small areas, external embryonic development, transparent embryos, high fecundity, and lower maintenance costs (64). Furthermore, numerous methods for genetic manipulation and generation of zebrafish lines with specific genetic alterations are feasible (63, 64).

Chemical mutagenesis through exposure to Ethylnitrosourea (ENU) is one of the most widely utilized techniques for genetic manipulation in the zebrafish model (63-67). ENU mutagenesis strategies permit the establishment of libraries of mutation-carrying zebrafish; these libraries may be screened for mutations in specific genes of interest (Fig. 1.2) (66, 68). To establish a mutant library, wild-type male zebrafish are exposed to ENU and subsequently bred to wild-type females, and the F1 male progeny are sacrificed for collection of DNA and sperm samples (66, 68). Banked DNA may be screened efficiently by large-scale resequencing and/or TILLING (Targeting Induced Local Lesions IN genomes) strategies to identify mutations in a particular gene (68). A mutation of interest found in a particular DNA sample may be recovered by using the corresponding sperm sample for *in vitro* fertilization (68). Resurrection and establishment of the mutation in a zebrafish line are achieved by inbreeding of subsequent generations (68).

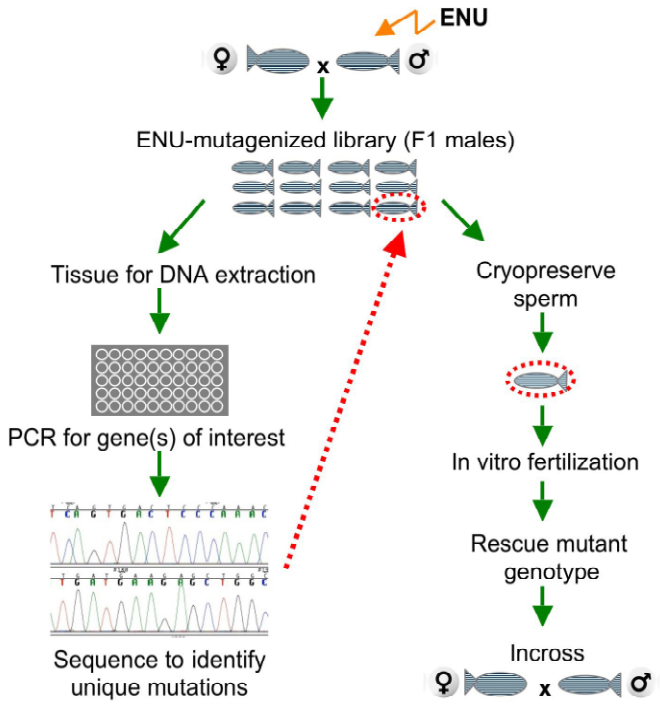

Fig. 1.2 Generation and screening of an ENU-mutagenized zebrafish library. Wildtype adult male zebrafish are exposed to ENU and subsequently crossed to wildtype female zebrafish. The F1 males from this cross are sacrificed for sperm cryopreservation and DNA extraction. DNA samples from the ENU-mutagenized library can be screened for mutations in genes of interest by PCR and sequencing. If a mutation of interest is found, the matching cryopreserved sperm sample is used for *in vitro* fertilization to rescue the mutant genotype.

Screening of ENU-mutagenized libraries has been used to recover mutations in the zebrafish recombination-activating gene 1 (*rag1*), *tp53*, and adenomatous polyposis coli gene (*apc*) (69-71). Both the *tp53*-mutant and *apc*-mutant zebrafish lines exhibited increased cancer susceptibility, demonstrating conservation of function of these tumor suppressor genes across vertebrate species (70, 71).

Zebrafish *brca2*

The zebrafish *brca2* gene was recently described and mapped to chromosome 15 (72). The zebrafish *brca2* gene is 16,391 base pairs with 27 exons, and encodes a 2,874 amino acid protein (Fig. 1.3). Zebrafish *brca2* contains a large exon 11, similar to other species. A genomic analysis of zebrafish *brca2* revealed highly conserved domains and conservation of synteny for neighboring genes (72). Conserved domains include the BRC repeats in exon 11, which are required for BRCA2-RAD51 binding, and multiple DNA binding domains in the C-terminal portion of the protein (Fig. 1.3 and Appendix I).

Zebrafish gonads are comparable to mammalian gonads

The basic morphology, structural organization and intercellular relationships of zebrafish ovaries and testes have been described. The adult zebrafish ovary is a bilobed structure with numerous connective tissue folds (ovigerous lamellae) that contain developing oocytes and follicles (73). Somatic cell populations in the zebrafish ovary include follicle cells (analogous to granulosa cells in mammalian

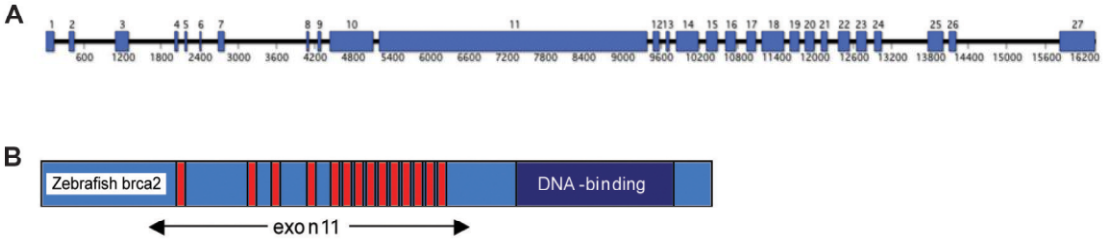

Fig. 1.3 Structure of zebrafish *brca2*. (A)The zebrafish *brca2* gene (NCBI NC_007126.4) is 16,391 base pairs with 27 exons. (B) Zebrafish *brca2* encodes a 2,874 amino acid protein (NCBI NP_001103864.2). Conserved domains include the Rad51-binding BRC repeats (red bars) and the DNA binding domain (dark blue box), which consists of several individual motifs, including a helix (residues *2021-2212*), tower (residues *2376-2417*), and three "OB" domains (residues *2596-2737*, *2214-2346*, *2596-2743*). Other conserved domains are indicated in Appendix I.

ovaries), thecal cells, the ovarian surface epithelium, and components of the fibrovascular stroma (73). Unlike mammalian follicles, in which multiple layers of granulosa cells surrounding a developing oocyte, zebrafish oocytes are surrounded by a single layer of follicle cells (73). The ovarian surface epithelium in zebrafish is a thin, flattened layer of epithelial cells that covers underlying developing follicles (73). The earliest developmental stage is the oogonium, which resides in nests and is distinguished from somatic cells by its relatively large size and nuclear:cytoplasmic ratio (73). Subsequent development phases of oocytes are categorized as stages I through V, based on criteria established by light and electron microscopy (Table 1.3) (73). After oocytes are recruited to develop, they arrest in diplotene I until they complete maturation (73). Oocytes are surrounded by somatic cells at the completion of Stage I, which forms the definitive follicle (73).

Multiple morphologic changes occur in and around developing oocytes as they continue to mature. These include development of a vitelline envelope in the cytoplasm (Stage II); proliferation of follicular and thecal cells around oocytes (Stage II); and onset of vitellogenesis (Stage III) (73). Vitellogenesis refers to the accumulation of yolk in the cytoplasm; yolk is derived from vitellogenin, a precursor produced by the liver and transported by endocytosis into developing oocytes (73). Oocytes complete maturation when they are ovulated into the oviduct (73).

Like mammalian species, oocyte maturation and follicle development in the zebrafish ovary are primarily directed by the pituitary gonadotropins FSH (follicle stimulating

Cell type	Developmental stage	Major events	Distinguishing histologic features
Oogonia	Oogenesis stage	Oogonia begin meiosis I	– Up to 20 µm in diameter – Reside in nests – Distinguished from somatic cells by their relatively large size and low nuclear:cytoplasmic ratio
Stage I oocyte	Primary growth stage	Oocytes progress through prophase I and arrest in diplotene I	– Up to 140 µm in diameter – Large nuclei, peripherally located nucleoli, and small amounts of cytoplasm – At completion of stage I, oocyte surrounded by follicle cells
Stage II oocyte	Cortical alveolus stage	Formation of channels across vitelline envelope that contain microvilli from oocyte and surrounding follicle cells	– 140 to 340 µm in diameter – Surrounded by follicle cells – Formation of intracytoplasmic vesicles (cortical alveoli) – Formation of a tripartite vitalline envelope
Stage III oocyte	Vitellogenic stage	Vitellogenesis begins – the hepatically derived protein vitellogenin is sequestered by the oocyte and converted to yolk	– Up to 690 µm in diameter – Cytoplasm expanded by numerous yolk globules
Stage IV oocyte	Maturation	Oocytes reinitiate meiosis and progress to metaphase II	– Up to 750 µm – Histologically similar to Stage III oocytes
Stage V oocyte	Mature eggs	Eggs are ovulated into the oviduct	– Up to 750 µm – Histologically similar to Stage III oocytes

Table 1.3 Stages of oogenesis in zebrafish. Oocyte staging, developmental events, and histologic features are derived from Selman et al., 2003.

hormone) and LH (luteinizing hormone) (74). There are also complex intercellular signaling pathways within the ovarian microenvironment that further regulate oogenesis, similar to what occurs in mammalian ovaries (74). This paracrine signaling network involves growth hormones (e.g. activin and follistatin), and steroid hormones (e.g. maturation-inducing steroids and estradiol), which control the onset and progression of oocyte maturation (74).

The mature zebrafish testis shares many features of mammalian testes (Table 1.4). The testis is organized into the tubular compartment, containing developing germ cells and Sertoli cells, and the intertubular/interstitial compartment, containing Leydig cells and vascular, structural, and neural elements (75, 76). Fish species undergo cystic spermatogenesis, which indicates that cytoplasmic extensions from Sertoli cells encircle and support a single group of clonally derived, synchronously developing germ cells (75, 76). This structural unit is referred to as a spermatocyst (75, 76). Within a testicular tubule, there are multiple differently sized spermatocysts containing germ cells at different stages of development (75, 76). The process of spermatogenesis is conserved among vertebrates and includes three phases: 1) the mitotic or spermatogonial phase; 2) the meiotic phase; and 3) the spermiogenic phase (75, 76). Each phase incorporates specific populations of germ cells, namely spermatogonia (mitotic phase), primary and secondary spermatocytes (meiotic phase), and spermatids and spermatozoa (spermiogenic phase) (Table 1.4) (75, 76). The first meiotic prophase is relatively long, due to the complexities of chromosomal

Cell type	Phase of development	Major events	Defining histologic features
Type A_{und} spermatogonia (undifferentiated)	Mitotic/spermatogonial	Mitotically active – may undergo symmetric or asymmetric divisions, i.e. daughter cells may undergo the same or different fates	– Occur singly – Large nucleus (~8.6 μm diameter) – Scant heterochromatin and 1 – 2 compact nucleoli – Relatively large cytoplasmic volume
Type A_{diff} spermatogonia (differentiated)	Mitotic/spermatogonial	Mitotically active with incomplete cytokinesis	– Occur in cysts with 2 – 8 germ cells – Smaller nucleus than Type A_{und} spermatogonia – Scant heterochromatin and 2 – 3 small nucleoli – Relatively large cytoplasmic volume
Type B early spermatogonia	Mitotic/spermatogonial	Mitotically active with incomplete cytokinesis	– Occur in cysts with ≥ 16 germ cells – Increased heterochromatin, often in round clumps – Elongated/round nucleus and reduced cytoplasm
Type B late spermatogonia	Mitotic/spermatogonial	Mitotically active with incomplete cytokinesis	– Occur in cysts with ≥ 16 germ cells – Increased heterochromatin, often in round clumps associated with nuclear envelope – Smaller round nucleus and reduced cytoplasm
Leptotene-zygotene spermatocytes	Meiotic	Meiotic prophase I	– Occur in cysts – Large, round clear nucleus with small dots of heterochromatin around nuclear periphery
Pachytene spermatocytes	Meiotic	Meiotic prophase I	– Occurs in cysts – The most frequent and largest meiotic germ cells – Dense nucleus, prominent lines of chromatin
Diplotene spermatocytes	Meiotic	Complete meiotic prophase I	– Occur in cysts – Maximal chromatin condensation – Typically found with metaphasic figures
Secondary spermatocytes	Meiotic	Enter and complete meiotic prophase II	– Occur in cysts – Small cells with round, dense nucleus – Often found with metaphasic figures
E1 spermatids (early)	Spermiogenic	Undergo final morphologic changes – Nuclear condensation – Loss of cytoplasmic bridges – Elimination of organelles and cytoplasm – Flagellum formation	– Flagellum is perpendicular to nucleus
E2 spermatids (intermediate)	Spermiogenic		– Flagellum becomes parallel to nucleus
E3 spermatids (final)	Spermiogenic		– Flagellum is centralized

Table 1.4 Stages of spermatogenesis in zebrafish. Cell staging, development events, and major histologic features are derived from Leal et al., 2009 and Schulz et al., 2009.

alignments and meiotic recombination; thus, the majority of spermatocytes observed at any given time in testicular tubules are primary spermatocytes (75).

Similar to mammals, the pituitary gonadotropins FSH and LH are the most important regulators of testicular physiology; however, the specific roles for these hormones in steroidogenesis are not well defined (75). Several growth factors in fish species have been identified that are produced by Sertoli cells to regulate germ cell proliferation (75). In addition, a number of steroid hormones, including androgens, progestins, and estrogen, have been shown to regulate spermatogenesis in a manner similar to mammalian testes (75).

Juvenile gonad development in zebrafish

Although structural and functional organization of the gonads is conserved in zebrafish, gonad development in zebrafish occurs differently than in mammalian species. Immature zebrafish experience a period of so-called "juvenile hermaphroditism" during development, which refers to development of a "juvenile ovary" in immature zebrafish of both sexes (Fig. 1.4) (77). The timing of this phase is variable within a population of zebrafish (78, 79). Generally, zebrafish undergo juvenile ovary development between 3 to 4 weeks of age (78, 79), although juvenile ovary development has been reported to begin as early as 12 days post fertilization (dpf) (77). This variability among timing of gonad development may be related to body size (78).

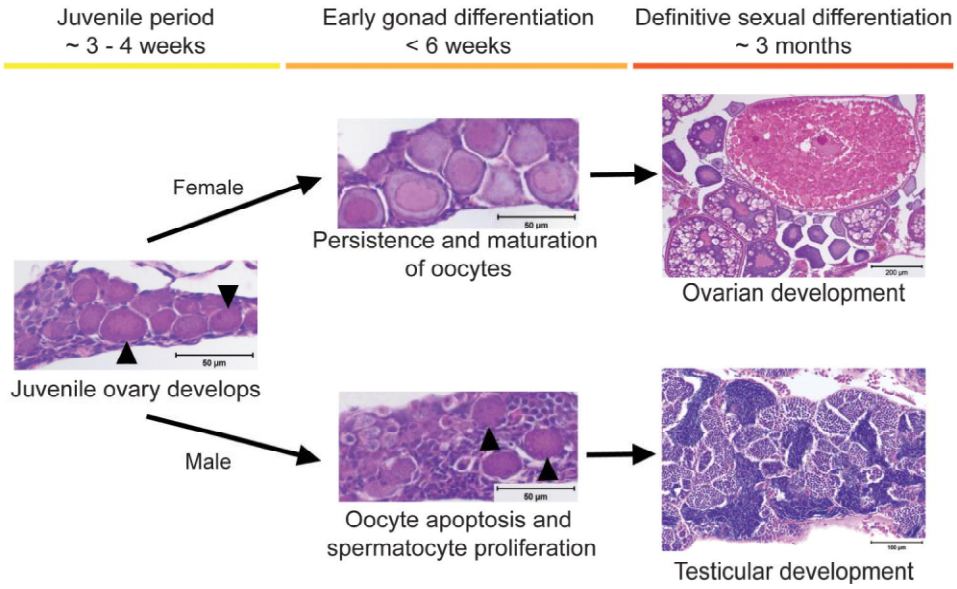

Fig. 1.4 Juvenile gonad development in zebrafish. During the juvenile period, wildtype zebrafish develop a juvenile ovary characterized by the presence of perinucleolar oocytes (arrowheads). Female sexual differentiation is characterized by continued maturation of oocytes and ovarian development. Male sexual differentiation requires degeneration and apoptosis of perinucleolar oocytes and spermatocyte proliferation before testicular development occurs. Scale bars, 50 µm (juvenile period, early gonad differentiation); 200 µm (ovarian development); 100 µm (testicular development).

During this period, all wildtype zebrafish develop immature oocytes in the juvenile gonads (77). Histologically identifiable cell populations in the juvenile ovary include oogonia, early meiotic stage primary oocytes, and perinucleolar oocytes (78). Perinucleolar oocytes, which are distinguished by large nuclei, basophilic cytoplasm, and peripheralized nucleoli, are used as the defining feature of the juvenile ovary in studies of zebrafish gonad development (78, 80). While all zebrafish develop perinucleolar oocytes, the extent of oocyte development and duration of oocyte retention is highly variable within populations of putative male zebrafish (79). The reasons for this variation among male zebrafish are not known (79).

As zebrafish continue to mature, female zebrafish exhibit retention, proliferation, and continued differentiation of oocytes (78, 79). Small numbers of apoptotic germ cells can be found in presumptive female gonads during this period (80). In contrast, gonads from presumptive male zebrafish exhibit degeneration and apoptosis of numerous germ cells (77, 78, 80). Subsequently, presumptive male gonads develop small groups of germ cells in cyst-like clusters surrounded by somatic cells, which represent nascent spermatogonial cysts (78). Male and female zebrafish reach sexual maturity at approximately three months of age (81).

Interestingly, the germ cell compartment plays a relatively greater role in gonad differentiation and sex determination in zebrafish than in mammals. In zebrafish, as in other animal species, primordial germ cells (PGCs) are specified early in development and follow a chemotactic gradient to colonize the genital ridge (82). If

PGC migration is blocked, resulting in apoptotic loss of PGCs in early embryogenesis, zebrafish will invariably develop as males (83, 84). The gonadal somatic tissues in these PGC-ablated zebrafish develop into tubular structures resembling testes, and express the male-specific genes *amh* and *sox9a* (85). Similarly, homozygous mutations in genes that are critical for germ cell survival and development, such as *nanos1*, *ziwi*, and *zili*, result in development of all-male zebrafish populations (86-88). These studies indicate that primordial germ cells play a fundamental role in gonadogenesis and sex determination in zebrafish.

Zebrafish sex determination: similarities and differences to mammalian species

Zebrafish, like many animal species, are sexually dimorphic as adults. Although some fish species can experience sex reversal after reaching sexual maturity, zebrafish do not undergo sex reversal once final gonadal development has occurred (89). The processes that direct sexual differentiation and gonadogenesis in zebrafish are not fully understood (90, 91).

An important difference between zebrafish and mammalian species is that zebrafish do not have defined sex chromosomes (92, 93). Whereas male and female animals possess X and Y chromosomes that dictate sexual differentiation and gonad development (94), sex determination in zebrafish appears to involve multiple autosomal genes (95-97). In addition, development of male or female populations in many fish species can be affected by environmental factors, such as water temperature, pH, and dissolved oxygen content [(98) and reviewed in (89)]. The lack

of defined sex chromosomes is not unique to zebrafish; however, there are examples of fish species which do possess an X and Y sex-determining system, such as the Japanese medaka (99).

Although zebrafish sex determination is not directed by defined X and Y chromosomes, the downstream signaling pathways that regulate testicular or ovarian differentiation appear to be conserved (75, 91). In male mammals, testicular differentiation is directed by the *Sry* gene, which induces *SOX9* expression in Sertoli cell precursors (100). SOX9 activates expression of the *anti-Müllerian hormone* gene (*AMH*), inducing regression of the Müllerian ducts (101, 102). AMH also blocks expression of the aromatase gene *Cyp19a1*, thus preventing conversion of androgens to estrogens (103). In the absence of *Sry* in female mammals, *SOX9* levels do not increase; thus, aromatase mediates androgen-to-estrogen conversion, the Müllerian ducts persist, and the embryonic gonad undergoes feminization (104-106).

In zebrafish, an *Sry*-like gene has not been defined. However, key downstream genes that are critical for mammalian sex determination are also found in zebrafish. There are two *sox9* genes in zebrafish (*sox9a* and *sox9b*) (107), which are the result of a genomic duplication event during teleost evolution (108). Similarly, there are two *cyp19a1* genes in zebrafish (*cyp19a1a* and *cyp19a1b*) (109). In adult zebrafish, the *sox9* genes are expressed in multiple tissues; interestingly, *sox9a* is expressed in testes, while *sox9b* is expressed in ovaries (107). *cyp19a1a* expression is limited to the ovary in adult zebrafish (109). Zebrafish *amh* is expressed in Sertoli cells in adult

testes, and in follicular cells in adult ovaries (110), similar to patterns of *Amh* expression in mammals (111). These expression patterns in adult zebrafish gonads imply that *sox9, cyp19a1*, and *amh* play conserved roles in sex determination.

Analyses of *sox9a*, *amh*, and *cyp19a1a* expression in developing zebrafish gonads provide further evidence that the roles for these genes in male versus female gonad development are conserved. Undifferentiated gonads exhibit expression of all three genes (110). Early testicular development correlates to increased expression of *sox9a* and *amh* and loss of *cyp19a1a* expression (110). In contrast, early ovarian development is characterized by expression of only *cyp19a1a* (110). Several microarray analyses comparing gene expression in both adult and juvenile gonads have supported these data, and have also suggested that expression patterns temporally coincide to stages of juvenile gonad development (95, 96, 112).

These studies indicate that conserved signaling pathways for sex differentiation exist in zebrafish, which are comparable to the signaling pathways that direct sex determination that occur in mammals. However, no single gene that is responsible for directing sex determination and gonad differentiation has yet been identified in zebrafish.

In summary, previous studies of gonadal development, structural organization, and intercellular signaling in zebrafish indicate that many of these elements are conserved in comparison to mammalian species. However, certain features of gonadal

morphogenesis and sex determination are distinctly different between zebrafish and mammalian species. These similarities and differences are important factors to consider when using the zebrafish as a comparative model for gonadal pathophysiology.

Thesis goals and outline

BRCA2 is critical for error-free repair of double-strand DNA breaks in many cell types, and mutations in *BRCA2* impact both DNA damage repair in somatic cells as well as meiotic progression in germ cells. While the loss of homologous recombination repair processes in BRCA2-deficient cells is thought to lead to neoplastic transformation, much remains unclear about the process of BRCA2-associated carcinogenesis. Studies of *Brca2* mutation in murine models have provided limited insight due to early embryonic lethality, and studies in viable models have not explained the link between *BRCA2* mutation and ovarian cancer. Zebrafish represent a novel alternate model for studying *brca2* mutation that may provide new insights into these topics.

The proposed studies are designed to generate a zebrafish model for *brca2* mutation to investigate the effects of *brca2* mutation *in vivo*, from embryonic development to adulthood. This model will incorporate three known risk factors for human ovarian cancer: *BRCA2* mutation, age, and reproductive history. These studies will include investigation of *brca2*-associated tumorigenesis and contribution of other genetic factors in cancer development. The hypothesis underlying this proposal is that female

zebrafish with *brca2* mutations comparable to mutations in humans with hereditary ovarian cancer will provide a model system in which to assess recognized risk factors for ovarian cancer and identify collaborating factors in ovarian carcinogenesis. The three specific aims designed to test this central hypothesis are:

- To characterize the zebrafish ovarian surface epithelium in immature and adult wildtype and mutant female zebrafish with different reproductive histories.
- To assess the expression and role of *brca2* during zebrafish development.
- To determine the effects of specific *brca2* mutations on ovarian tumorigenesis in zebrafish.

Establishing a model for *BRCA2*-associated cancer in a genetically tractable model such as the zebrafish provides a unique opportunity to investigate and identify collaborative factors in carcinogenesis, and represents a potential *in vivo* system for assessing novel therapeutic interventions.

Chapter 2 will focus on evaluating the zebrafish as a model for BRCA2-associated cancer, particularly ovarian cancer. In these studies, the expression patterns of *brca2* during development and in adulthood are examined in order to determine the potential results of *brca2* mutation. Histologic characteristics of the zebrafish ovary and testis are evaluated to establish a basis from which to assess zebrafish gonadal pathophysiology. Additionally, the potential for using reproductive history as a risk factor is tested through studies of breeding and nonbreeding wildtype zebrafish.

In Chapter 3, a *brca2*-mutant zebrafish line is established with a mutation in exon 11, a mutation similar in location and type to humans with hereditary ovarian cancer (17). The effects of *brca2* mutation on zebrafish embryogenesis and gonad development are investigated with this model. These studies will show that *brca2* is not required for embryogenesis in zebrafish, but is essential for spermatogenesis in adult males. In addition, these investigations demonstrate that *brca2* is required for ovarian development in zebrafish.

Chapter 4 explores the mechanisms for failure of ovarian development in *brca2*-mutant zebrafish and the effects of *brca2* mutation on tumorigenesis. In these studies, germ cell apoptosis during gonadal development is determined to be critical in preventing ovarian development in *brca2*-mutant zebrafish. In adults, *brca2* mutation is associated with tumor development in reproductive tissues. Concomitant mutations in *brca2* and *tp53* result in accelerated tumorigenesis in multiple tissues, and are associated with primary tumor development in the ovary. These studies indicate that the role for *BRCA2* mutation in reproductive tumorigenesis, and the synergistic effect of *TP53* mutation on this process, are conserved in zebrafish.

Chapter 2: The zebrafish as model for *brca2*-associated ovarian cancer

Introduction

Despite numerous diagnostic and therapeutic advances in oncologic research and clinical practice, human ovarian cancer remains a leading cause of morbidity and mortality in women (1). Significantly, the long-term survival rate for women diagnosed with ovarian cancer has remained largely unchanged over the last several decades (2). This lack of progress is attributable at least in part to lack of knowledge about ovarian cancer pathogenesis, particularly the early stages of disease (20).

There are few known risk factors for ovarian cancer, and *BRCA2* is among a small number of genes associated with hereditary ovarian cancer (12, 15, 18, 28). Thus far, insights gained from traditional murine models into *BRCA2*-associated carcinogenesis are limited (61, 62). Therefore, new animal models are needed for the study of ovarian pathophysiology and *BRCA2* mutation *in vivo*.

We used the zebrafish as a model for investigating two known risk factors for ovarian cancer: *BRCA2* mutation and reproductive history. In these studies, we assessed the suitability of zebrafish as a comparative model for studying adult gonads, particularly the ovary. We examined the expression of *brca2* in zebrafish during early development and in the adult gonads. Finally, we evaluated the applicability of long-term controlled breeding experiments in zebrafish for modeling reproductive history as an ovarian cancer risk factor.

Materials and Methods

Histologic evaluation and staging of adult wildtype zebrafish ovaries and testes. Adult wildtype AB* male and female zebrafish were euthanized in an overdose of 0.4% Tricaine Methanesulfonate, fixed overnight in 4% Paraformaldehyde (PFA; Boston Bioproducts, Ashland, MA), and transferred to 70% ethanol. Sections were routinely processed for preparation of Hematoxylin and Eosin (H & E) sections (Histoserv Inc., Gaithersburg, MD). Ovarian (73) and testicular (76) morphology and development were staged as described.

Immunohistochemistry for cytokeratin expression in zebrafish, rabbit, macaque, and human ovaries. Adult wildtype AB* female zebrafish were euthanized and fixed as described. Sections were routinely processed for paraffin embedding and sectioning (Histoserv Inc.). Paraffin-embedded blocks containing formalin-fixed rabbit and macaque ovary specimens were provided by Dr. Matthew Starost (Veterinary Diagnostic and Research Services, NIH). Unstained sections of formalin-fixed, paraffin-embedded normal human ovarian tissue were acquired from an archive of human tissues (Laboratory of Pathology, NCI, NIH). Unstained sections from each species were routinely processed for immunohistochemistry by Histoserv Inc. (Appendix II) with a mouse monoclonal anti-cytokeratin specific for the Type II cytokeratins 1, 5, 6, and 8 (1:150; Clone PCK-26, Sigma-Aldrich, St. Louis, MO).

Construction of RNA probes for zebrafish brca2. Three plasmids were constructed for transcription of RNA probes to detect zebrafish *brca2* by whole-mount in situ

hybridization (WISH) and in situ hybridization (ISH): pBSII-SK+/brca2-ex27, pBSII-SK+/brca2-3', and pBSII-SK+/brca2-5'. The pBSII-SK+/brca2-ex27 plasmid contained a 330 bp fragment of zebrafish *brca2* genomic DNA. Primers created *HindIII* and *XbaI* restriction sites on the ends of the PCR product. The pBSII-SK+/brca2-3' plasmid contained a 3828 bp fragment from the 3' end of zebrafish *brca2* cDNA. The reverse primer created a *NotI* restriction site at the 3' end of the PCR product. The pBSII-SK+/brca2-5' plasmid contained a 2484 bp fragment from the 5' end of zebrafish *brca2* cDNA. The forward primer created a *SalI* restriction site on the 5' end of the PCR product. The primer sequences used for plasmid constructs are given in Appendix III.

Each insert was amplified by PCR and cloned into pBSII-SK+. For pBSII-SK+/brca2-ex27, the insert and pBSII-SK+ were digested with *HindIII* and *XbaI*. For pBSII-SK+/brca2-3', the insert and pBSII-SK were digested with *NotI* and *BamHI* (this insert had a naturally occurring *BamHI* restriction site at the 5' end). For pBSII-SK+/brca2-5', the insert and pBSII-SK+ were digested with *SalI* and *BamHI* (this insert had a naturally occurring *BamHI* restriction site at the 3' end). After restriction digestion, inserts and plasmids were gel-purified with a QIAquick Gel Extraction Kit (QIAGEN, Valencia, CA) according to the manufacturer's protocol. Inserts and plasmids were ligated with T4 DNA ligase (Invitrogen, Carlsbad, CA) according to the manufacturer's protocol, and ligation reactions were used to transform DH5-α chemically competent *E. coli* (Invitrogen) according to the manufacturer's protocol. Plasmids were prepared with a Plasmid Maxi Kit (QIAGEN).

For each construct, 2 μg of plasmid DNA were linearized and purified (PCR Purification Kit; QIAGEN) according to the manufacturer's protocol. Antisense and sense RNA labeled with Digoxigenin (DIG) were transcribed using DIG RNA Labeling Mix and T7 or T3 RNA polymerases (Roche, Mannheim, Germany) according to the manufacturer's protocol. After transcription, DIG-labeled RNA was treated with 0.05U/μl RNase-free DNase I (Invitrogen) and ethanol-precipitated. RNA quantity and quality were assessed by absorbance at 260 nm and by RNA-denaturing formaldehyde gel electrophoresis.

Embryo collection and processing for WISH. Embryos were collected from incrosses of wildtype AB* zebrafish and staged according to Kimmel et al. (113). Approximately 50 embryos were collected at each of the following time points: 0.75 hours post fertilization (hpf) (2-cell); 2.75 hpf (mid-blastula); 6 hpf (shield); 11 hpf (early somitogenesis); 15 hpf (late somitogenesis); and 24 hpf (pharyngula). Embryos were washed twice with 1X PBS, fixed in 4% PFA overnight at 4°C, and washed twice with 1X PBS. Embryos collected after gastrulation (11, 15, and 24 hpf) were anesthetized with 0.4% Tricaine Methanesulfonate in blue water before fixation.

WISH for brca2. Fixed embryos were incubated in 100% methanol at -20°C overnight, washed with 100% acetone, and rehydrated with a series of methanol/1X PBS grades. Embryos were prehybridized in WISH hybridization buffer at 60°C for three hours. For hybridization, embryos were incubated in WISH hybridization

buffer containing either antisense or sense DIG-labeled RNA for zebrafish *brca2* (1 ng/μl) overnight at 60°C. Following hybridization, embryos were washed in the following series of washes: Wash I (60°C), Wash II (60°C), Wash III (60°C), Maleic Acid Buffer (room temperature). For blocking, embryos were incubated in WISH blocking solution for one hour. Embryos were incubated with WISH working antibody solution containing anti-DIG-AP antibody (1:5000; Roche) for two to three hours. Following antibody incubation, embryos were serially washed in PBTw buffer and washed twice in staining buffer. For detection, embryos were incubated in BM Purple substrate (Roche) for a minimum of five hours at room temperature or at 37°C. Embryos were then washed in 1X PBS, fixed overnight in 4% PFA, and stored in 1X PBS. *brca2* expression in wildtype AB* zebrafish embryos was analyzed in three independent experiments, each with 50 embryos per stage. The composition of reagents used in WISH experiments are given in Appendix IV.

ISH for brca2. Wildtype AB* zebrafish were euthanized and fixed as described above. Unstained 5μm sections were prepared under RNase-free conditions (Histoserv Inc.). Unstained sections were deparaffinized with Histoclear (Sigma-Aldrich) and rehydrated with a series of ethanol grades. Sections were incubated in proteinase K (5 μg/ml; Fermentas Inc., Glen Burnie, MD) in 1X PBS at 37°C and post-fixed in 4% PFA. Sections were incubated in 0.1M Triethanolamine Hydrochloride/0.25% Acetic Anhydride solution and subsequently dehydrated in a series of ethanol grades. Sections were prehybridized in ISH hybridization buffer for two hours at 55°C or 60°C. Sections were hybridized in ISH hybridization buffer

with either antisense or sense DIG-labeled RNA for zebrafish *brca2* (400 ng/ml or 800 ng/ml) at 55°C or 60°C overnight. Following hybridization, sections were washed three times in 50% Formamide/50% 2X SSC at 55°C or 60°C, and subsequently passed through a series of 2X SSC and block buffer washes. Sections were incubated in ISH blocking solution or 1X Blocking Solution (5X In Situ Hybridization Blocking Solution; Vector Laboratories Inc., Burlingame, CA) for thirty minutes at room temperature and incubated in ISH working antibody solution containing anti-DIG-AP antibody (1:500; Roche) for two hours at room temperature. Following antibody incubation, sections were washed with block buffer and color buffer washes. For detection, sections were incubated in BCIP/NBT working solution (BCIP/NBT AP Substrate Kit; Vector Laboratories Inc.) for a minimum of two to three hours. Sections were then washed in stop buffer, briefly dehydrated in an ethanol grade series, air-dried, and coverslipped with Permount (Fisher Scientific, Pittsburg, PA). Staging of gonads after ISH was performed as described (73, 76), and *brca2* expression in gonads was analyzed in at least three independent experiments. The composition of reagents used in ISH experiments are given in Appendix IV.

Zebrafish breeding experiments. Embryos were collected from an incross of wildtype AB* zebrafish and raised to adulthood. At three months of age, zebrafish were organized into the following cohorts: breeding females (n = 16), breeding males (n = 16), nonbreeding females (n = 18), and nonbreeding males (n = 18). Breeding zebrafish were bred once every two weeks, and were generally set up as pairs in breeding boxes to assess individual breeding success. Egg production in individual

female zebrafish was scored by assessing the approximate number of eggs produced, and results were recorded as relative egg production per female with the following scale: 0, no eggs laid; 1, < 50 eggs laid; 2, 50 – 100 eggs laid; 3, > 100 eggs laid. At six-month intervals from the onset of breeding experiments, four adults from each cohort were collected, euthanized, and fixed as described above (Appendix V).

Embryo imaging. Embryos were imaged in glycerol/1X PBS solution with a Leica MZ16 stereomicroscope and camera (Leica DFC420) with Leica Imaging Suite. Images were minimally processed with Adobe Photoshop Version 10.0.1.

Imaging of zebrafish sections. Histologic sections were imaged with an Olympus BX41 and camera (Diagnostics Instruments 14.2 color mosaic) with SPOT software (Version 4.6.4.3, 1997-2006). Images were minimally processed with Adobe Photoshop Version 10.0.1.

Results

Cell populations are conserved between mammalian and zebrafish gonads.

Histologic analyses of gonads from adult wildtype zebrafish demonstrated that the basic structural organization and cell populations observed in zebrafish ovary and testis were similar to adult mammalian gonads. In the zebrafish ovary, germ cell stages identified histologically included oogonia, stage I oocytes, stage II oocytes, and stage III oocytes (Fig. 2.1A). Oogonia were generally present in small clusters

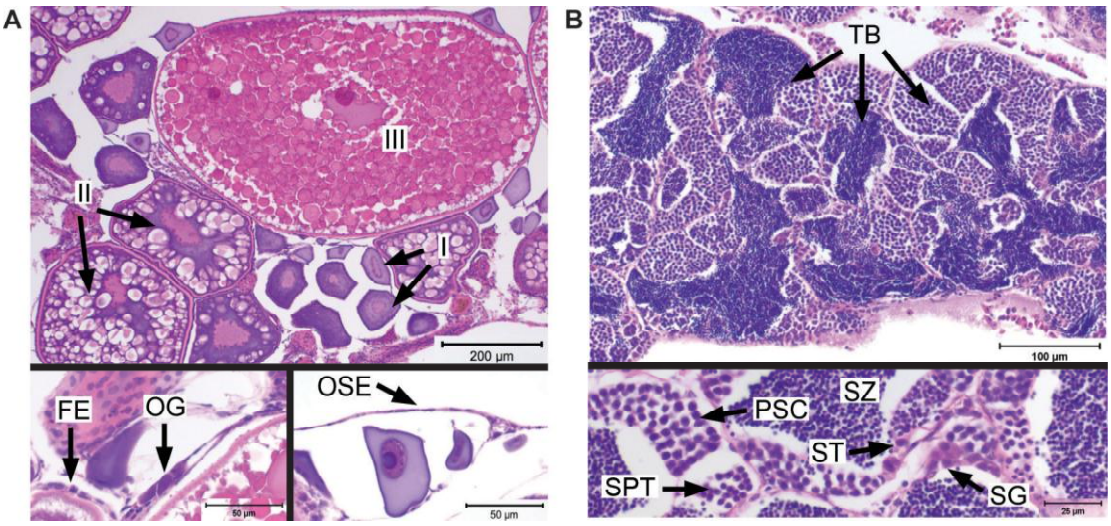

Fig. 2.1 Wildtype zebrafish ovary and testis. (A) The ovary contains developing oogonia and developing oocytes; stage II and III oocytes are enveloped by follicular epithelium, and the ovary is covered by the ovarian surface epithelium. (B) The testis is composed of tubules containing spermatogonia, primary spermatocytes, secondary spermatocytes, and spermatozoa; PSC and SSC develop in spermatocysts surrounded by Sertoli cells. I, stage I oocyte; II, stage II oocyte; III, stage III oocyte; OG, oogonia; FE, follicular epithelium; OSE, ovarian surface epithelium; TB, tubule; SG, spermatogonia; PSC, primary spermatocytes; SSC, secondary spermatocytes (not shown); SPT, spermatids; SZ, spermatozoa; ST, Sertoli cells. Scale bars, 200 µm (A, top panel); 50 µm (A, bottom panels; 100 µm (B, top panel); and 25 µm (B, bottom panel).

embedded in the ovarian stroma and exhibited small amounts of dark eosinophilic cytoplasm and a small dark basophilic nucleus. Stage I oocytes exhibited moderately abundant, pale to dark basophilic cytoplasm, and large amphophilic nuclei with one or more prominent nucleoli. Stage II oocytes had abundant basophilic cytoplasm containing numerous clear to pale eosinophilic vacuoles, and large eosinophilic nuclei with peripheralized chromatin. Stage III oocytes exhibited abundant cytoplasm filled with eosinophilic globular material (yolk protein (73)), and a large eosinophilic nucleus with peripheralized chromatin. Stage II and stage III oocytes exhibited a rim of brightly eosinophilic material subjacent to the cellular margin (vitelline envelope (73)). Stage II and II oocytes were surrounded by a single layer of epithelial cells forming the follicular epithelium (Fig. 2.1A). The ovarian surface epithelium formed a flattened single cell layer overlying the ovary (Fig. 2.1A).

In the zebrafish testis, germ cell stages identified histologically included spermatogonia, type I spermatocytes, type II spermatocytes, spermatids, and spermatozoa (Fig. 2.1B). Spermatogonia were present individually or in small clusters at the junctions of testicular tubules, and had eosinophilic cytoplasm and large basophilic nuclei. Primary spermatocytes were present in defined clusters along the margins of tubules, and had prominent basophilic nuclei and scant cytoplasm. Secondary spermatocytes were infrequently observed; while similar to primary spermatocytes in organization and cytological characteristics, secondary spermatocytes were approximately half the size of primary spermatocytes and often exhibited metaphasic nuclei. Spermatids were present in defined cellular clusters

along the margins of tubules, and exhibited small, dark basophilic nuclei and inapparent cytoplasm. Spermatozoa formed dense clusters in the centers of tubules, and had small, dark basophilic nuclei and inapparent cytoplasm. Clusters of spermatocytes were delineated by Sertoli cells, which exhibited flattened, elongated eosinophilic cytoplasm and small, dark basophilic nuclei (Fig. 2.1B).

Pancytokeratin immunoreactivity is conserved in ovarian surface epithelium.

Human ovarian surface epithelium (OSE) expresses keratin types 7, 8, 18, and 19, which is characteristic of simple epithelia (8). To determine if cytokeratin expression in OSE is conserved among mammalian and zebrafish species, sections of normal ovary from human, macaque, rabbit, and zebrafish were evaluated for immnunohistochemical detection of Type II cytokeratins (keratins 1, 5, 6, and 8). Human (accession NP_00226.41) and zebrafish (accession NP_956374.1) keratin 8 are 79% identical. This antibody was selected because the manufacturer indicated that it exhibits cross-reactivity across a variety of species. Immunohistochemistry for cytokeratins on ovary specimens demonstrated strong, specific cytokeratin immunoreactivity in the OSE from each species (Fig 2.2).

brca2 is ubiquitously expressed during embryogenesis in wildtype zebrafish embryos.

WISH for *brca2* on wildtype AB* embryos from the 2-cell stage through 24 hours post-fertilization (hpf) indicated that *brca2* was abundantly expressed in early cleavage-stage embryos (Fig. 2.3), corresponding to maternal mRNA produced

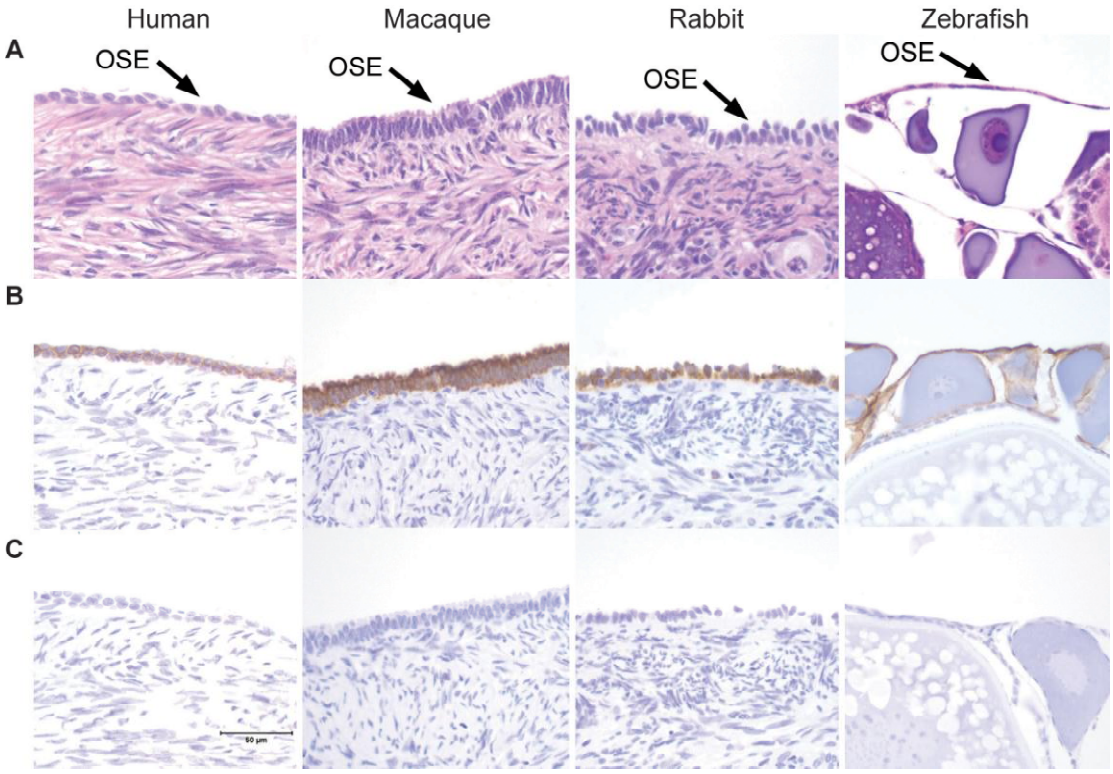

Fig. 2.2 Pancytokeratin expression is conserved in zebrafish OSE. (A) Ovarian surface epithelium (OSE) from human, macaque, rabbit, and zebrafish ovary with normal ovarian morphology. (B) The OSE from each species shows specific pancytokeratin immunoreactivity. Sections were counterstained with Hematoxylin. (C) Negative controls (secondary antibody only). Sections were counterstained with Hematoxylin. Scale bar, 50 µm.

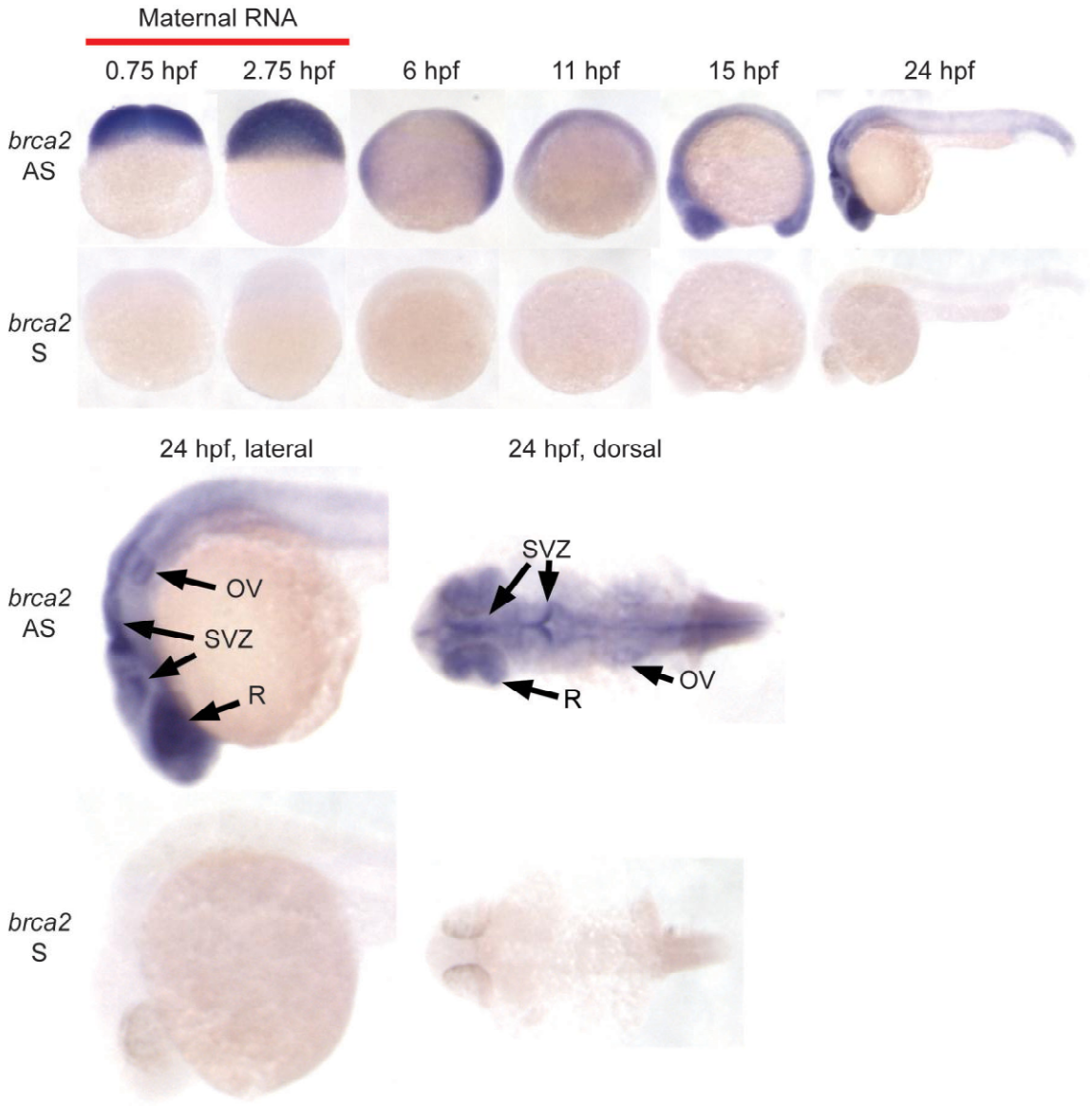

Fig. 2.3 *brca2* expression in wildtype zebrafish embryos. WISH for *brca2* expression in zebrafish embryos with antisense (AS, top panels) and sense (S, bottom panels) probes at the indicated stages demonstrates expression of *brca2* throughout embryogenesis. SVZ, subventricular zone; OV, otic vesicle; R, retina.

during oogenesis (114). At 24 hpf, *brca2* was highly expressed in the developing brain, eye, and ear, with highest expression in the subventricular regions and the developing retina (Fig. 2.3).

brca2 is expressed in the CNS of zebrafish larvae and the immature gonad of juvenile zebrafish.

WISH for *brca2* on wildtype AB* larvae at 2 days post fertilization (dpf) through 5 dpf demonstrated that *brca2* expression was maintained in the developing eye, ear, and subventricular regions of the CNS (Fig. 2.4). There was an overall decline in the intensity of *brca2* expression as maturation progressed (Fig. 2.4). At 4 dpf and 5 dpf, some zebrafish larvae exhibited *brca2* expression in the developing intestinal tract (Fig. 2.4, arrows).

ISH for *brca2* in sections of gonads from 30 dpf wildtype AB* zebrafish showed *brca2* expression in putative premeiotic germ cells and perinucleolar oocytes (Fig. 2.5). *brca2* was not expressed in less mature germ cells and was not detected in other tissue types (data not shown).

brca2 is expressed in adult zebrafish gonads.

ISH for *brca2* in wildtype zebrafish ovaries showed *brca2* expression in developing and mature oocytes, with strongest expression in the most mature oocytes (Fig. 2.6A).

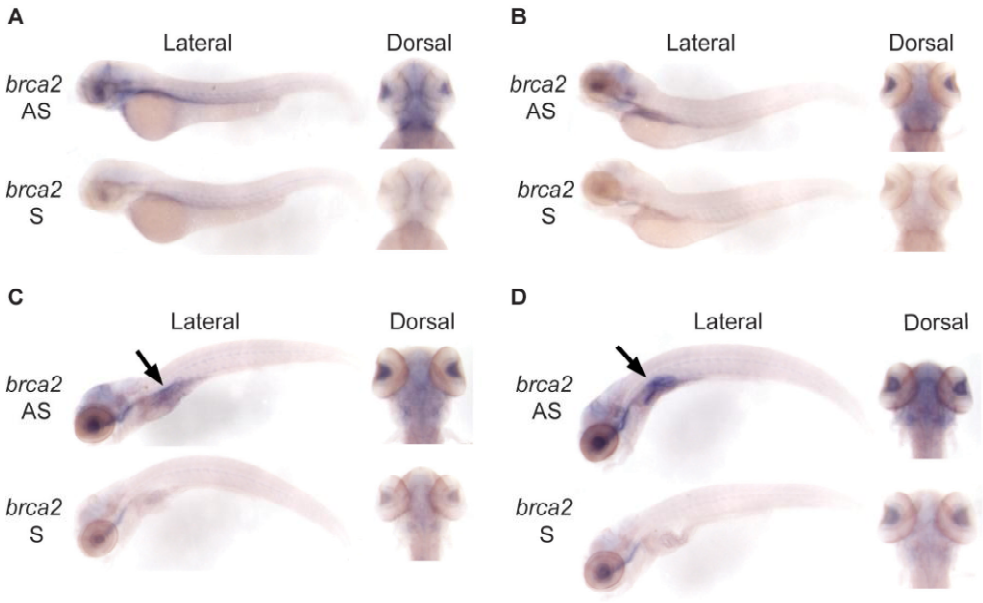

Fig. 2.4 *brca2* expression in wildtype zebrafish larvae. WISH for *brca2* expression in zebrafish larvae with AS and S probes at 2 dpf (A), 3 dpf (B), 4 dpf (C), and 5 dpf (D) demonstrates expression of *brca2* in the developing eye, ear, and CNS. *brca2* was also expressed in the developing intestinal tract at 4 dpf and 5 dpf (arrows).

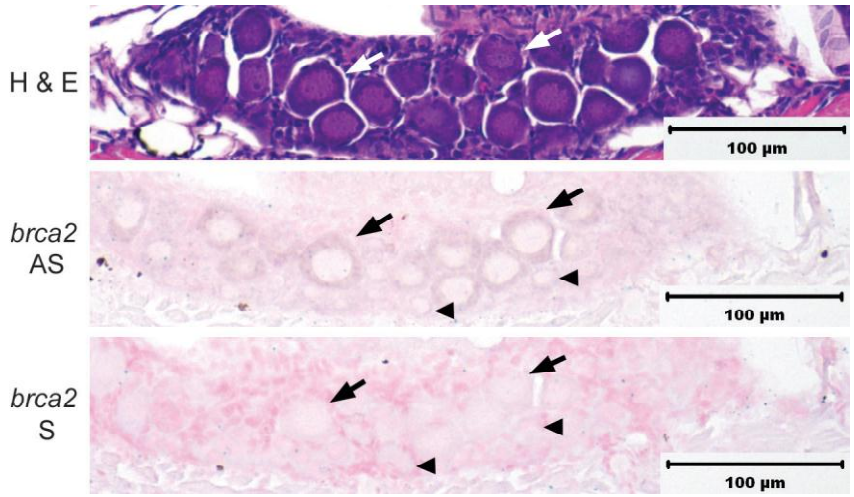

Fig. 2.5 *brca2* expression in wildtype juvenile zebrafish gonads. ISH for *brca2* expression in serial sections of juvenile gonads with AS (middle panel) and S (lower panel) probes shows that *brca2* is expressed in perinucleolar oocytes (arrows) and in putative premeiotic germ cells (arrowheads). An H&E serial section of juvenile gonad is included for anatomic reference (upper panel). Scale bars, 100 µm.

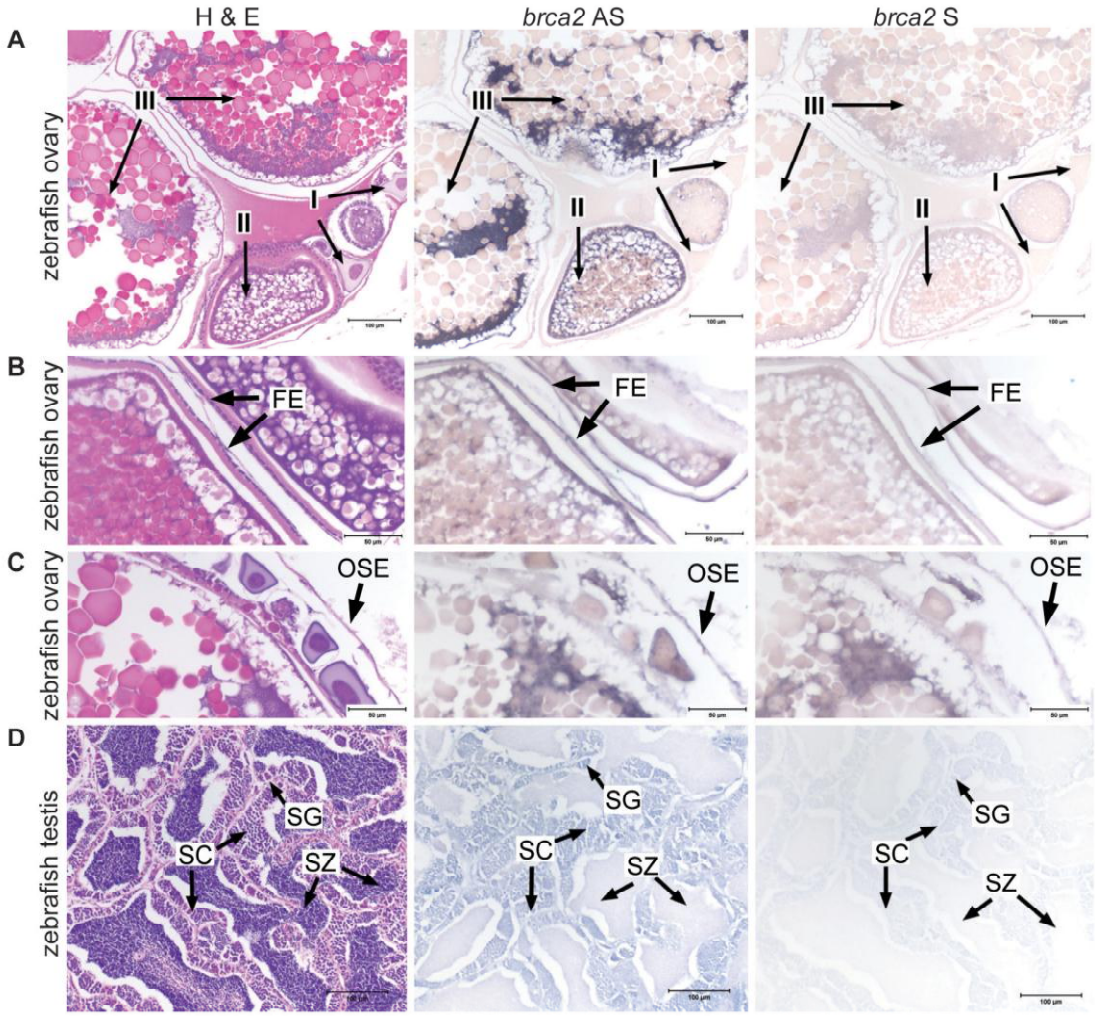

Fig. 2.6 *brca2* expression in adult zebrafish gonads. In situ hybridization for *brca2* expression in serial sections of adult zebrafish ovary with AS (middle panels) and S probes (right panels) indicates that *brca2* is expressed in oocytes (A), follicular epithelium (B), and ovarian surface epithelium (C). In situ hybridization for *brca2* expression in serial sections of adult zebrafish testis (D) indicates that *brca2* is expressed in spermatogonia and spermatocytes (arrows). Hematoxylin and eosin sections of ovary and testis (left panels) are provided for anatomic reference. I, stage I oocyte; II, stage II oocyte; III, stage III oocyte; FE, follicular epithelium; OSE, ovarian surface epithelium; SG, spermatogonia; SC, spermatocytes; SZ, spermatozoa. Scale bars, 100 µm (A and D); 50 µm (B and C).

brca2 was additionally expressed in the follicular epithelium (Fig. 2.6B) and the ovarian surface epithelium (Fig. 2.6C). In adult wildtype testes, *brca2* was expressed in spermatogonia and developing spermatocytes; mature spermatozoa did not express *brca2* (Fig. 2.6D).

Wildtype adult female zebrafish demonstrate disparate breeding histories.

Analyses of breeding history and egg production demonstrated that individual wildtype female zebrafish can experience widely variable reproductive histories (Fig. 2.7). Among individual females, egg production ranged from none to greater than 100 embryos produced per breeding cycle. Failure of egg production was often intermittent, and some females would remain infertile for up to 14 weeks before resuming egg production. Variability in breeding history was more pronounced with increased age. During these studies, one breeding female zebrafish died unexpectedly after 10 months of breeding; thus, this female's breeding history was not included in analyses of egg production. Histologic examination of the ovaries from this female zebrafish revealed chronic granulomatous oophoritis with fibrosis and retention of degenerating yolk material in the gonoduct (data not shown).

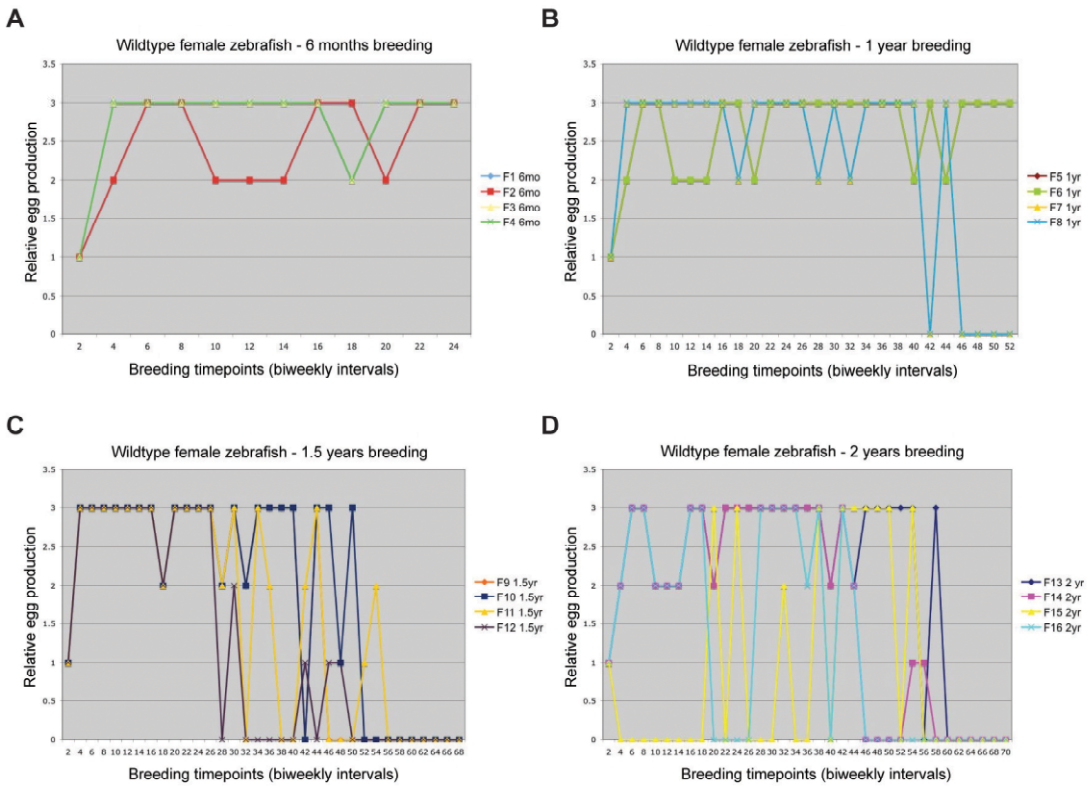

Figure 2.7 Relative egg production among wildtype female zebrafish. Wildtype female zebrafish were bred at biweekly intervals for 6 months (A), 1 year (B), 1.5 years (C), and 2 years (D). Relative egg production for individual females was scored as follows: 0, no eggs laid; 1, < 50 eggs laid; 2, 50 – 100 eggs laid; 3 > 100 eggs laid. Each color indicates an individual female zebrafish.

Discussion

These studies were designed to evaluate the zebrafish as a model for studying gonadal pathophysiology and *brca2*. Initial analyses focused on examining normal gonadal morphology in the zebrafish. Observations of germ cell development and stromal cell populations in wildtype AB* zebrafish ovaries and testes were similar to previous studies of zebrafish gonadal morphology (73, 75, 76). While ovarian thecal cells and testicular Leydig (interstitial) cells were not readily identifiable in routine histologic sections, these cell populations have been identified by other methods in zebrafish gonads (73, 75, 76). These studies indicate that germ cell and somatic cell populations with conserved intracellular structural organization are identifiable by routine histology in zebrafish ovaries and testes.

While no tissue-specific markers for the ovarian surface epithelium have been identified, expression of keratins 7, 8, 18, and 19 is characteristic of this tissue (8). Immunohistochemistry for type II cytokeratins, which include keratin 8, demonstrated that pancytokeratin immunoreactivity in the ovarian surface epithelium is conserved across multiple species, including zebrafish. These findings are an additional indication that ovarian structure is similar in zebrafish as compared to other species. These histologic and immnunohistochemical studies in wildtype AB* zebrafish gonads thus provide a basis for assessing zebrafish gonadal pathophysiology.

The ovarian cancer susceptibility gene *BRCA2* has been extensively investigated in mouse models after a link between *BRCA2* mutation and ovarian cancer was first discovered in 1994 (28). Evaluations of *Brca2* expression in mouse embryos from day 6.5 to day 19 indicate that *Brca2* is strongly expressed during embryogenesis (115-117). *Brca2* expression is most abundant in rapidly dividing tissues, including the ventricular zone, neuroepithelium of the eye, walls of the cerebral hemispheres, and other tissues (115-117).

In preparation for establishing a *brca2*-mutant zebrafish line, *brca2* expression during embryogenesis was evaluated. The data presented herein demonstrate that in zebrafish, *brca2* is strongly expressed throughout early embryogenesis from the two-cell stage up to 24 hpf. These findings complement a previous study of *brca2* expression during zebrafish embryogenesis (118). As development progresses beyond 24 hpf, *brca2* expression is maintained in the developing CNS, eye, and intestine. Regions of highest expression in zebrafish are similar to those described in mice (115-117), indicating that the pattern of *BRCA2* expression is conserved between mammalian and zebrafish embryos.

Importantly, *brca2* is strongly expressed at the two-cell stage, well before the onset of zygotic gene transcription in cleavage cycle ten (~ 1000 cell stage, ~ 3 hpf) (119). Thus, maternally provided *brca2* is available for DNA repair before zygotic transcription begins. In contrast, the highest levels of *Brca2* expression in mice occurred around embryonic day 13.5 (117). As zygotic transcription in mammalian

embryos begins before implantation at the 1 – 2 cell stage (120, 121), the majority of *Brca2* RNA present during mouse embryogenesis is likely to be derived from the zygotic genome, rather than provided maternally.

To build upon these studies of *brca2* in zebrafish embryos, developing and adult zebrafish were evaluated for *brca2* expression by ISH. In juvenile and adult zebrafish, *brca2* expression was restricted to the gonads. Juvenile wildtype zebrafish expressed *brca2* in putative premeiotic germ cells and perinucleolar oocytes; *brca2* expression was not detected in less mature germ cells. In zebrafish, meiosis begins in a subset of the germ cell population during gonadal development (77, 122). BRCA2 is required for repair of planned double-strand DNA breaks generated during meiotic recombination, which occurs in prophase I (34, 58). Thus, *brca2* expression in germ cells entering meiosis in the juvenile zebrafish gonad is compatible with the known function of BRCA2 in meiotic prophase.

Adult wildtype female zebrafish expressed *brca2* in both germ cell and somatic cell populations in the ovary. Oocytes expressed *brca2* throughout oogenesis, with accumulation of abundant *brca2* in the most mature oocytes. Expression of *brca2* in mature oocytes corresponds to the high levels of *brca2* expression observed in early-stage zebrafish embryos. In addition, *brca2* is expressed in the follicular epithelium and the ovarian surface epithelium. Studies of *Brca2* expression in mouse ovaries have demonstrated similar expression patterns in the ovarian surface epithelium and follicular epithelium (116).

In adult wildtype male zebrafish, *brca2* is expressed in spermatogonia and in primary and secondary spermatocytes. Zebrafish spermatogenesis is comparable to spermatogenesis in mammalian species; primary spermatocytes, which can be identified by their size and nuclear morphology, are in meiotic prophase of the cell cycle (75). Thus, *brca2* expression in zebrafish primary spermatocytes correlates with meiotic progression. These findings are similar to studies of *Brca2* expression in mouse testes, which demonstrate that *Brca2* is expressed during spermatogenesis, especially in spermatocytes in meiotic prophase (116). In humans, BRCA2 localizes to unsynapsed regions of meiotic chromosomes in human spermatocytes (123). Both zebrafish and mice exhibit *Brca2* expression in populations of cells that are mitotically active (116), but are not in meiosis, which may indicate additional requirements for *Brca2* in DNA repair during spermatogenesis.

Studies of *brca2* expression during embryogenesis and in juvenile and adult zebrafish demonstrated that patterns of expression are conserved between zebrafish and mice. This may reflect similar functions for *brca2* during development and in adult gonads in these species, an important consideration for comparative models. In addition, these findings will be important for analyzing the effects of *brca2* mutation in zebrafish.

Analyses of breeding history over a two-year period in wildtype female zebrafish revealed that reproductive rates could not be uniformly controlled among individual

females, particularly with increasing age. The occurrence of granulomatous oophoritis, which was observed in one zebrafish from the breeding group that died during the study, is a recognized problem of uncertain etiology among breeding female zebrafish (124), and may have contributed to intermittent or sustained infertility in this population of females. These studies indicate that reproductive history as a risk factor for ovarian cancer is not easily evaluated by comparing individual zebrafish. Analyzing reproductive history among large groups of zebrafish, rather than performing relative comparisons within a group, could possibly diminish the effects of individual biologic variability.

The morphologic, immunohistochemical, and in situ hybridization studies presented in this chapter demonstrate that the zebrafish is a feasible animal model for studying comparative gonadal pathophysiology and the role of *brca2* in embryogenesis, development, and tumorigenesis. The abundant maternal RNA for *brca2* present in early embryogenesis suggests that maternally provided *brca2* could sustain *brca2*-mutant zebrafish embryos. This would circumvent the early embryonic lethality that occurs in most *Brca2*-mutant mouse models and facilitate establishment of a *brca2*-mutant zebrafish line.

Chapter 3: Generating and characterizing a *brca2*-mutant zebrafish line

Introduction

The identification and establishment of knockout models in zebrafish have traditionally involved forward genetic screens of mutagenized zebrafish (125). More recently, a variety of techniques have evolved that allow identification and establishment of zebrafish lines with mutations in specific genes of interest. Ethylnitrosourea (ENU)-mutagenized libraries of zebrafish DNA and cryopreserved sperm provide an important resource for generating mutant zebrafish lines (63-67). Unique ENU-induced mutations have been identified in a number of cancer susceptibility genes in zebrafish, leading to the generation of zebrafish models for mutations in *tp53*, *apc*, and *rag1*, among others (69-71).

In this chapter, a *brca2*-mutant zebrafish line derived from an ENU-mutagenized library is characterized. This zebrafish line carries a nonsense mutation in *brca2* exon 11 (*brca2*^{Q658X}), a mutation similar in location and type to *BRCA2* mutations in humans with hereditary breast and ovarian cancer (17). Analyses of the *brca2*^{Q658X} mutation in zebrafish demonstrate the impact of *brca2* mutation on embryonic survival, development, gonadogenesis, and sexual differentiation. Strikingly, these studies identify a critical role for *brca2* in zebrafish ovarian development.

Materials and Methods

Identification and establishment of a brca2-mutant zebrafish line. A previously-established ENU-mutagenized library (68) was screened by PCR and sequencing with overlapping primer pairs spanning zebrafish *brca2* exon 11. Sequence data was analyzed with PolyPhred (http://droog.gs.washington.edu/polyphred/), and a zebrafish line carrying a C to T point mutation that produces a glutamine (Q) to stop codon (X) change was identified. The mutant line was recovered by *in vitro* fertilization (IVF) as previously described (68). Following recovery by IVF, *brca2*^{Q658X} heterozygous zebrafish were outcrossed to wildtype EK or AB* zebrafish. The *brca2*^{Q658X} mutant line is referenced in the Zebrafish Model Organism Database (ZFIN) with mutant allele designation *brca2*^{hg5}.

Genotyping for the brca2^{Q658X} *mutation*. Zebrafish were anesthetized in 0.4% Tricaine Methanesulfonate in system water and a portion of the caudal fin was clipped. Fin tissue was digested in 100µl of DNA extraction buffer with 0.2mg/ml proteinase K (Fermentas Inc.) at 50 – 55ºC for a minimum of two hours followed by ten minutes at 95ºC. The dCAPS-Finder 2.0 program (126) was used to design primers to detect the *brca2*^{Q658X} point mutation. These primers amplified a 379 bp fragment of *brca2* and created an *Alu*I restriction site based on the presence of the *brca2*^{Q658X} point mutation. PCR products were incubated with *Alu*I digestion buffer (0.07 U/µl *Alu*I in 1X Tango buffer; Fermentas Inc.) at 37ºC for a minimum of two hours. Digested PCR products were analyzed by gel electrophoresis (2.5% agarose in 1X Tris/Borate/EDTA (TBE) buffer with 0.3 – 0.6 µg/ml Ethidium Bromide).

Establishing a dose curve for gamma-irradiation of zebrafish embryos. Embryos from incrosses of wildtype AB* zebrafish were collected. At approximately 4.5 hours post-fertilization (hpf), zebrafish embryos were placed in 4 ml blue water media (NaCl, 0.57g/L; Methylene Blue, 0.002%), in 60 mm Petri dishes and were irradiated with an Eldorado 8 Cobalt-60 Teletherapy machine (MDS Nordion, Ottawa, Ontario, Canada, formerly AECL Ltd). The dose rate varied from 140-150 cGy/min during the course of this study. Decay corrections were done monthly, and full electron equilibrium was ensured for all irradiations. Zebrafish embryos received the following dosages: 0 Gy, 0.1 Gy, 0.5 Gy, 1.0 Gy, 5.0 Gy, 10.0 Gy, and 20.0 Gy. Sixty embryos were irradiated at each dose interval.

Acridine Orange assay for apoptosis analyses in vivo. Embryos were dechorinated by hand at 24 hpf, soaked in Acridine Orange (Sigma; 2 µg/ml in blue water) for 30 minutes at 28.5°C, and washed twice in blue water. Live embryos were anesthetized with 0.4% Tricaine Methanesulfonate and evaluated for Acridine Orange staining with a Zeiss Stemi SV11Apo stereomicroscope. Images were captured with Openlab modular imaging software (Improvision/Perkin Elmer Inc.) and minimally processed with Adobe Photoshop Version 10.0.1.

Irradiation and apoptosis analyses of embryos collected from incrosses of brca2^{Q658X} heterozygotes. Embryos were collected from incrosses of *brca2*^{Q658X} heterozygotes. At 4 – 5 hpf, embryos were irradiated as described above with the following dosages:

0 Gy, 1.0 Gy, and 5.0 Gy. Embryos were evaluated for apoptosis by Acridine Orange staining and imaged as described previously.

Phenotypic analysis of adult brca2-mutant zebrafish. Adult zebrafish collected from incrosses of *brca2*^{Q658X} heterozygous zebrafish were evaluated both grossly and histologically. Zebrafish were euthanized and fixed as described in Chapter 2. Specimens were routinely processed for paraffin embedding and preparation of 5µm H & E sections (Histoserv Inc.).

Assessment of meiotic progression in testes from adult male zebrafish. Testes from ten adult males (5.5 months of age) of each genotype were dissected and grouped by genotype for fixation as described in Chapter 2. To determine the total percentage of spermatocysts containing cells in meiosis, five tubules were randomly selected from each of ten testis sections for a total of fifty tubules. Tubules in which the tubular lumen and margins could not be reasonably ascertained were disregarded, and sections without at least five well-defined tubules in cross section were not included. For each tubule, the total number of spermatocysts was counted and the number of spermatocysts containing spermatocytes with meiotic figures was recorded (Table 3.1). The numbers of spermatocysts per tubule from testes of each *brca2* genotype were compared by unpaired t-tests (Table 3.1). The numbers of meiotic spermatocysts per tubule from testes of each *brca2* genotype were compared by unpaired t-tests with Welch's correction (Table 3.1).

Assessment of apoptosis in adult zebrafish testes by TUNEL assay. 5 µm unstained sections of testes from ten adult males (5.5 months of age) of each genotype were used for TUNEL labeling with a commercially available kit (In Situ Cell Death Detection Kit, AP; Roche). After TUNEL labeling, sections were counterstained with Nuclear Fast Red Solution (Sigma-Aldrich Co.) and mounted with Clear-Mount (Electron Microscopy Services, Hatfield, PA). TUNEL assays were performed with each sample set in three independent experiments.

Assessment of apoptosis in adult zebrafish testes by caspase-3 immunohistochemistry. 5 µm unstained sections of testes from ten adult males (5.5 months of age) of each genotype were deparaffinized in xylene and rehydrated through a series of ethanol grades. Sections were incubated in 3% H_2O_2/70% methanol to block endogenous peroxidase activity. For antigen retrieval, sections were incubated in 1X DAKO Target Retrieval Solution with steam (DAKO, Glostrup, Denmark). DAKO Protein Block and normal goat serum were used for blocking. Endogenous biotin activity was blocked with a commercially available kit (Vector Laboratories Inc.). For detection of cleaved caspase-3, a rabbit polyclonal anti-cleaved caspase-3 antibody (1:200 dilution; Cell Signaling, Boston, MA) was used with a goat anti-rabbit biotinylated secondary antibody (1:400 dilution; DAKO). Detection was achieved by incubating sections with a preformed avidin:biotinylated enzyme complex (Vectastain ABC Kit; Vector Laboratories Inc.) followed by application of 3,3'-diaminobenzidine tetrahydrochloride (DAB-Plus Substrate Kit; Invitrogen). After detection, sections

were counterstained with Mayer's Hematoxylin Solution (Sigma-Aldrich Co.), dehydrated, and coverslipped.

Histologic analysis of gonadal development. Juvenile zebrafish were collected at 21, 31, 41, and 51 days post fertilization (dpf), euthanized, genotyped, and fixed as described in Chapter 2, and specimens were grouped in tissue cassettes by genotype. 21 dpf juveniles were embedded in 2% agarose prior to placement in tissue cassettes. Juvenile gonad development was staged as described (77, 78). Ten sections were screened per group; specimens were assessed for the presence of gonadal tissue, presence of identifiable perinucleolar oocytes in gonads (signifying juvenile ovary formation), presence of spermatogonia in spermatogonial cysts (signifying testicular differentiation), and proliferation and differentiation of oocytes (signifying ovarian differentiation).

Results

brca2^{Q658X}*-mutant zebrafish are viable.*

To establish a *brca2*-mutant zebrafish model, we screened an Ethylnitrosourea (ENU)-mutagenized library for mutations in *brca2* exon 11 (Fig. 3.1). We identified a zebrafish line carrying a C to T point mutation that produces a glutamine (Q) to stop codon (X) change (Fig. 3.2A). The *brca2*^{Q658X} mutation was routinely detected by PCR and restriction digestion; the PCR product from the *brca2*^{Q658X} mutant allele migrates at a lower molecular weight than the wildtype allele (Fig. 3.2B). Embryos collected from incrosses and outcrosses of *brca2*^{Q658X} heterozygous zebrafish were

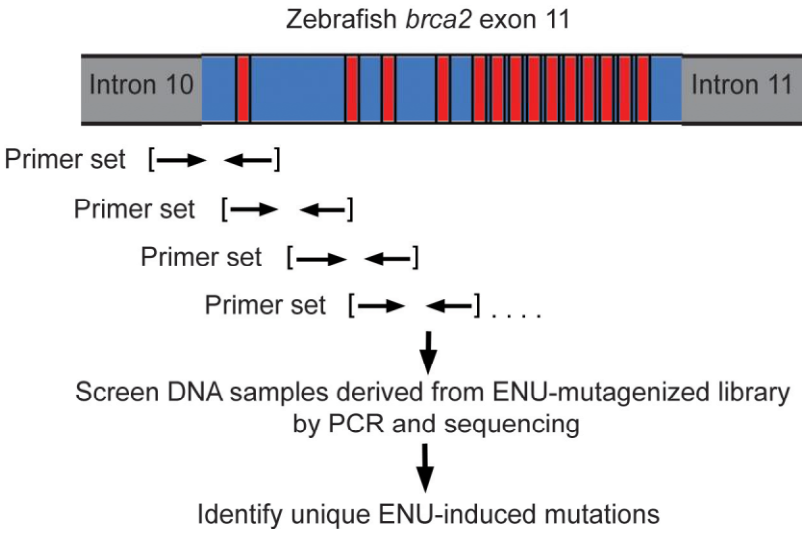

Fig. 3.1 Screening an ENU-mutagenized library for mutations in *brca2* exon 11. A previously established ENU-mutagenized library was screened for mutations in exon 11 of zebrafish *brca2* by PCR and sequencing. Overlapping primer sets spanned the length of exon 11.

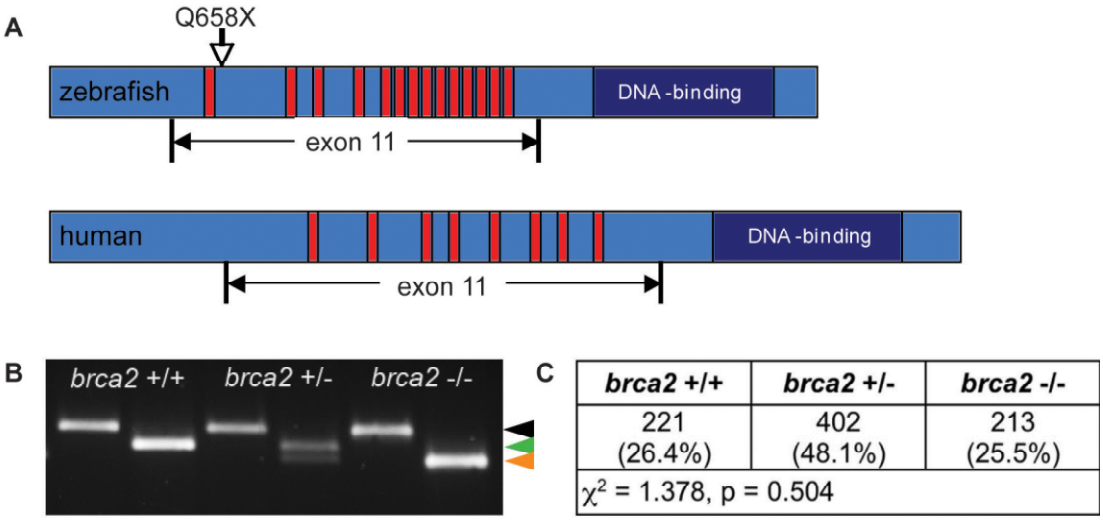

brca2 +/+	brca2 +/-	brca2 -/-
221 (26.4%)	402 (48.1%)	213 (25.5%)
$\chi^2 = 1.378$, p = 0.504		

Fig. 3.2 *brca2*^{Q658X} mutant zebrafish line. (A) Schematic of zebrafish *brca2* (upper) compared to human *BRCA2* (lower). Red bars represent the Rad51-binding BRC repeats and the dark blue box represents the DNA binding domain. The zebrafish *brca2*^{Q658X} mutation (C1971T;Q658X) described herein is shown relative to its position within exon 11. (B) The zebrafish *brca2*^{Q658X} mutation is identifiable by PCR and restriction digestion. Gel electrophoresis resolves PCR products from the wildtype allele (344 bp, green arrowhead), mutant allele (318 bp, orange arrowhead), and undigested PCR product (379 bp, black arrowhead). (C) Genotypes of progeny from incrosses of *brca2*^{Q658X} heterozygotes conform to expected Mendelian ratios. The percentages of observed genotypes were not statistically significantly different than expected ($\chi^2 = 1.378$, p = 0.504).

phenotypically normal (data not shown). Genotyping data collected on zebrafish derived from twelve different incrosses of *brca2*^{Q658X} heterozygous zebrafish yielded wildtype, heterozygous, and homozygous mutant zebrafish in expected Mendelian ratios, indicating that *brca2*^{Q658X} homozygotes were fully viable (Fig. 3.2C).

brca2^{Q658X} *mutation is not associated with increased apoptosis in embryos following exposure to ionizing radiation.*

To determine the effects of *brca2* mutation on DNA repair capacity in zebrafish, embryos from incrosses of *brca2*^{Q658X} heterozygotes were exposed to ionizing radiation during early embryogenesis. To establish an irradiation dose curve, wildtype zebrafish embryos were exposed to ionizing radiation over the following range: 0 Gy, 0.1 Gy, 0.5 Gy, 1.0 Gy, 5.0 Gy, 10.0 Gy, and 20.0 Gy. After irradiation, embryos were evaluated for morphologic defects and for apoptosis *in vivo* by Acridine Orange staining (Appendix VI).

Irradiation doses of 0 Gy, 1.0 Gy, or 5.0 Gy were selected for irradiation of embryos from incrosses of *brca2*^{Q658X} heterozygotes because these doses induced relatively low levels of apoptosis in wildtype embryos, and might therefore reveal increased susceptibility to radiation-induced apoptosis in *brca2*^{Q658X}-mutant embryos. Cohorts of embryos from three separate clutches were exposed to 0 Gy, 1.0 Gy, or 5.0 Gy at approximately 4 – 5 hpf. Apoptosis was evaluated *in vivo* by Acridine Orange staining approximately 24 hours after irradiation (Fig. 3.3). While increased levels of

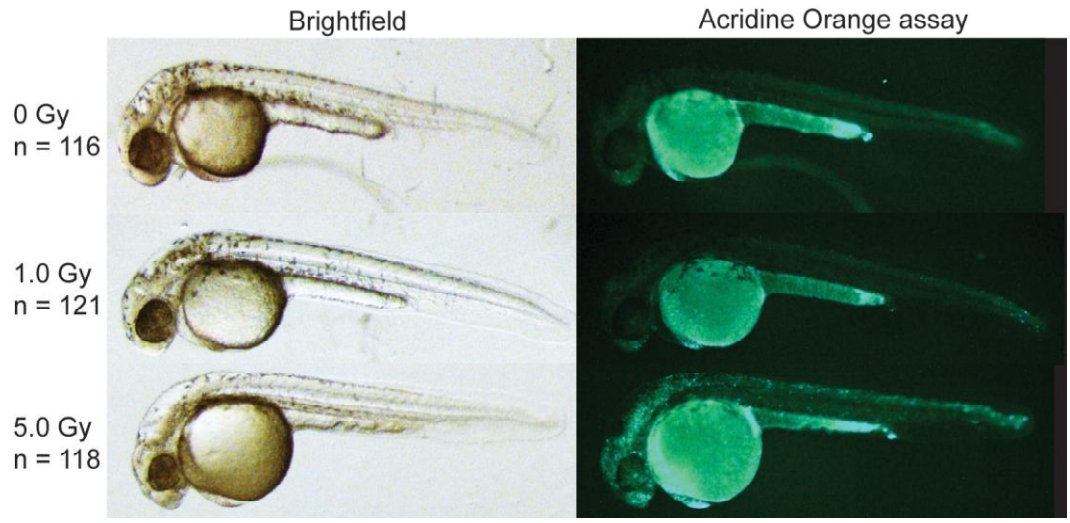

Fig. 3.3 *brca2*^{Q658X}-mutant zebrafish are not more susceptible to ionizing radiation. Representative examples of embryos that were derived from incrosses of *brca2*^{Q658X} heterozygotes and exposed to ionizing radiation (0, 1.0 Gy, or 5.0 Gy) at 4 – 5 hpf. The total numbers of embryos derived from incrosses of *brca2*^{Q658X} heterozygotes in each irradiation dose group are indicated at the left. At approximately 24 hpf, irradiated embryos were stained with Acridine Orange to detect apoptotic cells in vivo. Within each dose group, no significant differences in morphologic appearance or level of apoptosis were observed by visual inspection among individual zebrafish.

apoptosis were observed with increasing irradiation dose, no difference in distribution or intensity of Acridine Orange staining was apparent within dose groups. A subset of embryos that exhibited decreased swimming behavior at 3 dpf after irradiation was sacrificed for genotyping. No correlation was found between *brca2* genotype and reduced swimming behavior.

Following *in vivo* analyses for apoptosis, embryos from each dosage group were raised to adulthood and monitored for approximately 1.5 years (0 Gy, n = 92; 1.0 Gy, n = 97; 5.0 Gy, n = 94). During this period, a small number of zebrafish from these cohorts were found dead or were euthanized (Appendix VII). These data did not reveal a pattern in morbidity or mortality associated with *brca2* genotype or with irradiation dose.

brca2^{Q658X}*-mutant zebrafish are phenotypically male and exhibit aberrant spermatogenesis.*

At sexual maturity, all *brca2*^{Q658X} homozygotes were phenotypically male, while wildtype and *brca2*^{Q658X} heterozygous cohorts both included similar ratios of male and female zebrafish (Fig. 3.4A). *brca2*^{Q658X} homozygotes induced egg laying in fertile wildtype female zebrafish, but eggs collected from these crosses were unfertilized.

Upon histologic examination of the gonads, adult wildtype and *brca2*^{Q658X} heterozygotes had either mature ovaries or testes, and gonadal sex was consistent

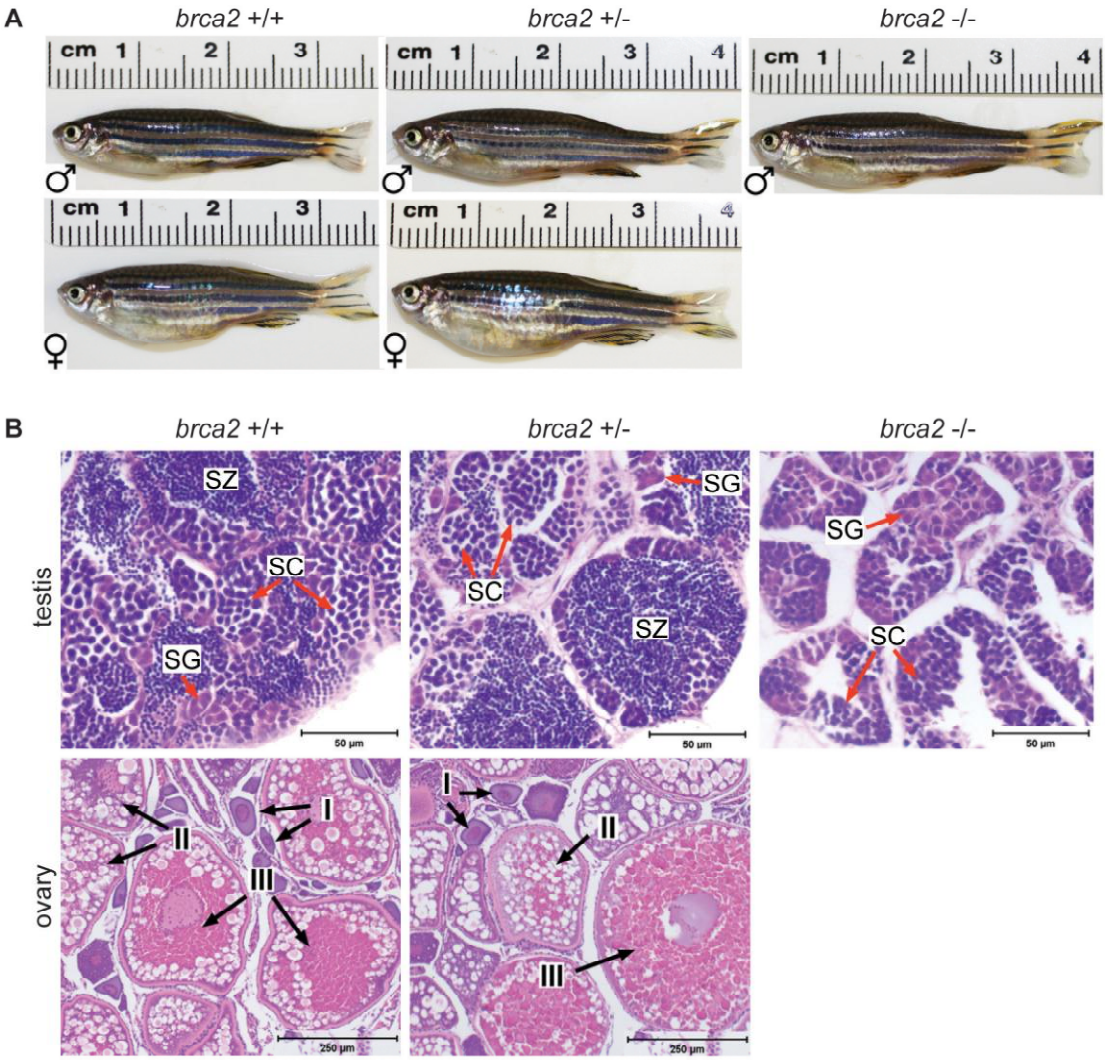

Fig. 3.4 *brca2*^{Q658X} homozygous zebrafish are phenotypically male and exhibit aberrant spermatogenesis. (A) Wildtype and *brca2*^{Q658X} heterozygotes exhibit distinctly male or female phenotypes, while *brca2*^{Q658X} homozygotes are phenotypically male. (B) Gonads from zebrafish of each genotype reflect observed male or female phenotypes in (A). Spermatogenesis is complete in testes from wildtype and *brca2*^{Q658X} heterozygotes. Testes from *brca2*^{Q658X} homozygotes contain only spermatogonia and primary spermatocytes. Ovaries from wildtype and *brca2*^{Q658X} heterozygotes are similar and contain developing and mature oocytes. SG, spermatogonia; SC, spermatocytes; SZ, spermatozoa; I, stage I oocyte; II, stage II oocyte; III, stage III oocyte. Scale bars, 50µm (testis); 250 µm (ovary).

with predicted sex based on physical features and behavior (Fig. 3.4A, B). In comparison, *brca2*^{Q658X} homozygotes had only testes (Fig. 3.4B). Spermatogenesis was arrested in testes from *brca2*^{Q658X} homozygotes, with only spermatogonia and primary spermatocytes present (Fig. 3.4B). Spermatogenesis was complete in testes from male wildtype and *brca2*^{Q658X} heterozygotes (Fig. 3.4B). The ovaries from female wildtype and *brca2*^{Q658X} heterozygotes were morphologically similar, with complete oocyte development and maturation (Fig. 3.4B).

brca2^{Q658X}*-mutant zebrafish exhibit meiotic arrest and clonal apoptosis of spermatocytes in adult testes.*

To further analyze spermatogenesis in *brca2*^{Q658X} homozygotes, germ cell progression through meiosis was evaluated in sections of testes from adult male zebrafish of each genotype. Testes from adult *brca2*^{Q658X} homozygotes had increased numbers of spermatocysts containing spermatocytes with meiotic nuclear morphology (Fig. 3.5A). Quantitative analysis of meiotic spermatocysts revealed that meiotic progression was arrested in testes from *brca2*^{Q658X} homozygotes. The numbers of spermatocysts containing spermatocytes in meiosis were statistically significantly higher in testes from adult *brca2*^{Q658X} homozygotes compared to testes from wildtype ($p = 0.0026$) and *brca2*^{Q658X} heterozygotes ($p = 0.0009$) (Table 3.1).

Meiotic arrest in adult *brca2*^{Q658X} homozygotes testes was accompanied by extensive spermatocyte apoptosis; in contrast, apoptotic cells were rare in mature testes from wildtype and *brca2*^{Q658X} heterozygotes. TUNEL assay (Fig. 3.5B) and

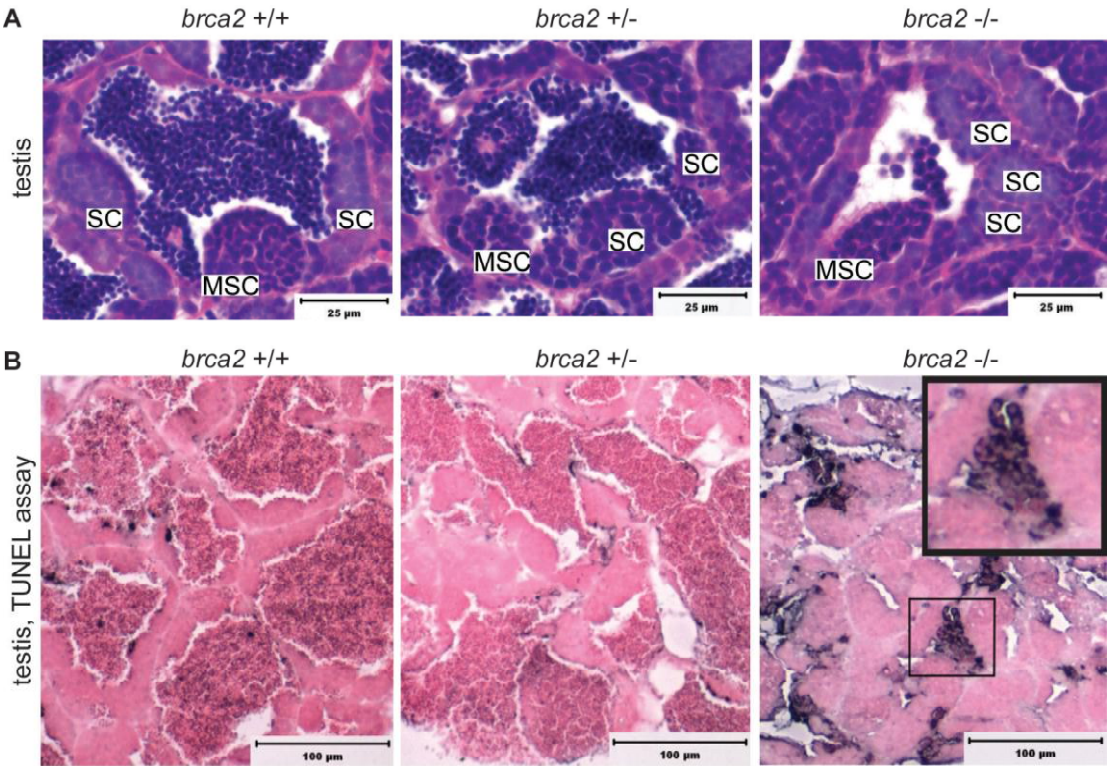

Fig. 3.5 *brca2*^{Q658X} homozygous zebrafish exhibit meiotic arrest and apoptosis of spermatocytes. (A) Testes from wildtype, *brca2*^{Q658X} heterozygotes, and *brca2*^{Q658X} homozygotes. Spermatocytes in testes from *brca2*^{Q658X} homozygotes undergo chromatin condensation in preparation for meiosis, but further meiotic stages are not present. (B) TUNEL staining of testes from wildtype, *brca2*^{Q658X} heterozygotes, and *brca2*^{Q658X} homozygotes. Multiple clusters of apoptotic spermatocytes are present in testes from *brca2*^{Q658X} homozygotes (inset). SC, spermatocyst; MSC, meiotic spermatocyst. Scale bars, 25 µm (A); 100 µm (B).

***brca2* genotype**	**# spermatocysts per 50 tubules**	**# meiotic spermatocysts per 50 tubules**	**% of meiotic spermatocysts**
Wild-type zebrafish	338	15	4%
brca2^{Q658X} heterozygous zebrafish	364	14	4%
brca2^{Q658X} homozygous zebrafish	351	38	11%
Comparisons	**p-value**	**p-value**	
Wild-type and *brca2*^{Q658X} heterozygous zebrafish	0.2867	0.8422	
Wild-type and *brca2*^{Q658X} homozygous zebrafish	0.5074	0.0026	
brca2^{Q658X} heterozygous and *brca2*^{Q658X} homozygous zebrafish	0.6423	0.0009	

Table 3.1 Quantitative analysis of meiotic spermatocysts in zebrafish testes. The numbers of meiotic spermatocysts were quantitated as a percentage of the total number of spermatocysts in 50 tubules from 10 zebrafish of each *brca2* genotype. The numbers of spermatocysts per 50 tubules were compared between *brca2* genotypes by unpaired t-tests (GraphPad Software, www.graphpad.com/quickcalcs/ttest1.cfm). The numbers of meiotic spermatocysts were compared among *brca2* genotypes by unpaired t-tests with Welch's correction (GraphPad Prism Version 5.0).

immunohistochemistry for cleaved caspase-3 (Appendix VIII) on sections of testes demonstrated multiple apoptotic spermatocytes in adult *brca2*^{Q658X} homozygotes, with apoptotic spermatocytes often forming distinct cell clusters (Fig. 3.5B, inset).

brca2^{Q658X}*-mutant zebrafish do not develop juvenile ovaries.*

To determine the stage at which *brca2* mutation affects sexual differentiation, gonads from juvenile zebrafish of each *brca2* genotype were examined by histology at intervals between 21 days and 51 days post fertilization (dpf). During this period, all zebrafish normally develop "juvenile ovaries", which contain gonocytes, early meiotic oocytes, and perinucleolar oocytes (77, 78). With maturation, males undergo oocyte loss and proliferation of spermatogonia and spermatocytes, while oocyte proliferation and differentiation continues in females (77, 78).

Gonad development in wildtype and *brca2*^{Q658X} heterozygotes was similar at all time points. At 21 dpf, the gonads from zebrafish of both genotypes were undifferentiated and contained gonocytes and scant stroma (Fig. 3.6A). At 31 dpf, gonads were classified into four morphologic types: undifferentiated (similar to gonads at 21 dpf); juvenile ovary; presumptive ovary; and presumptive testis (Fig. 3.6B). Juvenile ovaries were distinguished by the presence of perinucleolar oocytes (Fig. 3.6B, short arrows). Presumptive ovaries exhibited numerous enlarged oocytes, while presumptive testes exhibited developing spermatogonial cysts with reduction or loss of perinucleolar oocytes (Fig 3.6B). By 41 and 51 dpf, definitive gonad

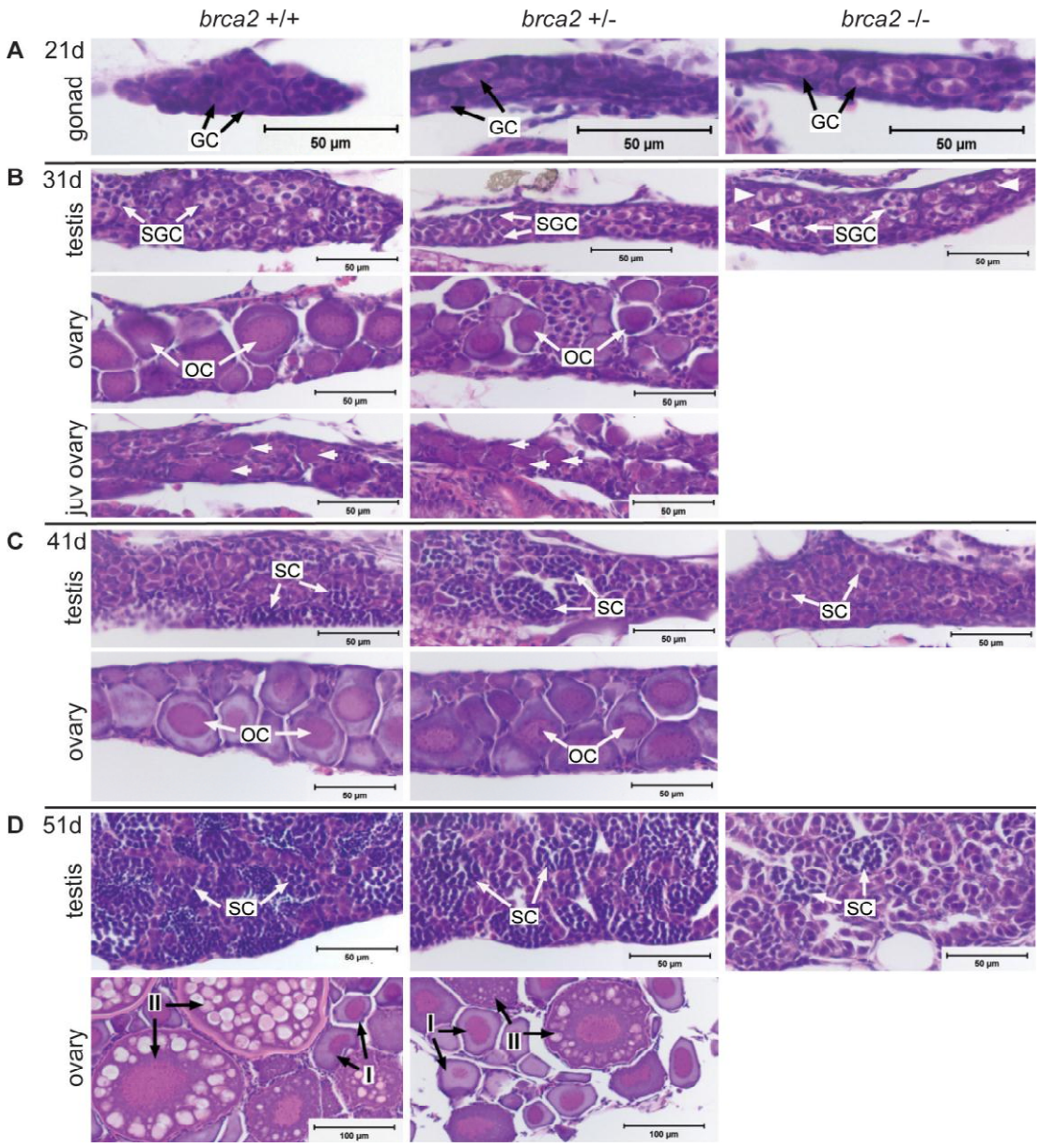

Fig. 3.6 Failure of ovarian development occurs in *brca2*^{Q658X} homozygous zebrafish. (*A*) Gonads from wildtype, *brca2*^{Q658X} heterozygotes, and *brca2*^{Q658X} homozygotes zebrafish are indistinguishable at 21 days post fertilization (dpf). (*B*) At 31 dpf, wildtype and *brca2*^{Q658X} heterozygotes exhibit juvenile ovaries, early testicular differentiation, or early ovarian differentiation, whereas *brca2*^{Q658X} homozygotes exhibit only early testicular differentiation. Perinucleolar oocytes in juvenile ovaries are indicated by short arrows. Putative premeiotic germ cells are indicated by arrowheads. (*C*, *D*) At 41 and 51 dpf, wildtype and *brca2*^{Q658X} heterozygotes exhibit continued maturation of testes or ovaries, while *brca2*^{Q658X} homozygotes exhibit only testicular development. Go, gonocyte; sgc, spermatogonial cyst; oc, oocyte; sc, spermatocyst; I, stage I oocyte; II, stage II oocyte. Scale bars, 50 µm (100 µm in 51dpf ovaries).

differentiation into ovaries or testes was apparent in wildtype and *brca2*^{Q658X} heterozygotes (Fig. 3.6C, D).

In contrast, oocyte differentiation was not observed in gonads from *brca2*^{Q658X} homozygotes at any time point. At 21 dpf, gonads from *brca2*^{Q658X} homozygotes were similar to gonads from wildtype and *brca2*^{Q658X} heterozygotes (Fig. 3.6A). At 31 dpf, gonads from *brca2*^{Q658X} homozygotes were classified as undifferentiated or presumptive testes (Fig. 3.6B). Presumptive testes contained germ cells and clusters of round cells encircled by somatic cells, consistent with developing spermatogonial cysts. In gonads from some *brca2*^{Q658X} homozygotes, large cells with prominent nuclei and vacuolated cytoplasm were present (Fig. 3.6B, arrowheads); these cells may be premeiotic germ cells, and were not observed in gonads from wildtype or *brca2*^{Q658X} heterozygotes. Unlike testes from wildtype and *brca2*^{Q658X} heterozygotes, few spermatocysts were observed in developing testes at 41 dpf in *brca2*^{Q658X} homozygotes (Fig. 3.6C). By 51 dpf, spermatocysts in testes from *brca2*^{Q658X} homozygotes contained only spermatogonia and primary spermatocytes, and fewer spermatocysts were present compared to wildtype and *brca2*^{Q658X} heterozygotes (Fig. 3.6D). No perinucleolar oocytes were observed in developing gonads from *brca2*^{Q658X} homozygotes at any time point.

Discussion

The *brca2*^{Q658X}-mutant zebrafish line identified and established in these studies carries a nonsense mutation in exon 11 of *brca2* that is predicted to result in

truncation of the brca2 protein. This mutation is similar in location and type to humans with *BRCA2* mutations (17), and thus this mutant zebrafish line is well suited for studying *BRCA2*-associated carcinogenesis. In humans, the majority of pathologic mutations in *BRCA2* are point mutations or small insertions or deletions that truncate the BRCA2 protein (3, 26). When these mutations occur in the "ovarian cancer cluster region" of *BRCA2* exon 11, epidemiologic evidence suggests an increased incidence of ovarian cancer relative to breast cancer in affected families (16, 29).

Multiple incrosses of *brca2*^{Q658X} heterozygous zebrafish revealed that *brca2*^{Q658X} homozygotes were viable. This is in marked contrast to the majority of *Brca2*-mutant mouse models, in which homozygous *Brca2* mutation is typically associated with early embryonic lethality (see Chapter 1, Table 1.2). This difference may reflect the relatively late onset of zygotic gene transcription in zebrafish embryos, which begins in cleavage cycle ten (119). Since maternal *brca2* is abundant in early-stage zebrafish embryos (Chapter 2, Fig. 2.3), it is likely that maternal RNA sustains *brca2*^{Q658X} homozygotes during early development.

Biallelic mutation or loss of *BRCA2* in cultured cells is associated with increased sensitivity to DNA-damaging agents (31, 35). Similarly, blastocyst explants derived from *Brca2*-mutant mouse embryos at embryonic day 3.5 are highly sensitive to irradiation (50). BRCA2 is required for error-free repair of double-strand DNA breaks through the process of homologous recombination (31, 32); thus, mutation or

loss of *BRCA2* would be expected to reduce a cell's capacity for DNA repair. Accordingly, *BRCA2*-deficient cells that are exposed to DNA-damaging agents exhibit numerous foci of unrepaired DNA and failure of RAD51 to colocalize to sites of DNA damage (30, 31, 35).

We assessed the effects of DNA damage in *brca2*-mutant zebrafish embryos by exposing embryos from incrosses of *brca2*^{Q658X} heterozygotes to ionizing radiation during the mid-blastula stage. Irradiated and nonirradiated embryos were subsequently screened *in vivo* for apoptosis. There was no apparent difference in embryonic development or level of apoptosis among embryos from incrosses of *brca2*^{Q658X} heterozygotes after irradiation; further, no significant long-term effects were observed in these populations of zebrafish. Several possibilities may address these findings. Firstly, DNA repair is known to be highly efficient in zebrafish embryos (127). Furthermore, zebrafish embryos exhibit accurate DNA repair through the process of nonhomologous end-joining (127), an alternate repair process for dsDNA breaks that is considered to be more "error-prone" in other animals (31, 128). Finally, *brca2*-mutant zebrafish are supplied with abundant maternal RNA for *brca2*. Thus, there may be sufficient levels of brca2 present through the mid-blastula stage for repair by homologous recombination to occur. In combination, these factors may prevent *brca2*-mutant zebrafish embryos from experiencing higher levels of sustained DNA damage and/or cellular apoptosis in comparison to wildtype embryos.

While the *brca2*^{Q658X} mutation did not induce an embryonic phenotype, studies of adult *brca2*^{Q658X} homozygotes demonstrate a conserved role for *brca2* in zebrafish germ cell development and spermatogenesis. *BRCA2* is required in germ cells for repair of double-strand DNA breaks generated during prophase of meiosis I, with loss of *BRCA2* resulting in meiotic arrest (58, 129). In mice, *Brca2* is expressed during spermatogenesis, especially during meiotic prophase (115, 116). Similarly, *brca2* is highly expressed in primary spermatocytes in wildtype zebrafish testes (Chapter 2, Fig. 2.6), which are in meiotic prophase (75). Thus, incomplete spermatogenesis and meiotic arrest in testes from *brca2*^{Q658X} homozygotes are in accordance with these findings. TUNEL staining and cleaved caspase-3 immunoreactivity revealed extensive apoptosis in *brca2*^{Q658X} homozygous testes, with apoptotic spermatocytes frequently present in discrete clusters. These findings appear to reflect apoptosis of spermatocyte clones, since zebrafish spermatocytes are clonally derived from a single germ cell and organized into discrete groups referred to as spermatocysts (75).

Analyses of juvenile *brca2*-mutant zebrafish demonstrated that immature *brca2*^{Q658X} homozygotes fail to form juvenile ovaries during the process of gonad development, in contrast to what is regularly observed in wildtype zebrafish (77, 78). Thus, these studies reveal an important role for *brca2* in ovarian development, raising questions about the participation of *brca2* in primordial germ cell-stromal cell signaling in the immature gonad. *BRCA2* is also known as *FANCD1*, and is a member of the Fanconi anemia (FA) family of proteins that regulate DNA damage response and repair (43). Interestingly, gonadal dysmorphogenesis and hypogonadism are observed in some

patients with mutations in various FA genes, although these studies are limited (130). Hypogonadism and meiotic arrest in germ cells have been reported in mouse models with mutations in several FA genes, including a *Brca2*-deficient mouse model that was rescued with human *BRCA2* (58, 131). Similar findings are described in mice homozygous for hypomorphic *Brca2* mutations (52, 54-56) and in rats with homozygous *Brca2* mutation (59).

Gonad development in *brca2*^{Q658X} homozygous zebrafish may be additionally influenced by disrupted meiosis, since meiotic progression in germ cells is characteristic of developing female gonads. In wildtype animals, female germ cells initiate meiosis during embryogenesis, while male germ cells remain quiescent until sexual maturity (132, 133). Thus, the temporal requirements for BRCA2 may differ in female versus male gonads (Appendix IX). Stromal cells and germ cells interact in the immature gonad to induce or repress the onset of meiosis in female versus male animals, respectively, and these interactions are tied to ovarian or testicular differentiation (132, 134, 135). *brca2*-deficient germ cells in the immature gonad are likely to be meiotically incompetent, similar to *brca2*-deficient germ cells in the adult zebrafish testes. Therefore, failure of meiotic progression in *brca2*-deficient germ cells during development may promote testicular differentiation.

Targeted mutations of meiosis-specific genes in mouse models, including genes *Spo11*, *Mlh1*, *Msh5*, and *Dmc1*, are associated with varying degrees of gonadal dysplasia and germ cell degeneration and loss in both male and female mice (136).

Interestingly, the point at which germ cell loss occurs and the degree of meiotic arrest in germ cells appears to influence the extent of ovarian dysgenesis. Mutations in *Msh5* and *Dmc1*, which cause total germ cell arrest early in prophase I and oocyte degeneration at birth, are generally associated with failure of follicle formation and gonadal degeneration (136, 137). In comparison, some oocytes from *Mlh1* mutant mice can progress beyond metaphase I, and these mice exhibit relatively normal folliculogenesis and ovarian morphology (137). Interestingly, testicular degeneration is not typical of male mice with mutations in meiosis-specific genes, even though they experience germ cell loss (138). From these observations, it has been suggested that germ cells are only required for maintenance of ovarian morphology, not testicular morphology (138). While there does not appear to be a fundamental requirement for meiosis-specific genes in mammalian sex determination, these studies demonstrate nonetheless that meiotically competent primordial germ cells are important for proper gonadal morphogenesis.

mlh1 is the only meiosis-specific gene that has been studied previously in zebrafish. MLH1 is required for synaptonemal complex formation in meiotic prophase (139). Zebrafish that are homozygous for the *mlh1* mutation exhibit reduced germ cell development or germ cell arrest, reduced fertility, spermatocyte apoptosis, and inviable offspring with frequent aneuploidy (140). Interestingly, both male and female *mlh1*-mutant zebrafish develop, and some fertile zebrafish of both sexes are described (140, 141). Gonadal development during the juvenile period was not described for *mlh1*-mutant zebrafish, so germ cell morphology during the onset of

meiosis is unknown. The observation that some *mlh1*-mutant female zebrafish are fertile suggests that enough germ cells in the juvenile gonad are able to enter meiosis and become perinucleolar oocytes, leading to ovarian differentiation.

A zebrafish line with homozygous mutation of the FA gene *fancl* was recently described. In this model, homozygous *fancl* mutation resulted in development of all-male zebrafish (142). *fancl*-mutant zebrafish showed an early bias toward testicular differentiation with increased germ cell apoptosis during juvenile gonad development (142). In contrast to *brca2*^{Q658X} homozygotes, *fancl*-mutant zebrafish exhibited limited early perinucleolar oocyte differentiation, and adult male *fancl*-mutant zebrafish were fertile (142). These findings further suggest that meiotic progression, as well as apoptosis in germ cells, may impact zebrafish gonadal development.

In summary, these studies in zebrafish have demonstrated the following: 1) *brca2* is not required for embryonic survival; 2) *brca2* mutation does not increase embryonic sensitivity to ionizing radiation; 3) *brca2* mutation results in an all-male phenotype characterized by incomplete spermatogenesis, meiotic arrest, and spermatocyte apoptosis; and 4) *brca2* is essential for ovarian development. In contrast to mouse models, *brca2* mutation in zebrafish does not affect embryogenesis, which is likely attributable to abundant maternal mRNA for *brca2*. However, *brca2* is critical for meiotic progression in germ cells. While *brca2* plays a conserved role in zebrafish spermatogenesis, the importance of *brca2* in zebrafish ovarian development is a novel finding that raises new questions about *BRCA2*-associated ovarian cancer.

Chapter 4: *brca2* in zebrafish gonadogenesis and tumorigenesis

Introduction

Establishment of a viable *brca2*-mutant zebrafish line has revealed that *brca2* is essential for zebrafish ovarian development. Evidence from humans and animal models with mutations in multiple genes from the Fanconi Anemia family, including *BRCA2*, indicate that this interrelated group of proteins influence gonadal morphogenesis (58, 130, 131, 143). However, the role for *BRCA2* in gonadal development is poorly defined, and an absolute requirement for *BRCA2* in ovarian development has not been previously demonstrated. Further, the link between *BRCA2* mutation and human ovarian cancer is not understood.

In this chapter, the mechanisms by which *brca2* mutation affects zebrafish ovarian development are explored. In addition, the role for *brca2* mutation in reproductive tumors and the collaborative effects of *brca2* mutation and homozygous *tp53* mutation on tumorigenesis are investigated. These studies indicate that germ cell apoptosis in *brca2*^{Q658X} homozygotes is a critical factor in gonad development. In adulthood, *brca2* functions as a tumor suppressor gene in zebrafish. Adult *brca2*^{Q658X} homozygotes develop testicular tumors, and tumorigenesis in multiple tissues is accelerated by homozygous *tp53* mutation in both *brca2*^{Q658X} heterozygotes and homozygotes. Thus, *brca2* plays critical roles in both ovarian development and cancer susceptibility.

Materials and Methods

Construction of RNA probes for zebrafish vasa. A plasmid containing 849 bp of the zebrafish *vasa* cDNA (pExpress-1-vasa; Clone #9787706, Open Biosystems/Thermo Scientific, Huntsville, AL) was used to amplify a 549 fragment. The insert was cloned into pCRII-TOPO (Invitrogen) according to the manufacturer's protocol. Cloning reactions were used to transform One-Shot chemically competent *E. coli* (Invitrogen) according to the manufacturer's protocol. Preparation of the pCRII-TOPO-vasa plasmid and transcription of DIG-labeled RNA were performed as described in Chapter 2.

Whole-mount in situ hybridization (WISH) for vasa expression in embryos from incrosses of brca2^{Q658X} heterozygotes. Embryos from incrosses of *brca2*^{Q658X} heterozygous zebrafish were used for analyses of *vasa* expression at 24 hpf and 4 dpf. WISH with antisense and sense probes for *vasa* on 24 hpf embryos was performed as described in Chapter 2. WISH with antisense and sense probes for vasa on 4 dpf larvae was performed as described in Chapter 2 with the following modifications: 1) larvae were genotyped before WISH by amputating a portion of the tail for DNA extraction and genotyping; 2) larvae were depigmented in 3% H_2O_2/0.5% KOH as described (144); 3) after fixation, larvae were incubated in 0.5 µg/ml proteinase K (Fermentas Inc.) in 1X PBS on ice for ten to fifteen minutes. Approximately 50 embryos at 24 hpf were analyzed in three independent experiments and approximately 25 – 50 embryos of each genotype were analyzed at 4 dpf in two independent experiments. After WISH for *vasa* in 24 hpf embryos, 25 – 35 embryos

from two independent experiments were individually imaged, and subsequently genotyped for the *brca2*^{Q658X} mutation. For imaging, embryos were positioned in individual wells of a 1% agarose mold and imaged with a Leica MZ16 stereomicroscope and camera (Leica DFC420) with Leica Imaging Suite. Embryos that were genotyped after WISH were prepared as described (86) with minor modifications (volume of DNA extraction buffer increased to 21 µl).

Immunohistochemistry for cleaved caspase-3 in juvenile zebrafish. Juvenile zebrafish from an incross of *brca2*^{Q658X} heterozygous zebrafish were collected at 28 dpf, euthanized, genotyped, and fixed as described in Chapter 3. After fixation, zebrafish were grouped by genotype. For each specimen, the head, dorsal musculature, and tail were removed and the trunk was embedded in agarose molds (2.0% agarose in distilled water). Agarose molds were placed in tissue cassettes for routine processing (Histoserv). Immunohistochemistry for cleaved caspase-3 was performed as described in Chapter 3.

Preparation of tdTomato-nos1-3'UTR construct. A plasmid containing a GFP-nos1-3'UTR construct (145) (pSP64-GFP-3'UTRnos1) was acquired from the laboratory of Dr. Erez Raz (Munster, Germany). Two new plasmids were constructed: pSP64-mCherry-3'UTRnos1 and pSP64-tdTomato-3'UTRnos1. To create pSP64-mCherry-3'UTRnos1, the pmCherry plasmid (Clontech, Mountain View, CA) was used for amplification of an 893 bp fragment of mCherry. The reverse primer created an *XhoI* restriction site at the 3' end of the PCR product and there was a *BamHI* restriction site

at the 5' end. The mCherry insert was gel-purified and the pSP64-GFP-3'UTRnos1 plasmid and insert were digested with *BamHI* and *XhoI*. Purification, ligation, transformation, and plasmid preparation of pSP64-mCherry-3'UTRnos1 were performed as described in Chapter 2. To create pSP64-tdTomato-3'UTRnos1, the pSP64-mCherry-3'UTRnos1 and the ptdTomato plasmid (Clontech) were digested with *AgeI* and *XhoI*. Purification, ligation, transformation, and plasmid preparation of pSP64-tdTomato-3'UTRnos1 were performed as described in Chapter 2. Preparation of tdTomato-3'UTRnos1 capped mRNA was performed with a commercially available kit according to the manufacturer's protocol (mMESSAGE mMACHINE Kit; Applied Biosystems/Ambion, Austin, TX).

Preparation of donor embryos for primordial germ cell transplants. *tg(bactin2:EGFP)zp5* zebrafish embryos were acquired from Zebrafish International Resource Center (ZIRC). Adult *tg(bactin2:EGFP)zp5* were incrossed and embryos collected from these crosses were used as donor embryos. At the one- to two-cell stage, donor embryos were injected with tdTomato-nos1-3'UTR RNA (300 pg/injection) and Oregon Green dextran conjugate (Invitrogen; 5 ng/injection) in 0.1M KCl using a microinjector (Harvard Instruments, PLI-100). After injection, donor embryos were incubated at 26 – 28°C. At approximately 2 hpf, donor embryos were dechorinated with 0.05% Pronase (Sigma), rinsed in system water, and collected into glass or agarose-coated plastic plates containing 30% Danieau's medium and 200 µg/ml Penicillin-Streptomycin (Gibco/Invitrogen).

Preparation of recipient embryos for primordial germ cell transplants. Embryos were collected from incrosses of *brca2*^{Q658X} heterozygous zebrafish. At the one-cell stage, embryos were injected with 1 ng of dead-end morpholino (dnd MO) (84) in 1X Danieau's medium and 0.025% Phenol Red using a microinjector (World Precision Instruments, PV-820). After injection, embryos were incubated at 26 – 28°C. At approximately 2 hpf, embryos were dechorinated with 0.05% Pronase (Sigma), rinsed in system water, and collected into glass or agarose-coated plastic plates containing 30% Danieau's medium and 200 µg/ml Penicillin-Streptomycin (Gibco).

Primordial germ cell transplant into embryos collected from incrosses of brca2^{Q658X} *heterozygotes.* At approximately 2.5 hpf, donor and recipient embryos were placed in agarose ramps in 30% Danieau's medium and 200 µg/ml Penicillin-Streptomycin (Gibco). Cells were collected from the margins of donor embryos with pulled glass capillary needles that were attached by flexible tubing to a 10-ml syringe. Donor cells were transplanted into the animal pole of recipient embryos. After transplant, recipient embryos were placed on glass or agarose-coated plastic plates in 1X Danieau's medium and 200 µg/ml penicillin-streptomycin and incubated at 26 – 28°C. Transplanted embryos were screened at 24 or 48 hpf for the presence of cells expressing GFP/Oregon Green and/or tdTomato in the region of the gonadal ridge.

Analyses of adult chimeric zebrafish. Chimeric zebrafish were raised to adulthood, genotyped for the *brca2*^{Q658X} mutation, and sexed by phenotypic features. Each chimeric zebrafish was individually bred to fertile wildtype AB* zebrafish.

Approximately 100 eggs collected from each of these crosses were screened by microscopy. Chimeric zebrafish which did not generate fertilized eggs in these crosses were considered sterile. Chimeric zebrafish which generated fertilized eggs in these crosses were considered fertile. Viable embryos from chimeric-wildtype zebrafish crosses were incubated at 26 – 28°C and screened daily for mortality and morphologic development. At 3 – 5 dpf, between 16 – 40 embryos from each breeding pair were individually digested in 30 – 50 µl DNA lysis buffer with 0.2 mg/ml Proteinase K (Fermentas Inc.) for DNA extraction. Individual embryos were genotyped for the *brca2*^{Q658X} mutation as described in Chapter 3. Individual embryos were also genotyped for the *(bactin2:EGFP)zp5* transgene according to the protocol provided by the supplier.

Histologic analyses of tumorigenesis in zebrafish testes. Aged adult wildtype, *brca2*^{Q658X} heterozygous, and *brca2*^{Q658X} homozygous male zebrafish were euthanized between the ages of 10 and 16 months. The testes were dissected, grouped by genotype, and fixed as described in Chapter 3, and placed in tissue cassettes for routine processing (Histoserv Inc.).

Introduction of tp53^{M214K} *mutation.* Zebrafish embryos homozygous for the *tp53*^{M214K} mutation were acquired from ZIRC. Adult *tp53*^{M214K} homozygous zebrafish were crossed with *brca2*^{Q658X} heterozygotes to establish a cohort of *brca2*^{Q658X} heterozygous;*tp53*^{M214K} heterozygous zebrafish. Progeny from an incross of *brca2*^{Q658X} heterozygous;*tp53*^{M214K} heterozygous zebrafish were genotyped for the

brca2^{Q658X} mutation as described or by sequencing. Progeny were also genotyped for the *tp53*^{M214K} mutation either by following the protocol provided by the supplier or by DNA sequencing.

Analyses of tumorigenesis in adult zebrafish. Adult zebrafish were regularly monitored for evidence of morbidity or overt tumor development. Tumor development in the *tp53*^{M214K} homozygous parental line was defined by gross observation of macroscopically identifiable tumors in live or euthanized zebrafish as described (70). A subset of *tp53*^{M214K} homozygous zebrafish was additionally screened by histology to confirm diagnosis. Progeny from an incross of *brca2*^{Q658X} heterozygous;*tp53*^{M214K} heterozygous zebrafish were evaluated for macroscopic tumor development and by histology. The ages at tumor onset in each genotype of zebrafish were compared by unpaired t-tests.

Results

Germ cell designation and colonization of the genital ridge and germ cell survival in brca2^{Q658X}*-mutant zebrafish.*

Development of all-male populations has been described in zebrafish with embryonic loss of primordial germ cells (PGCs) or failure of PGCs to migrate to the embryonic gonadal ridge (84, 85). Therefore, we evaluated embryos from incrosses of *brca2*^{Q658X} heterozygous zebrafish for the presence and appropriate localization of PGCs at 24 hpf and 4 dpf by WISH for the germ cell marker *vasa* (Fig. 4.1A). *Vasa* expression in 24 hpf embryos indicated no apparent difference in PGC numbers or

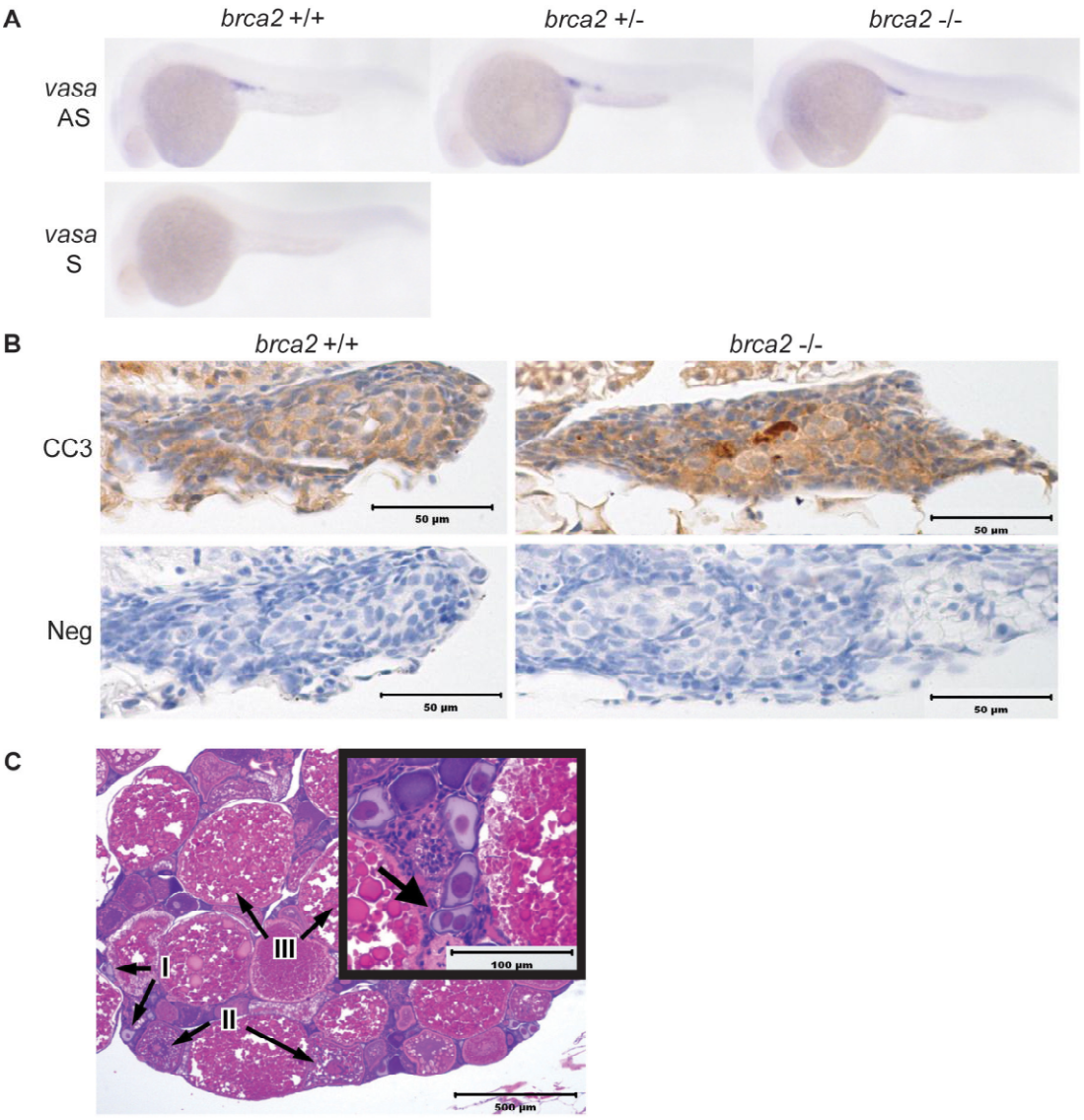

Fig. 4.1 Germ cell specification and survival in *brca2*^{Q658X} homozygotes. (A) WISH with antisense (AS) and sense (S) RNA probes for *vasa* indicates appropriate migration to and colonization of the gonadal ridge in wildtype, *brca2*^{Q658X} heterozygous, and *brca2*^{Q658X} homozygous embryos. (B) Immunohistochemistry for cleaved caspase-3 in juvenile gonads from wildtype and *brca2*^{Q658X} homozygotes. Multiple apoptotic cells are present in gonads from juvenile *brca2*^{Q658X} homozygotes. (C) Homozygous *tp53*^{M214K} mutation rescues ovarian development in *brca2*^{Q658X} homozygotes, but female *brca2*^{Q658X} homozygous;*tp53*^{M214K} homozygous zebrafish develop binucleate oocytes (inset). CC3, anti-cleaved caspase-3; neg, negative control (secondary antibody only). Scale bars, 50 µm (B); 500 µm (C); 100 µm (C, inset).

localization in wildtype, *brca2*^{Q658X} heterozygotes, or *brca2*^{Q658X} homozygotes (Fig. 4.1A). Similar results were observed at 4 dpf (Appendix X).

While the *brca2*^{Q658X} mutation did not appear to affect embryonic PGC designation, germ cell survival was impaired in juvenile gonads from *brca2*-mutant zebrafish. Immunohistochemistry for cleaved caspase-3 on gonads from *brca2*^{Q658X} homozygotes at 28 dpf demonstrated multiple apoptotic cells (Fig. 4.1B). In contrast, apoptotic cells were rare in gonads from wildtype zebrafish at 28 dpf (Fig. 4.1B).

Homozygous tp53 mutation rescues ovarian development in brca2^{Q658X}*-mutant zebrafish.*

To determine how germ cell apoptosis might impact gonad development in *brca2*-mutant zebrafish, *brca2*^{Q658X} heterozygotes were crossed with *tp53*^{M214K} homozygotes (70). *brca2*^{Q658X} heterozygous;*tp53*^{M214K} heterozygous zebrafish were subsequently incrossed, and progeny were raised to adulthood.

Histologic examination of the gonads from seven adult *brca2*^{Q658X} homozygous;*tp53*^{M214K} homozygous zebrafish that died or were euthanized due to tumor development revealed that two zebrafish had developed ovaries (Fig. 4.1C). Oogenesis appeared complete in female *brca2*^{Q658X} homozygous;*tp53*^{M214K} homozygous zebrafish. However, the ovaries contained multiple binucleate oocytes (Fig. 4.1C, inset), which were not observed in female *brca2*^{Q658X} heterozygous;*tp53*^{M214K} homozygous or *tp53*^{M214K} homozygous zebrafish.

Adult phenotypically male *brca2*^{Q658X} homozygous;*tp53*^{M214K} homozygous zebrafish were outcrossed to fertile wildtype female zebrafish, but eggs collected from these crosses were unfertilized. Attempts to breed phenotypically female *brca2*^{Q658X} homozygous;*tp53*^{M214K} homozygous zebrafish were unsuccessful.

PGC transplant rescues fertility in brca2^{Q658X}*-mutant zebrafish.*

To determine whether *brca2*-mutant stromal cells impact gonad development, PGCs were transplanted into embryos from incrosses of *brca2*^{Q658X} heterozygous zebrafish (Fig. 4.2). The endogenous PGCs in transplanted embryos were ablated via injection with dnd MO (84) prior to transplant. To confirm successful PGC ablation in recipient embryos, a subset of embryos were screened by WISH for *vasa* after injection with dnd MO (Appendix XI). PGCs were collected from *tg(bactin2:EGFP)zp5* zebrafish, which express EGFP under the control of the β-actin promoter (146). To maximize visibility of transplanted cells, donor embryos were injected with Oregon Green dextran conjugate (labeling all cells) and tdTomato-nos1-3'UTR RNA (labeling PGCs) (Fig. 4.3A).

Transplanted embryos were screened at 24 or 48 hpf for the presence of donor cells. Since the tdTomato-nos1-3'UTR RNA construct was not consistently detectable in donor embryos or transplanted embryos, embryos were screened for Oregon Green-positive cells that localized to the embryonic genital ridge (Fig. 4.3B). As

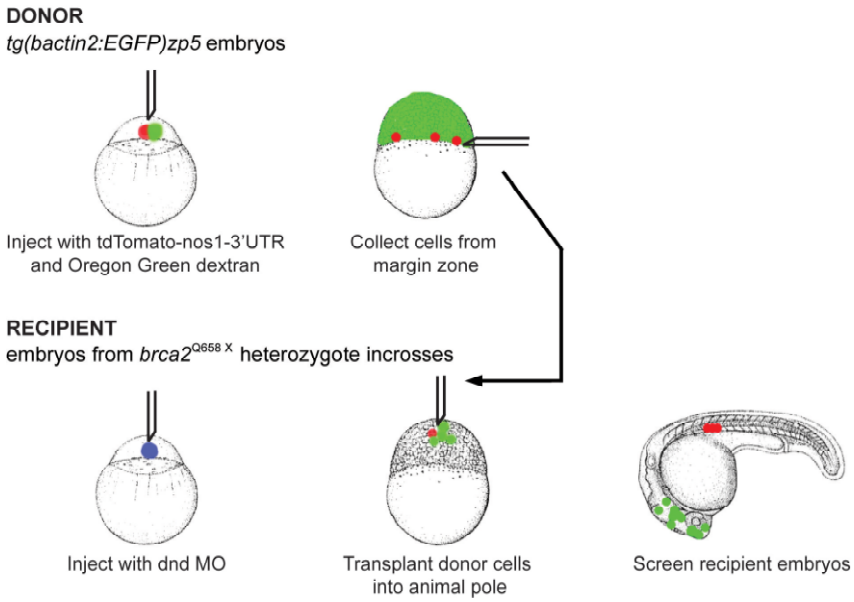

Fig. 4.2 Primordial germ cell transplant method. Donor embryos are collected from incrosses of *tg(bactin2:EGFP)zp5* zebrafish and coinjected at the 1-cell stage with tdTomato-nos1-3'UTR RNA and Oregon Green dextran conjugate. Recipient embryos are collected from incrosses of *brca2*^{Q658X} heterozygous zebrafish and injected at the 1-cell stage with dnd MO. When donor and recipient embryos have reached mid-blastula stage (2.5 – 3 hpf), donor cells are collected from the margin zone and injected into the animal pole of recipient embryos. Transplanted embryos are screened at 24 or 48 hpf for localization of transplanted germ cells to the embryonic genital ridge. Transplanted somatic cells do not migrate from the animal pole, and are incorporated into cephalic tissues.

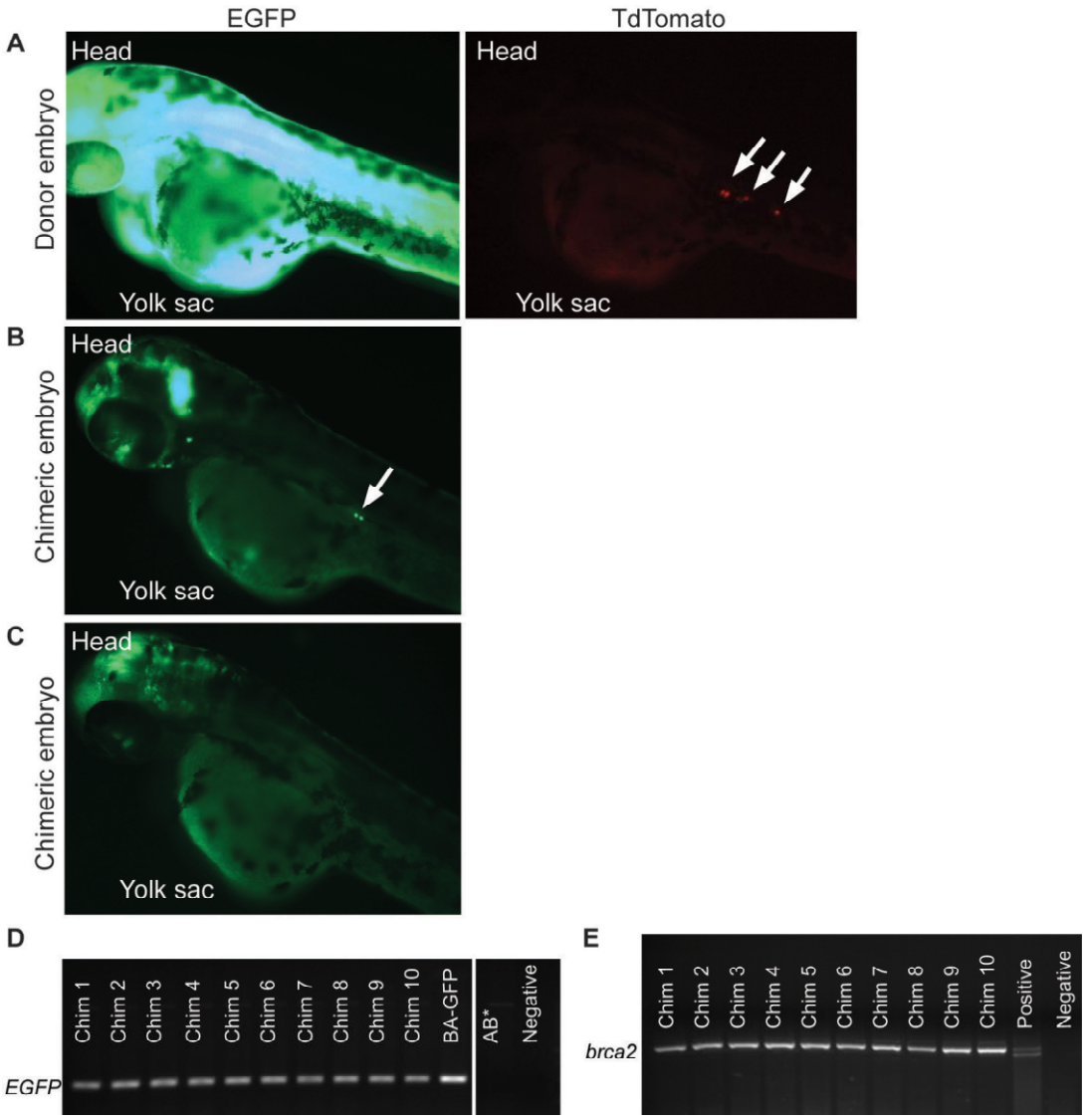

Fig. 4.3 Primordial germ cell transplantation and screening of chimeric embryos. (A) Donor embryos are injected with Oregon Green dextran (OG), labeling all cells, and tdTomato-nos1-3'UTR RNA, labeling primordial germ cells (white arrows). (B) Chimeric embryo with OG-positive primordial germ cells localized at the genital ridge (white arrow) and OG-positive somatic cells in the head and eye. (C) Chimeric embryo with OG-positive somatic cells only in the head and eye. (D) Genotyping for the *bactin2:EGFP* transgene in embryos from a cross of an adult chimeric *brca2*^{Q658X} homozygote and fertile wildtype female zebrafish shows that germ cells are derived from *tg(bactin2:EGFP)zp5* donors. Redundant controls have been removed from the gel image (white line). (E) Genotyping for the *brca2*^{Q658X} mutation in embryos from a cross of an adult chimeric *brca2*^{Q658X} homozygote and fertile wildtype female zebrafish shows that germ cells do not carry the *brca2*^{Q658X} mutation. Chim, embryo DNA from chimeric zebrafish-wildtype cross; BA-GFP, *tg(bactin2:EGFP)zp5* embryo DNA; AB*, embryo DNA from wildtype AB* zebrafish; Positive, DNA from a *brca2*^{Q658X} heterozygote; Negative, water control.

transplants were performed into the animal pole, somatic cells did not migrate, and remained in cephalic tissues in transplanted embryos (Fig. 4.3B, C).

Chimeric embryos were raised to adulthood and genotyped for the *brca2*^{Q658X} mutation. Chimeric *brca2*^{Q658X} heterozygotes (n = 12) and homozygotes (n = 8) were crossed to fertile wildtype AB* zebrafish to screen for fertility, and embryos were collected for analysis (Table 4.1). Chimeric wildtype zebrafish were not screened for fertility (n = 11). Fertile chimeras included one male *brca2*^{Q658X} homozygote, two male *brca2*^{Q658X} heterozygotes, and two female *brca2*^{Q658X} heterozygotes (Table 4.1). Embryos from crosses of chimeric and wildtype zebrafish carried the *bactin2:EGFP* transgene (Fig. 4.3D) and were wildtype for *brca2* (Fig. 4.3E). These data indicate successful ablation of endogenous germ cells and replacement with germ cells from *tg(bactin2:EGFP)zp5* donors in chimeric zebrafish. While PGC transplantation rescued fertility in one *brca2*^{Q658X} homozygote, this chimeric zebrafish was male.

brca2^{Q658X}*-mutant zebrafish are predisposed to testicular neoplasia.*

Since *BRCA2* mutations in humans are predominantly associated with cancer development in reproductive tissues, the testes from aged adult *brca2*^{Q658X} homozygotes were screened histologically for tumor development. Between ten and sixteen months of age, four out of thirteen (31%) of *brca2*^{Q658X} homozygotes developed testicular neoplasia (Fig. 4.4). Testicular tumors were of both somatic cell and germ cell origin and included undifferentiated stromal cell tumor (Fig. 4.4A, B), papillary cystadenoma (Fig. 4.4C), and seminoma (Fig. 4.4D). Additional changes in

	Adult chimera genotype and phenotype			Embryo genotype	
Specimen	***brca2*^{Q658X} genotype**	**Sex**	**Fertile/Sterile**	***tg(bactin2:EGFP)zp5***	***brca2*^{Q658X}**
1	+/-	M	F	Y	+/+
2	+/-	F	F	Y*	+/+
3	+/-	F	F	Y	+/+
4	+/-	M	F	Y	+/+
5	+/-	M	S		
6	+/-	M	S		
7	+/-	M	S		
8	+/-	M	S		
9	+/-	M	S		
10	+/-	M	S		
11	+/-	M	S		
12	+/-	M	S		
13	-/-	M	F	Y	+/+
14	-/-	M	S		
15	-/-	M	S		
16	-/-	M	S		
17	-/-	M	S		
18	-/-	M	S		
19	-/-	M	S		
20	-/-	M	S		

Table 4.1 Genotype and phenotype of chimeric *brca2*^{Q658X}-mutant zebrafish. Adult chimeric zebrafish were genotyped and subsequently outcrossed to fertile wildtype AB* zebrafish. Fertilized embryos collected from these crosses were genotyped for the *bactin2:EGFP)zp5* transgene and for the *brca2*^{Q658X} mutation to confirm ablation of endogenous PGCs and successful PGC transplant.

*The majority of embryos from this specimen were negative for the *bactin2:EGFP)zp5* transgene (40 embryos were genotyped individually from this cross). After beginning PGC transplants, it was found that small numbers of embryos from incrosses of tg(*bactin2:EGFP)zp5* zebrafish did not carry the (*bactin2:EGFP)zp5* transgene. In specimen 3, it is presumed that most of the transplanted donor PGCs did not carry the (*bactin2:EGFP)zp5* transgene. However, the endogenous germ cells for this specimen were successfully ablated, since all embryos derived from a cross to wildtype AB zebrafish were wildtype for the *brca2*^{Q658X} mutation.

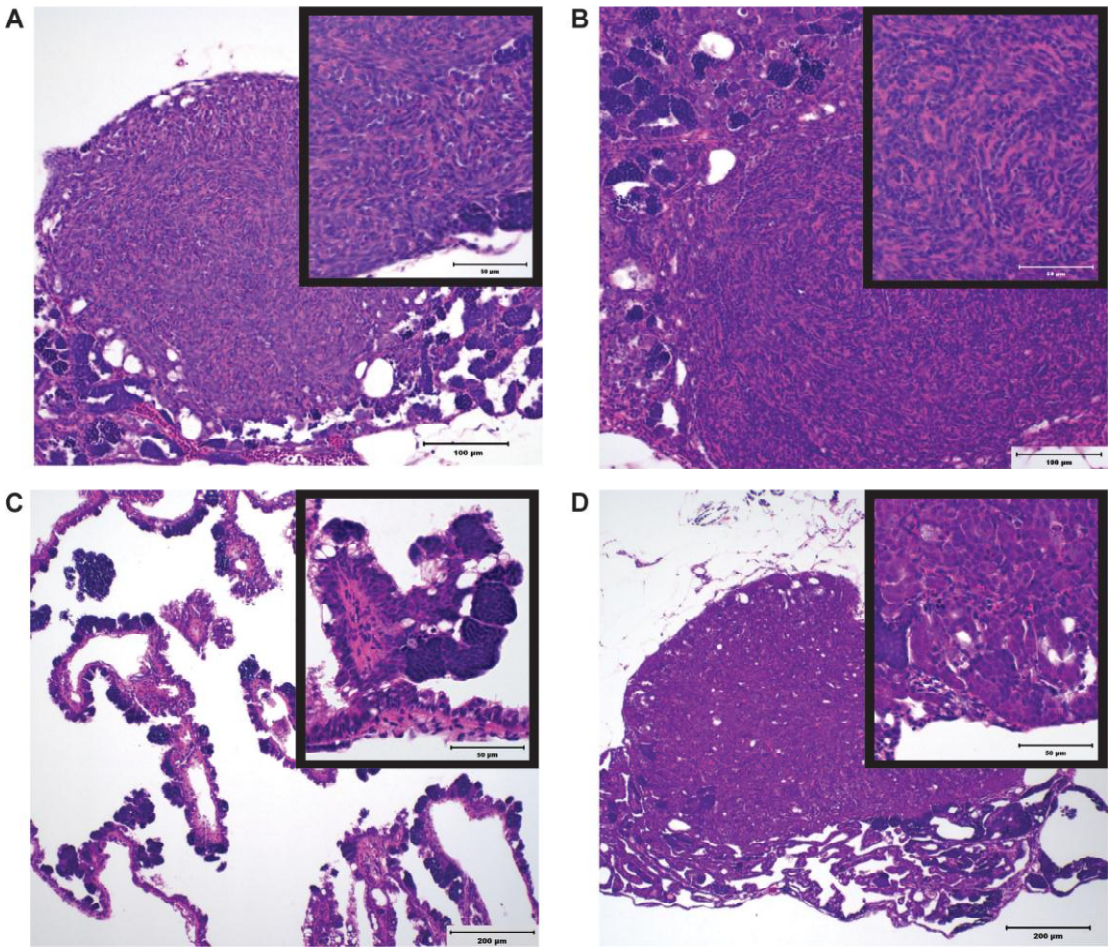

Fig. 4.4 *brca2*^{Q658X} homozygotes are predisposed to testicular neoplasias. (A) Undifferentiated stromal cell tumor from a *brca2*^{Q658X} homozygote. Neoplastic spindle cells form irregular bundles (inset). (B) Undifferentiated stromal cell tumor from a *brca2*^{Q658X} homozygote. Neoplastic spindle cells form irregular bundles around poorly defined tubular structures (inset). (C) Papillary cystadenoma from a *brca2*^{Q658X} homozygote. Neoplastic cells form papillary projections and are often vacuolated (inset). (D) Seminoma from a *brca2*^{Q658X} homozygote. Neoplastic cells have a high nuclear:cytoplasmic ratio and prominent nuclei and nucleoli (inset). Scale bars, 100 µm (50 µm in insets).

testes from aged adult *brca2*^{Q658X} homozygotes included germ cell hyperplasia and dysplasia and segmental testicular degeneration (Appendix XII).

In contrast, no testicular tumors were observed in age-matched cohorts of wildtype (n = 12) and *brca2*^{Q658X} heterozygotes (n = 12). Hyperplastic, dysplastic, and degenerative changes observed in testes from *brca2*^{Q658X} homozygotes were not seen in testes from wildtype and *brca2*^{Q658X} heterozygotes.

Collaborative effects of tp53 and brca2 mutations on tumorigenesis.

Analysis of tumorigenesis in zebrafish from an incross of *brca2*^{Q658X} heterozygous;*tp53*^{M214K} heterozygous zebrafish revealed that combined mutations in *brca2* and *tp53* accelerated the onset of tumor development (Fig. 4.5A and Table 4.2). The mean age at tumor onset was statistically significantly lower in both *brca2*^{Q658X} homozygous;*tp53*^{M214K} homozygous zebrafish and *brca2*^{Q658X} heterozygous;*tp53*^{M214K} homozygous zebrafish when compared to the tp53M214K homozygous parent line (Table 4.2). Of all tumor-bearing zebrafish collected from the *brca2*^{Q658X} heterozygous;*tp53*^{M214K} heterozygous zebrafish incross, only two were *brca2*^{Q658X} wildtype; *tp53*^{M214K} homozygous zebrafish, and the ages at tumor onset were similar to those observed in the tp53M214K homozygous parent line (Table 4.3).

The majority of tumors observed in both *brca2*^{Q658X} heterozygous;*tp53*^{M214K} homozygous zebrafish and *brca2*^{Q658X} homozygous;*tp53*^{M214K} homozygous zebrafish were malignant peripheral nerve sheath tumors (Table 4.3). Interestingly, in

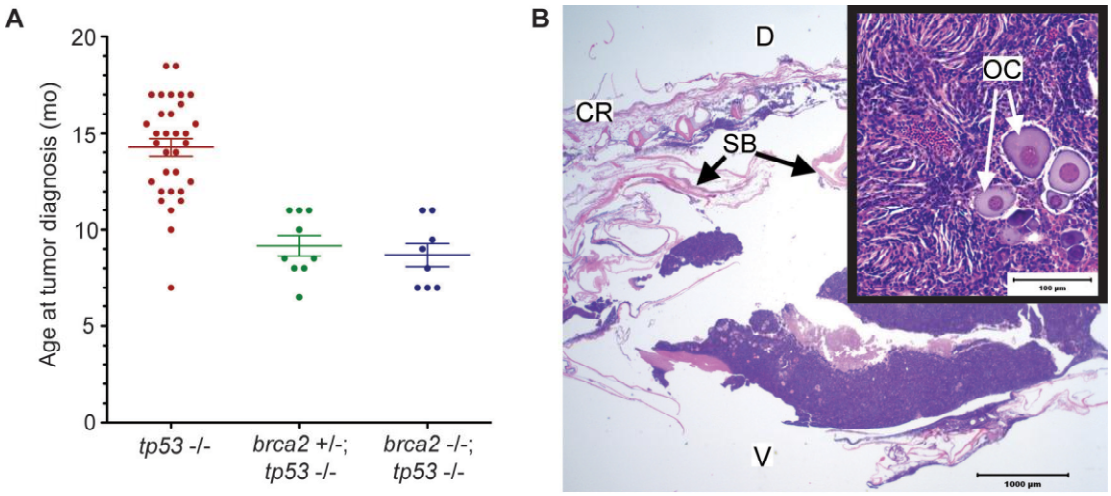

Fig. 4.5 Concomitant tp53 mutation accelerates tumorigenesis in both *brca2*^{Q658X} heterozygous and *brca2*^{Q658X} homozygous zebrafish. (A) Age at tumor onset is significantly lower in both *brca2*^{Q658X} homozygous;*tp53*^{M214K} homozygous zebrafish and *brca2*^{Q658X} heterozygous;*tp53*^{M214K} homozygous zebrafish compared to the *tp53*^{M214K} homozygous zebrafish parent line. (B) The ovary is a primary site for tumor development in *brca2*^{Q658X} heterozygous;*tp53*^{M214K} homozygous zebrafish, with oocyte entrapment (inset). OC, oocyte; CR, cranial; D, dorsal; V, ventral; SB, swim bladder. Scale bars, 1000 µm (B); 100 µm (B, inset).

	***brca2*^{Q658X} -/-;*tp53*^{M214K} -/-**	***brca2*^{Q658X} +/-;*tp53*^{M214K} -/-**	**tp53 ^{M214K} -/-**
Age at tumor onset (months)	7.0 7.0 8.0 7.0 9.0 9.5 11.0 11.0	6.5 8.0 8.0 8.5 8.5 10.0 11.0 11.0 11.0	7.0 10.0 11.0 11.5 11.5 12.0 12.0 12.0 12.5 12.5 13.0 13.0 14.0 14.0 14.5 14.5 15.0 15.0 15.0 15.0 15.5 15.5 16.0 16.0 16.5 17.0 17.0 17.0 17.0 17.0 18.5 18.5
Total	8	9	32
Mean age (months)	8.7	9.2	14.3

	***brca2*^{Q658X} -/-;*tp53*^{M214K} -/-**	***brca2*^{Q658X} +/-;*tp53*^{M214K} -/-**	
tp53 ^{M214K} -/-	$p < 0.0001$	$p < 0.0001$	
***brca2*^{Q658X} +/-; *tp53*^{M214K} -/-**	$p = 0.5643$		

Table 4.2 Analysis of ages at tumor onset in *brca2*^{Q658X}-mutant zebrafish with concomitant *tp53* mutation. Ages at tumor onset were statistically significantly lower in *brca2*^{Q658X} homozygous;*tp53*^{M214K} homozygous zebrafish, *brca2*^{Q658X} heterozygous;*tp53*^{M214K} homozygous zebrafish compared to the parent line of *tp53*^{M214K} homozygous zebrafish. Data sets were compared by unpaired t-tests (GraphPad Prism Version 5.0).

***brca2*^{Q658X} -/-; *tp53*^{M214K} -/-**				
Specimen	**Age (mo)**	**Sex**	**Diagnosis**	**Primary site(s)**
1	7.0	M	1) MPNST 2) MPNST	1) Coelom 2) Eye
2	7.0	F	1) MPNST	1) Ovary
3	7.0	M	1) MPNST 2) MPNST	1) Coelom 2) Eye
4*	8.0	ND	1) Eye mass with proptosis	1) Eye
5	9.0	M	1) MPNST	1) Coelom
6	9.5	ND	1) MPNST 2) MPNST 3) Cutaneous hemangiosarcoma	1) Coelom 2) Subpharyngeal 3) Tail
7	11.0	M	1) Seminoma	1) Testis
8	11.0	F	1) Rhabdomyosarcoma	1) Head
***brca2*^{Q658X} +/-; *tp53*^{M214K} -/-**				
Specimen	**Age (mo)**	**Sex**	**Diagnosis**	**Primary site(s)**
9	6.5	F	1) MPNST	1) Coelom
10	8.0	F	1) MPNST	1) Ovary
11	8.0	F	1) MPNST	1) Ovary
12	8.5	F	1) MPNST 2) MPNST	1) Coelom 2) Eye
13	8.5	M	1) Sarcoma	1) Coelom
14	10.0	F	1) Sarcoma	1) Ovary
15	11.0	M	1) MPNST 2) MPNST	1) Coelom 2) Eye
16	11.0	F	1) MPNST	1) Coelom
17	11.0	F	1) Intestinal adenocarcinoma 2) Cutaneous hemangioma	1) Intestine 2) Body wall
***brca2*^{Q658X} +/+; *tp53*^{M214K} -/-**				
Specimen	**Age (mo)**	**Sex**	**Diagnosis**	**Primary site(s)**
18	10.0	F	1) Primitive neuroectodermal tumor	1) Coelom
19	11.0	F	1) MPNST	1) Body wall
***tp53*^{M214K} -/- parent line**				
Specimen	**Age (mo)**	**Sex**	**Diagnosis**	**Primary site(s)**
20	7.0	F	1) MPNST	1) Liver
21	10.0	F	1) MPNST	1) Caudal coelom/ovary
22	11.0	F	1) MPNST	1) Caudal coelom/ovary
23	11.5	M	1) Rhabdomyosarcoma	1) Tail
24	11.5	F	1) MPNST	1) Coelom
25	12.0	M	1) MPNST 2) Rhabdomyosarcoma	1) Eye 2) Tail

Table 4.3 Histologic analyses of tumor types and primary sites of development in *brca2*^{Q658X}-mutant zebrafish with concomitant *tp53* mutation. Tumors in zebrafish from an incross of *brca2*^{Q658X} heterozygous;*tp53*^{M214K} heterozygous zebrafish and in a subset of zebrafish from the parent line of *tp53*^{M214K} homozygous zebrafish were evaluated histologically. MPNST, malignant peripheral nerve sheath tumor; ND, not determined. *Specimen 4 was not available for histologic analysis.

three out of seven female *brca2*^{Q658X} heterozygous;*tp53*^{M214K} homozygous zebrafish, the ovaries appeared to be the primary site for tumor development (Fig. 4.5B). Tumor development in one of two *brca2*^{Q658X} homozygous;*tp53*^{M214K} homozygous female zebrafish also appeared to primarily involve the ovary (Table 4.3). Primary tumorigenesis in the gonads was not typical of a subset of *tp53*^{M214K} homozygous zebrafish evaluated histologically (Table 4.3), and was not reported in characterization of the *tp53*^{M214K} zebrafish line (70).

While malignant peripheral nerve sheath tumors predominated, a variety of other malignancies were observed in both *brca2*^{Q658X} heterozygous;*tp53*^{M214K} homozygous zebrafish and zebrafish *brca2*^{Q658X} homozygous;*tp53*^{M214K} homozygous zebrafish (Fig. 4.6). Frequently, one or more zebrafish developed tumors in more than one anatomic location and/or developed more than one type of tumor (Table 4.3).

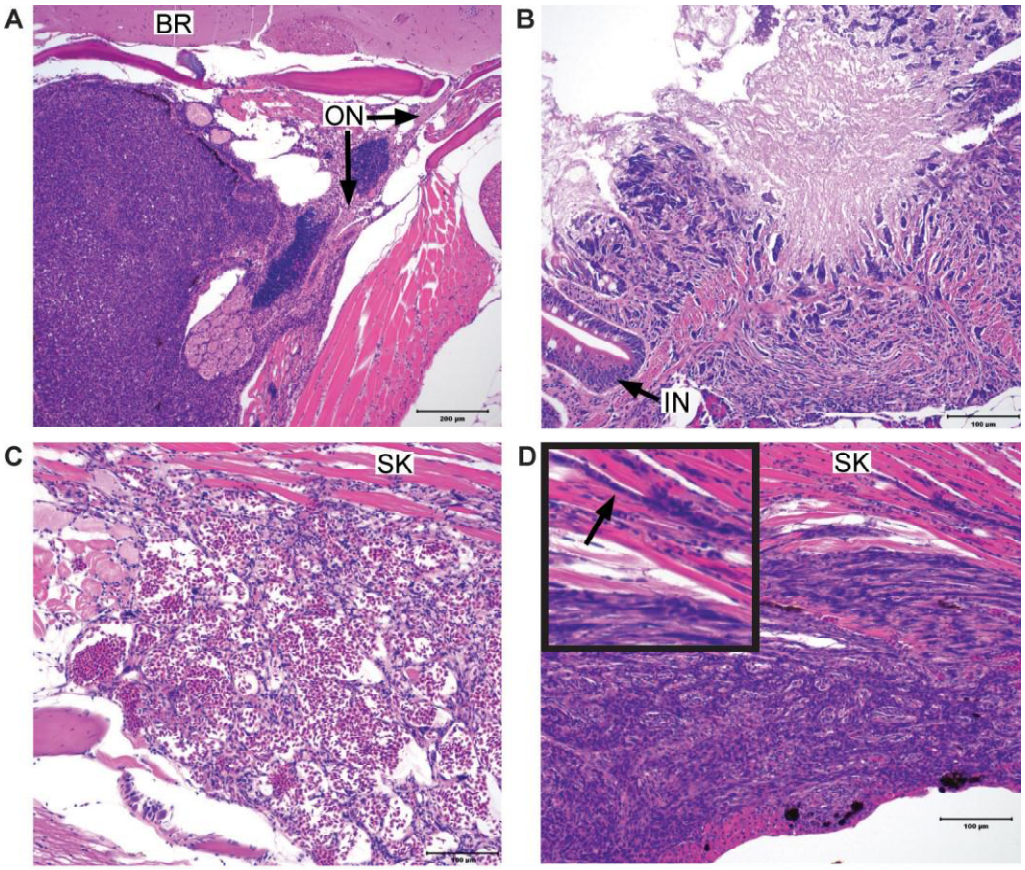

Fig. 4.6 *brca2*^{Q658X}-mutant zebrafish with concomitant homozygous *tp53* mutation develop a variety of solid tumors. (A) Intraocular malignant peripheral nerve sheath tumor with invasion around the optic nerve in a *brca2*^{Q658X} homozygous;*tp53*^{M214K} homozygous zebrafish. (B) Intestinal adenocarcinoma in a *brca2*^{Q658X} heterozygous;*tp53*^{M214K} homozygous zebrafish. (C) Intramuscular hemangiosarcoma in a *brca2*^{Q658X} homozygous;*tp53*^{M214K} homozygous zebrafish. (D) Rhabdomyosarcoma in a *brca2*^{Q658X} homozygous;*tp53*^{M214K} homozygous zebrafish with characteristic strap cells (inset, arrow). BR, brain; ON, optic nerve; IN, intestinal epithelium, SK, skeletal muscle. Scale bars, 200 µm (A); 100 µm (B, C, D).

Discussion

Investigation of the *brca2*^{Q658X} mutation in zebrafish revealed that *brca2* is dispensable for embryonic survival, but is critical for spermatogenesis and ovarian development. Since BRCA2 is known to be required in germ cells for meiotic recombination, meiotic failure in adult male *brca2*^{Q658X} homozygous testes demonstrates a conserved role for brca2 in germ cell maturation. However, little is known about the participation of BRCA2 in primordial germ cell-stromal cell interactions in the immature gonad. Thorough studies of gonadal morphogenesis are limited in *Brca2*-mutant mouse models (58), as well as in patients with *BRCA2* mutations (130). Thus, the *brca2*^{Q658X}-mutant zebrafish line provides a unique opportunity for investigating the effects of *brca2* mutation on gonad development.

Previous studies in zebrafish indicate that primordial germ cells (PGCs) are required for ovarian development in zebrafish. All-male populations of zebrafish develop when PGCs fail to migrate to the embryonic genital ridge (83, 84). Furthermore, germ cell depletion by gene mutation or knockdown generates predominantly male zebrafish populations with structurally and functionally male gonads (84, 85). However, WISH for the germ cell marker *vasa* indicated that PGC designation and colonization of the genital ridge were unimpaired in *brca2*-mutant zebrafish embryos. Therefore, failure of ovarian development in *brca2*^{Q658X} homozygotes suggests a disruption in stromal cell-germ cell interactions at later stages of gonad development.

Immunohistochemistry for cleaved caspase-3 in juvenile *brca2*-mutant zebrafish at 30 days of age demonstrated multiple apoptotic cells in gonads from *brca2*^{Q658X} homozygotes. Furthermore, homozygous *tp53* mutation rescued ovarian development in a small number of *brca2*^{Q658X} homozygotes. Together these data indicate that germ cell apoptosis is an important contributor to the failure of ovarian development observed in *brca2*^{Q658X} homozygotes. Apoptosis of perinucleolar oocytes is a normal occurrence during the transformation from juvenile ovaries to testes in male zebrafish (80). Numerous apoptotic cells may be observed in gonads of presumptive males, in contrast to presumptive females (80). This suggests that apoptotic loss of germ cells in the developing gonad may be an important signal for directing testicular differentiation in zebrafish.

As discussed in Chapter 3, meiotic arrest and subsequent germ cell degeneration is not associated with lack of ovarian development in mammalian species. However, some studies in mammalian species suggest that embryonic germ cells may play a role in maintaining the ovarian phenotype. Various animal models for ovarian sex reversal have demonstrated development of Sertoli-like cells and seminiferous-like cords in embryonic mammalian ovaries (147). Under these circumstances, development of male stromal elements was preceded by extensive germ cell loss (147). Thus, while the effects of germ cell depletion on zebrafish ovarian development are relatively more profound, germ cell survival in mammalian embryonic gonads is important for maintaining ovarian differentiation.

To investigate the role for primordial germ cells in gonad development in *brca2*^{Q658X} homozygotes, PGC transplant experiments were performed to replace endogenous, *brca2*-mutant germ cells with meiotically competent germ cells. PGC transplantation into embryos from incrosses of *brca2*^{Q658X} heterozygotes resulted in low numbers of fertile adult zebrafish. The use of *tg(bactin2:EGFP)zp5* embryos as donors was important in confirming that endogenous germ cells had been ablated and replaced by donor germ cells. While transplantation of meiotically competent PGCs rescued fertility in *brca2*^{Q658X} homozygotes, female chimeric *brca2*^{Q658X} homozygotes have yet to be recovered from these experiments. Previous studies of PGC transplantation in zebrafish have demonstrated that male populations of chimeric zebrafish are generated when single PGCs are transplanted to recipient embryos (148). As ovarian development in *brca2*^{Q658X} homozygotes was rescued by homozygous *tp53* mutation, failure to rescue ovarian development by germ cell transplantation may indicate that few PGCs were transplanted in initial transplant experiments.

Interestingly, multiple binucleate oocytes were present in the rescued *brca2*^{Q658X} homozygous;*tp53*^{M214K} homozygous ovaries. A role for *BRCA2* in cytokinesis has been previously suggested, with *BRCA2* knockdown or loss resulting in incomplete cell division (149). Aberrant or delayed cytokinesis has been described in embryonic fibroblasts derived from *Brca2*-deficient mice as well as in primary fibroblast cultures collected from human carriers of *BRCA2* mutations (149, 150). Failure of cytokinesis was not reported in cultured BRCA2-deficient cells (149, 150), in contrast to the binucleate oocytes observed in the rescued *brca2*^{Q658X} homozygous;*tp53*^{M214K}

homozygous ovaries. While the effects of *BRCA2* on cytokinesis remain controversial (151), the findings reported herein suggest an association between *BRCA2* mutation and aberrant cytokinesis.

The impact of *BRCA2* mutation on cancer susceptibility, particularly in reproductive tissues, is also conserved in zebrafish. In wildtype populations, aged male zebrafish demonstrate a relatively high frequency of seminomas (152, 153). Additionally, a high incidence of germ cell tumors has been reported in the *lamc1*^{cz61}-mutant zebrafish line, although the mutant locus associated with tumorigenesis was not identified (154). Adult *brca2*^{Q658X} homozygotes exhibited a propensity for testicular tumors that was not observed in age-matched siblings. Unlike previous reports of testicular tumorigenesis in zebrafish, *brca2*^{Q658X} homozygotes developed testicular tumors that were predominantly of somatic cell origin. In comparison, ovarian cancers in women with *BRCA2* mutations also arise from somatic cell populations (8-11). Thus, these findings in *brca2*^{Q658X} homozygotes demonstrate a conserved and primary role for *BRCA2* mutation in tumorigenesis of reproductive tissues.

Tumorigenesis in mice with hypomorphic or C-terminal mutations in *Brca2* has infrequently involved reproductive tissues. The most common tumors described in viable *Brca2*-mutant mice are lymphomas and carcinomas of the gastrointestinal tract (52, 54-56). A spectrum of tumor types was also reported in a *Brca2*-mutant rat model, although female Brca2-mutant rats did develop ovarian tumors (59). The cause for this interspecies variation is unclear, but may relate to differences in cancer

susceptibility, methods used to generate *BRCA2* mutation, and/or variability in the location of the *BRCA2* mutation in each model.

Concomitant homozygous *tp53*^{M214K} mutation accelerated tumorigenesis in multiple tissues in both *brca2*^{Q658X} heterozygotes and *brca2*^{Q658X} homozygotes. The majority of zebrafish developed malignant peripheral nerve sheath tumors, similar to those described previously in *tp53*^{M214K} homozygotes (70). However, female *brca2*^{Q658X} heterozygous;*tp53*^{M214K} homozygous and *brca2*^{Q658X} homozygous;*tp53*^{M214K} homozygous zebrafish exhibited a tendency for primary tumor development in the ovary, which was not typical of female zebrafish with homozygous *tp53*^{M214K} mutation alone (70). These observations, while limited in number, suggest a specific role for *brca2* mutation in gonad tumorigenesis, and imply collaborative effects of *tp53* and *brca2* mutations on tumorigenesis. Interestingly, combined mutations in *Brca2* and *Tp53* in mouse models have also been shown to reduce survival and increase tumor incidence (51, 57).

In humans, somatic mutations in *p53* are one of the most common genetic aberrations observed in ovarian cancer cells (19, 20). Recent studies have identified a so-called "p53 signature" lesion, referring to expression of p53 in morphologically normal epithelia, as an indication of *p53* mutation and an important precursor to malignant transformation (155). The p53 signature has been described with similar frequency in ovarian and tubular tissues from women with and without mutations in the *BRCA* genes (156), although some studies indicate a higher incidence of *p53* mutation in

BRCA-associated ovarian cancers (157). A recent model for the development of *BRCA*-associated ovarian cancer suggests that *p53* mutation in serosal or fimbrial epithelial cells occurs early in neoplastic transformation, and overt carcinogenesis is preceded by loss of heterozygosity for *BRCA1* or *BRCA2* (20). These studies thus indicate that *p53* mutation is an important event in *BRCA2*-associated carcinogenesis, similar to what has been observed in *brca2*-mutant zebrafish.

Several *in vitro* studies indicate that p53 physically interacts with multiple proteins involved in homologous and meiotic recombination, including RAD51, DMC1 and BRCA2 (158, 159). These interactions point to a mechanism for cell cycle control, perhaps providing the opportunity to detect abnormal synapses or recombinatorial events (158, 159). These findings suggest that aberrant or incomplete DNA repair occurring in mitosis or meiosis in BRCA2-deficient cells may persist with concurrent *p53* mutation, supporting the concept that mutations in *p53* and *BRCA2* act synergistically during carcinogenesis.

In summary, these studies demonstrate that *tp53*-mediated germ cell apoptosis plays a significant role in gonad development in *brca2*-mutant zebrafish. Meiotic failure in germ cells acts may act as an additional influence in this process. The role for *brca2* in cytokinesis is unclear; however, this model provides a unique opportunity to further explore this issue. Importantly, these studies indicate a conserved role for *brca2* in tumors of reproductive tissues, and support the concept that *tp53* mutation is a critical event in *brca2*-associated carcinogenesis.

Chapter 5: Conclusion and Discussion

Known risk factors for human ovarian cancer are few, and some risk factors, such as aging and reproductive history, are nonspecific or poorly understood (3, 4). A family history of breast or ovarian cancer remains the most well-defined predictor of ovarian cancer risk (18). The majority of these hereditary cases are associated with mutations in a small number of genes, which includes *BRCA2* (12, 15, 18). While mutations in *BRCA2* clearly confer an increased risk for ovarian cancer (28), the mechanistic link between *BRCA2* mutation and these tumors is not understood.

BRCA2 is required for homologous recombination following double-strand DNA breaks (31). In somatic cells, this process is necessary for optimal error-free repair after DNA damage occurs (30-32). Thus, the pathogenesis of *BRCA2*-associated carcinogenesis is thought to involve progressive accumulation of unrepaired or misrepaired DNA (30-32). *In vitro* data support this concept; BRCA2-deficient cell lines exhibit many genetic aberrations that are indicative of defects in DNA repair (32, 37). *In vivo* data from traditional murine models has been limited by early embryonic lethality in *Brca2* homozygous mutants in many studies (see Chapter 1, Table 1.2). Individual reports describing viable *Brca2*-mutant mice and rats have confirmed that mutations in *Brca2* are associated with increased cancer susceptibility (51, 55, 56, 59, 60). However, these studies have failed to further define the specific association between *BRCA2* mutation and reproductive tumors.

We developed the zebrafish as a novel model for studying *brca2* mutation *in vivo*. These studies were designed to investigate the effects of *brca2* mutation on embryogenesis, development, gonadal pathophysiology, and cancer susceptibility in zebrafish. The *brca2*-mutant zebrafish line described herein (*brca2*^{Q658X}) was derived from an ENU-mutagenized library, and carries a nonsense mutation in *brca2* exon 11. This mutation is similar in location and type to deleterious *BRCA2* mutations in women with hereditary breast and/or ovarian cancer (17). In preparation for studies of *brca2*^{Q658X}-mutant zebrafish, *brca2* expression during embryogenesis in wildtype AB* zebrafish was examined. Histologic, immunohistochemical, and in situ hybridization studies of juvenile gonads, ovaries, and testes from wildtype AB* zebrafish were also performed in order to establish a baseline for studying these tissues in *brca2*^{Q658X}-mutant zebrafish.

Since *Brca2* mutation profoundly affects embryonic development and survival in mouse models, we examined the expression of *brca2* throughout embryogenesis. The pattern of *brca2* expression in zebrafish embryos was similar to that observed in mouse embryos (115-117), suggesting that *brca2* may play a conserved role during embryogenesis in animal species. However, the source of this RNA (maternal or zygotic) during embryogenesis may be a critical difference in these species. Zebrafish embryos, which rely on maternal RNA until approximately the 1000 cell stage (119), have high levels of *brca2* RNA throughout embryogenesis. This indicates that abundant maternally provided *brca2* RNA is available from the earliest stages of development. In contrast, zygotic transcription in mammalian embryos

begins at the one or two-cell stage (120, 121). Because zebrafish embryos can rely on maternal RNA until a later developmental stage, the effects of *BRCA2* mutation may be more severe during embryogenesis in mammals.

Studies of *brca2*^{Q658X}-mutant zebrafish embryos indicate that maternal RNA for *brca2* may indeed be protective. No developmental phenotype was observed in association with heterozygous or homozygous *brca2*^{Q658X} mutation in zebrafish embryos. However, embryonic viability in *brca2*^{Q658X}-mutant zebrafish could also indicate reliance on other DNA repair mechanisms. Zebrafish embryos are capable of highly efficient and accurate DNA repair by processes other than homologous recombination (160). Thus, survival of *brca2*-deficient zebrafish embryos may be attributable to this characteristic as well.

Analyses of juvenile and adult *brca2*^{Q658X} homozygotes indicate that *brca2* is required for ovarian development in zebrafish. Adult *brca2*^{Q658X} homozygotes were all male, and exhibited aberrant spermatogenesis and testicular hypoplasia characterized by meiotic arrest and clonal apoptosis of spermatocytes. Histologic examination of germ cell morphology in *brca2*^{Q658X} homozygous testes showed that spermatogenesis was arrested after formation of primary spermatocytes. Primary spermatocytes enter and complete meiosis I during spermatogenesis (75, 76); thus, meiotic arrest at this stage in *brca2*^{Q658X} homozygotes is compatible with the known role for *brca2* in meiotic prophase I. These findings demonstrate that the requirement for *brca2* during meiosis is conserved in zebrafish.

Studies of juvenile *brca2*^{Q658X} homozygotes showed that *brca2* mutation prevents oocyte development during gonadogenesis, a process that normally occurs in all zebrafish during the juvenile period (77, 79). In addition, *brca2*^{Q658X} homozygous mutation is associated with increased germ cell apoptosis in juvenile gonads. These studies suggest two potential mechanisms for failure of ovarian development in *brca2*^{Q658X} homozygotes: 1) failure for germ cells to enter meiosis and form perinucleolar oocytes in the juvenile gonads; and 2) extensive germ cell apoptosis in the juvenile gonads. Both hypotheses imply that alterations in germ cell function or survival critically impact gonad development in zebrafish.

Evidence from animal models indicates that the onset of meiosis in embryonic germ cells is a function of somatic cell-germ cell signaling. Early studies of embryonic gonad development demonstrated that female germ cells cultured with embryonic male genital ridges fail to begin meiosis (132). In contrast, male germ cell cultured with female embryonic genital ridges enter meiotic prophase (132). More recent studies have defined some of the signaling pathways that initiate or repress meiosis in germ cells. In mouse embryos, signaling for meiotic initiation in germ cells begins with the production of retinoic acid (RA) from the embryonic mesonephros (134, 161, 162). Expression of genes responsive to RA signaling in female germ cells, including *Stra8* and *Dazl*, is required for meiotic initiation (134, 135). In male embryos, gonadal somatic cells express the RA-metabolizing enzyme Cyp26b1, thus preventing the onset of meiosis in male germ cells (134, 161, 162). Germ cells in female gonads

that do not express *Stra8* or *Dazl* do not enter meiosis (134, 135). These studies indicate that successful meiotic initiation in female gonads requires two elements: appropriate signaling from the mesonephros and gonadal stroma, and germ cells that can respond to these signals and enter meiosis.

As discussed in Chapter 3, gonad differentiation along male or female lines in mammalian species is generally dictated by chromosomal sex (94), and is not changed by meiotic failure in embryonic germ cells (58, 131, 136, 137). In contrast, germ cells have a significant role in directing male or female gonad development in zebrafish (83, 84, 90). If germ cells cannot initiate meiosis during zebrafish gonad development, this could alter somatic cell-germ cell signaling that would otherwise lead to ovarian differentiation. Germ cells in juvenile gonads from *brca2*^{Q658X} homozygotes are likely to be meiotically incompetent. Early meiotic and perinucleolar oocytes express *brca2* in wildtype juvenile zebrafish gonads. Since these cell types are not found in *brca2*^{Q658X} homozygotes, this implies a requirement for *brca2* in meiotic initiation and development of these cell populations. As *stra8* and *dazl* have not been described in zebrafish gonad development, their roles in these processes are unknown. However, the association between meiotic arrest in germ cells and testicular development in *brca2*^{Q658X} homozygotes suggests that meiotic initiation in germ cells is critical for ovarian development in zebrafish.

The second potential mechanism for failure of ovarian development involves apoptotic loss of germ cells in juvenile gonads. As discussed in Chapter 4, extensive

germ cell loss in mammalian embryonic gonads can lead to formation of seminiferous-like cords in females (147). Similarly, germ cell depletion during embryogenesis results in testicular differentiation in zebrafish (83-85). In our studies, homozygous *tp53* mutation rescued ovarian development in *brca2*^{Q658X} homozygotes. These data show that germ cell apoptosis is a key element for failure of ovarian development in *brca2*^{Q658X} homozygotes. Interestingly, studies of germ cell depletion in mammalian embryonic gonads indicate that loss of germ cells in female gonads at the meiotic stage, rather than the mitotic stage, can lead to transdifferentiation of granulosa cells and formation of seminiferous-like cords (147). Furthermore, studies in mouse models with germ cell loss during development suggest that germ cells are dispensable for testicular morphologic integrity in mammals (138). Therefore, it is possible that both meiotic failure and germ cell apoptosis work in combination to direct testicular development in *brca2*^{Q658X} homozygous zebrafish.

In addition to determining a novel role for *brca2* in zebrafish ovarian development, these studies demonstrate that the association between *brca2* mutation and tumorigenesis in reproductive tissues is conserved in zebrafish. Importantly, the majority of these tumors originated from somatic cell populations in the adult zebrafish testes. Similarly, ovarian carcinomas in women arise from epithelia of the ovarian surface or tubules (8-11), i.e. somatic cell populations, rather than germ cells. Homozygous *tp53* mutation accelerated tumorigenesis in both *brca2*^{Q658X} homozygotes and *brca2*^{Q658X} heterozygotes, and these mutations were associated with primary tumor development in the ovary in female zebrafish. Combined mutations in

p53 and *BRCA2* are also important factors in human ovarian carcinogenesis (19, 20). These findings in *brca2*^{Q658X}-mutant zebrafish are in contrast to tumor susceptibilities in viable *Brca2*-mutant rodent models, which are reported to develop a wide variety of tumor types (51, 55, 56, 59, 60). This variation among species may reflect differences in cancer susceptibility, methods used for generating *BRCA2* mutations, and/or variability in the location of the *BRCA2* mutation in these models.

The studies of *brca2*^{Q658X}-mutant zebrafish reported herein suggest a novel approach in considering the link between *BRCA2* mutation and human ovarian cancer. As discussed previously, *BRCA2* mutation in the ovarian surface epithelium or fimbria, followed by the accumulation of subsequent genetic changes, is thought to lead to neoplastic transformation (20). It is also possible that *BRCA2* mutation in germ cells adversely affects ovarian physiology, as was observed during gonad development in *brca2*^{Q658X}-mutant zebrafish. If so, altered intercellular signaling among germ cell and stromal cell populations might contribute to cellular transformation. In mammals, germ cells appear to play a significant role in both ovarian development and maintenance of the ovarian phenotype (147). The role for *BRCA2* in ovarian development and the effects of *BRCA2* mutation on intercellular signaling in the gonad are not known. Thus, the implications of these studies for *BRCA2*-associated ovarian cancer are as yet unclear. However, studying the effects of *brca2* mutation on gonad development and tumorigenesis in zebrafish has provided new insight into how germ cell-stromal cell interactions may relate to cancer susceptibility.

In summary, these studies have generated a novel zebrafish model for studying *brca2* mutation *in vivo*; established a conserved role for *brca2* in zebrafish spermatogenesis; discovered that *brca2* is required for ovarian development in zebrafish; shown that the association between reproductive tumorigenesis and *brca2* mutation is conserved in zebrafish; and demonstrated that *tp53* mutation is an important contributor to *brca2*-associated carcinogenesis. The *brca2*^{Q658X}-mutant zebrafish line represents an important resource for studying both gonadogenesis and *brca2*-associated carcinogenesis. This model has the potential to enable identification of genetic, environmental, or chemical modifiers that influence cancer susceptibility, and provides a new platform for studying the processes of gonad development and sex determination in vertebrate species.

Appendix I

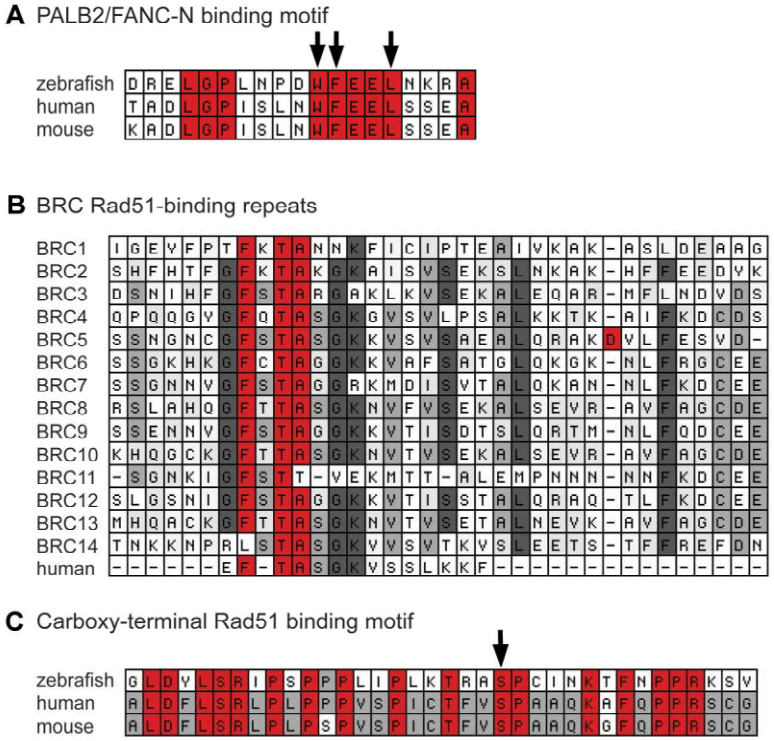

Amino acid sequence motifs found in zebrafish brca2**.** The zebrafish (accession number NP_001103864), mouse (accession number NP_001074470), and human BRCA2 (accession number NP_000050.2) were compared using MacVector (MacVector, Inc.) and sequence motifs were identified using InterProScan (163). The amino acid positions for each motif are given in parentheses. (A) Alignment of the 10-residue minimal PALB2-binding motif from human (*21-39*), mouse (*21-39*), and zebrafish (*10-28*) BRCA2. Identical residues are boxed in red. The arrows indicate the core interacting residues Trp31, Phe32, and Leu35 (164). (B) Alignment of the zebrafish brca2 BRC Rad51-binding repeat motifs to a consensus sequence from the eight human BRCA2 BRC repeats (165). The positions of the zebrafish BRC repeats are: 1 (*586-620*), 2 (*896-928*), 3 (*1003-1037*), 4 (*1129-1163*), 5 (*1238-1272*), 6 (*1295-1329*), 7 (*1361-1395*), 8 (*1401-1435*), 9 (*1445-1479*), 10 (*1488-1522*), 11 (*1533-1564*), 12 (*1573-1607*), 13 (*1617-1651*), 14 (*1685-1719*). Residues found in >90% of the sequences are boxed in red, >70% in dark grey, and >50% in light grey. The dashes indicate gaps in the alignment or no defined consensus. (C) Alignment of the BRCA2 carboxy-terminal Rad51-binding domain (166) from zebrafish (*2796-2831*), human (*3270-3305*), and mouse (*3193-3228*). Identical residues are boxed in red, and residues common in two sequences are boxed in grey. The arrow indicates the conserved CDK phosphorylation site (167).

Appendix II

Standard Immunohistochemistry Protocol provided by Histoserv, Inc. for detection of cytokeratin immunoreactivity in formalin-fixed paraffin-embedded sections.

1. Deparaffinize slides
2. Wash in distilled water
3. Pretreat slides at 85ºC for 20 minutes
4. Incubate in hydrogen peroxide solution for blocking
5. Was in distilled water wash
6. Incubate in bovine serum albumin (BSA) solution for blocking
7. Wash in Tris-buffered-saline-Tween-20 (TBST) buffer
8. Apply primary antibody – diluent for primary antibody is 1% BSA
9. Wash in TBST buffer
10. Apply secondary antibody – diluent for secondary antibody is 1% BSA
11. Wash in TBST buffer
12. Apply streptavidin-horseradish-peroxidase solution
13. Wash in TBST buffer
14. Develop slides with Diaminobenzidine (DAB)
15. Counterstain with Hematoxylin
16. Dehydrate and clear
17. Coverslip slides

Appendix III

Primer sequences for plasmid constructs	
Primer	*Sequence*
Brca2-3'-F	GTTTAGCTTCTAGAAATCTTATGCACCAA
Brca2-3'-R	gaatgcggccgcTCAGTCGTTCATCAGACCGTCC
Brca2-5'-F	gaatgtcgacgcggccgcCACACTCATGGCAGCATGTTTG
Brca2-5'-R	CGTTGAGTATGTCAGGATCCCATTC
Brca2-ex27-F	cacccaagcttACAAAACCTTCAATCCGCCAC
Brca2-ex27-R	gctctagaCCATCAGAGAACCACAGTAAACCAG
Vasa-F1	ATGTCCATCGCATAGGAAGAAC
Vasa-R1	GCTCCAGTCCAAACGAGTGATA
Cherry F	GCACCCCAGGCTTTACACTTTATGCTTCC
Cherry R	actcgagCGGCCGCGACTGTAGAATT
Primers sequences for genotyping	
Primer	*Sequence*
Dcap-mut-F2	TCCTGCACCAAGACCCCCTGTA*AG*C
Dcap-R	CTGTCAAAGTGCCATTTTCTTCAAG
Brca2-5	GTCTTGGAAGCATCACTAACACTCAC
Brca2-25	TGAGGCTATAGTAAAGGCAAAGGC
P53-03	CATATTCACAGACCACCAGCCC
P53-04	TCACACTAAAAGCATACCTCGCC
P53-F2	TCCTGTTTTTGCAGCTTGGTG
P53-R1	TGTTTCGGATAGCCTAGTGCGAG
EGFP-6	TTCTTCAAGTCCGCCATGCCCG
EGFP-3	GCACGCTGCCGTCCTCGATGTT

Lowercase = restriction enzyme recognition sequence
Italicized = base pair mismatch

Appendix IV

WHOLE-MOUNT IN SITU HYBRIDIZATION REAGENTS	
WISH hybridization buffer	▪ 50% formamide ▪ 5X SSC ▪ 5mM EDTA, pH 8.0 ▪ 0.1% Tween-20 ▪ 0.1% CHAPS ▪ 50µg/ml heparin ▪ 1mg/ml torula yeast RNA ▪ DEPC water
Maleic acid buffer	▪ 0.1M maleic acid, pH 7.5 ▪ 150mM NaCl
Wash I	▪ 50% formamide ▪ 2X SSC ▪ 0.15% CHAPS
Wash II	▪ 2X SSC ▪ 0.3% CHAPS
Wash III	▪ 0.2X SSC ▪ 0.3% CHAPS
Blocking solution	▪ 2% Blocking Reagent (Roche) ▪ 0.1M maleic acid buffer ▪ 5% fetal bovine serum
Working antibody solution	▪ Fixed embryos, ~100 from gastrula, somite, and segmentation stages ▪ 0.5 ml blocking solution
PBTw buffer	▪ 1X PBS ▪ 0.2% bovine serum albumin ▪ 0.1% Tween-20
Staining buffer	▪ 0.1M Tris-HCl, pH 9.5 ▪ 0.1M NaCl ▪ 50mM $MgCl_2$ ▪ 0.1% Tween-2
IN SITU HYBRIDIZATION REAGENTS	
ISH hybridization buffer	▪ 50% deionized formamide ▪ 4X SSC ▪ 10% dextran sulfate ▪ 5X Denhardt's solution ▪ 0.2 mg/ml salmon sperm DNA ▪ 0.25 mg/ml yeast tRNA ▪ DEPC water
Block buffer	▪ 100mM Tris-HCl, pH 7.5 ▪ 150mM NaCl
Blocking solution	▪ 1% Blocking Reagent (Roche) ▪ 5% FBS
Color buffer	▪ 100mM Tris-HCl, pH 9.5 ▪ 100mM NaCl ▪ 50mM $MgCl_2$
BCIP/NBT working solution	▪ BCIP/NBT Alkaline Phosphatase Substrate Kit (Vector Labs) ▪ Levamisole (Vector Labs), 1 drop/5 ml ▪ 0.001% Tween-20
Stop buffer	▪ 10mM Tris-HCl pH 8.0 ▪ 1mM EDTA, pH 8.0
MISCELLAENOUS REAGENTS	
Acridine Orange solution	▪ 5µg/ml Acridine Orange hemi (zinc chloride) salt (Sigma) in ddH_2O
DNA lysis buffer	▪ 10mM Tris-HCl, pH 8.0 ▪ 2mM EDTA ▪ 0.2% Triton-X100
DNA extraction buffer	▪ 10mM Tris-HCl, pH 8.4 ▪ 10mM EDTA, pH 8.0 ▪ 200mM NaCl ▪ 0.5% SDS
Tricaine methanesulfonate	▪ 0.4% tricaine (3-amino benzoic acid ethyl ester; ethyl m-aminobenzoate) ▪ 1.0% Na_2HPO_4
1X Danieau's medium	▪ 58mM NaCl ▪ 0.7mM KCl ▪ 0.4mM $MgSO_4$ ▪ 0.6mM $Ca(NO_3)_2$ ▪ 5.0mM HEPES pH 7.6

Appendix V

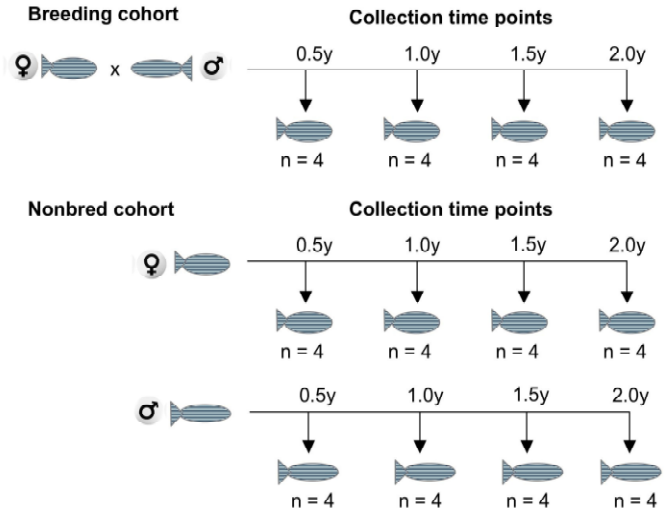

Wildtype AB* male and female zebrafish were divided into breeding and nonbred cohorts. All cohorts were maintained in sex-segregated tanks, and zebrafish in the breeding cohort were bred at biweekly intervals beginning at 3 months of age. Collection time points were determined with respect to the onset of breeding experiments.

Appendix VI

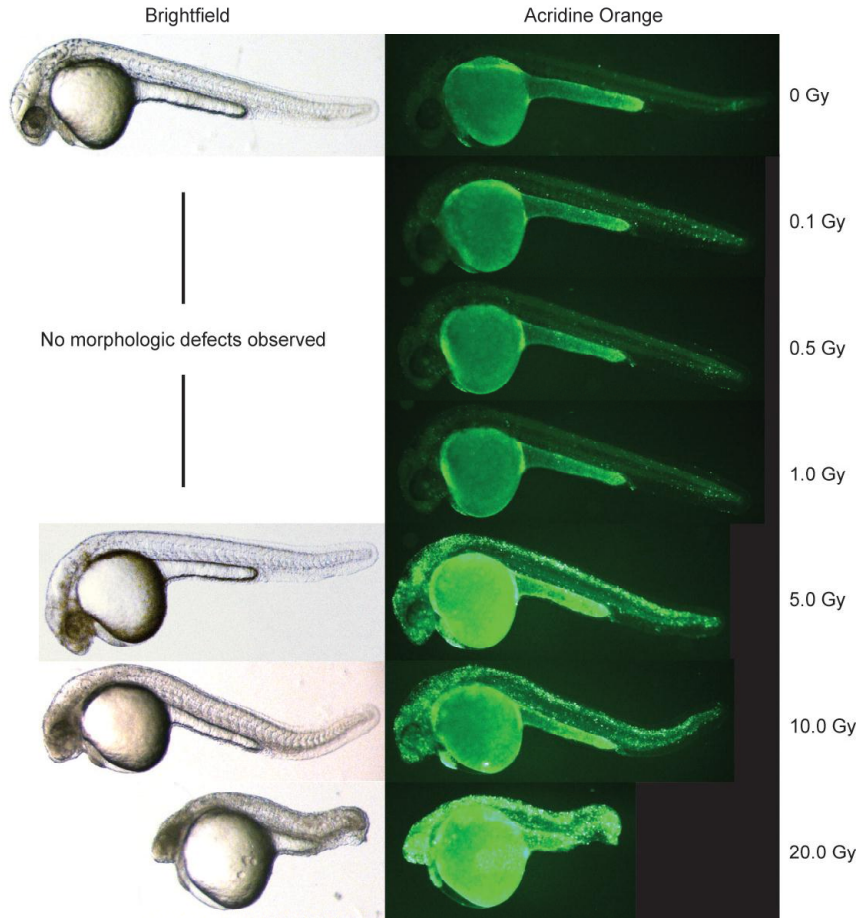

Wildtype zebrafish embryos were irradiated at 4.5 hpf at the following dose intervals: 0 Gy, 0.1 Gy, 0.5 Gy, 1.0 Gy, 5.0 Gy, 10.0 Gy, and 20.0 Gy. 60 embryos were irradiated at each dose interval. Irradiated embryos were stained with Acridine Orange solution at approximately 24 hpf to screen for apoptosis *in vivo*.

Appendix VII

Wildtype			
Specimen	**Age (mo)**	**Irradiation dose**	**Diagnosis**
1	6.0	0 Gy	ND
2	10.5	0 Gy	1) Cutaneous melanoma (tail)
3	13.0	5.0 Gy	ND
***brca2*^{Q658X} heterozygous**			
Specimen	**Age (mo)**	**Irradiation dose**	**Diagnosis**
4	13.0	0 Gy	1) Spermatocytic seminoma 2) Ultimobranchial carcinoma
5	13.5	5.0 Gy	ND
6	18.0	0 Gy	1) Ultimobranchial adenoma 2) Severe intracoelomic gas distension
***brca2*^{Q658X} homozygous**			
Specimen	**Age (mo)**	**Irradiation dose**	**Diagnosis**
7	17.0	0 Gy	1) Chronic granulomatous coelomitis, hepatitis, and pancreatitis with rare intralesional bacilli 2) Testicular hypoplasia with arrested spermatogenesis and mild germ cell dysplasia
8	17.5	5.0 Gy	ND
9	6.0	0 Gy	1) Musculoskeletal deformation 2) Testicular hypoplasia with arrested spermatogenesis
10	5.5	5.0 Gy	1) Severe granulomatous coelomitis with intralesional fungal hyphae and acid-fast bacilli 2) Testicular hypoplasia with arrested spermatogenesis

Zebrafish from an incross of *brca2*^{Q658X} heterozygotes were irradiated during embryogenesis and raised to adulthood. No significant long-term effects on morbidity or mortality were observed in *brca2*^{Q658X} -mutant zebrafish as compared to wildtype siblings.

Appendix VIII

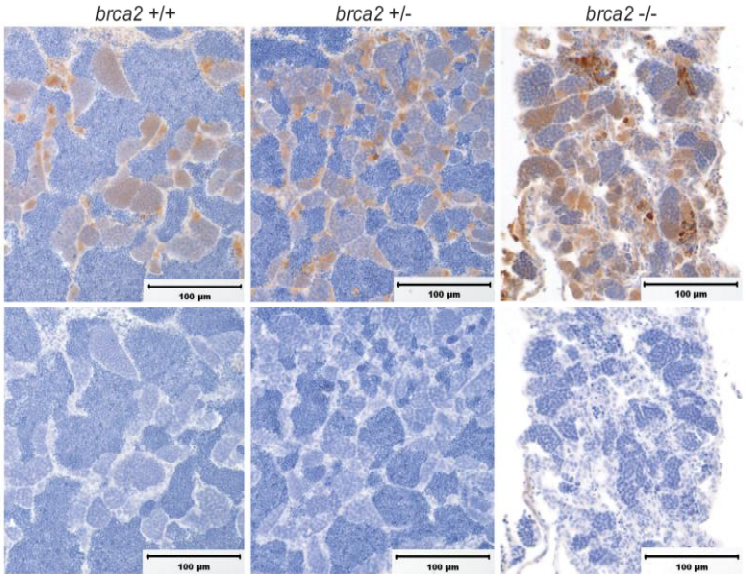

Immunohistochemistry for cleaved caspase-3 in testes from wildtype, *brca2*^{Q658X} heterozygotes, and *brca2*^{Q658X} homozygotes demonstrated numerous clusters of apoptotic cells in *brca2*^{Q658X} homozygous testes.

Appendix IX

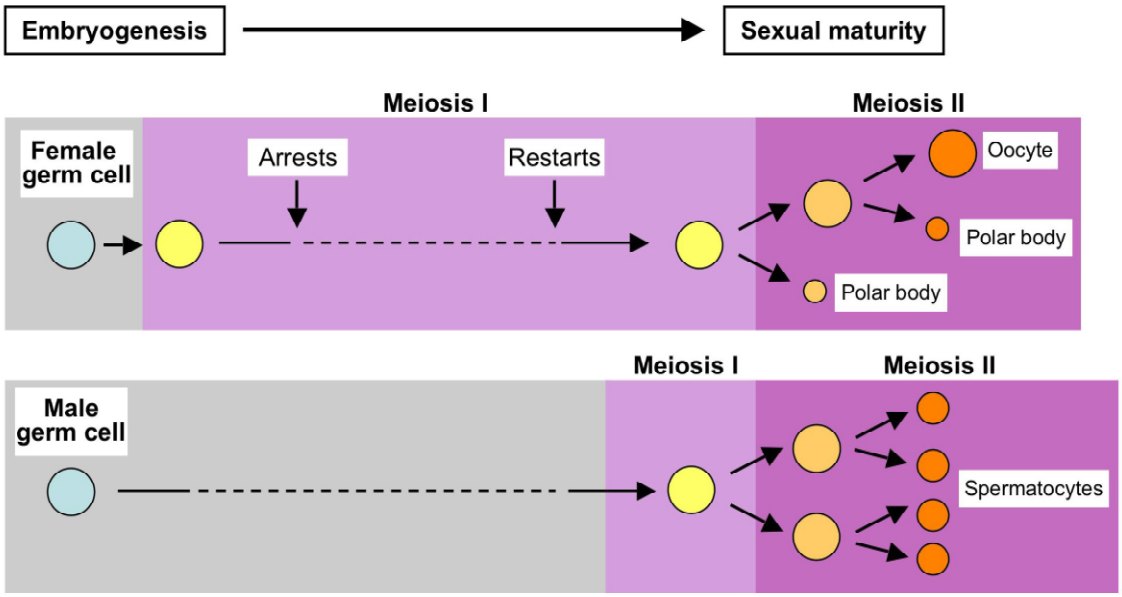
Embryogenesis
Sexual maturity
Meiosis I
Meiosis II
Female germ cell
Arrests
Restarts
Oocyte
Polar body
Polar body
Meiosis I
Meiosis II
Male germ cell
Spermatocytes

Appendix X

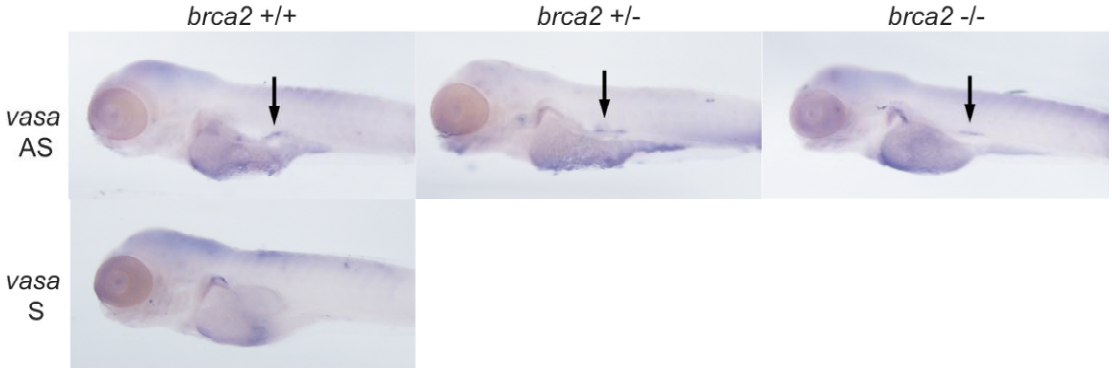

WISH for *vasa* at 4 dpf in wildtype, *brca2*^{Q658X} heterozygotes, and *brca2*^{Q658X} homozygotes indicated no apparent difference in primordial germ cell numbers or localization in *brca2*-mutant zebrafish.

Appendix XI

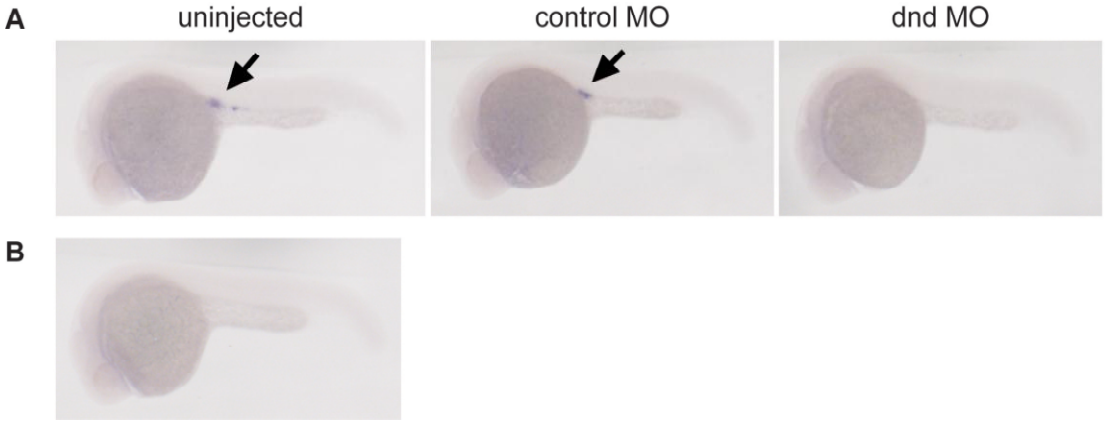

WISH with antisense (A) and sense (B) RNA probes for *vasa* at 24 hpf. Injected embryos received equivalent doses of control (scrambled) morpholino (MO) or dnd MO. The absence of *vasa*-expressing cells in embryos injected with dnd MO demonstrates successful ablation of endogenous germ cells.

Appendix XII

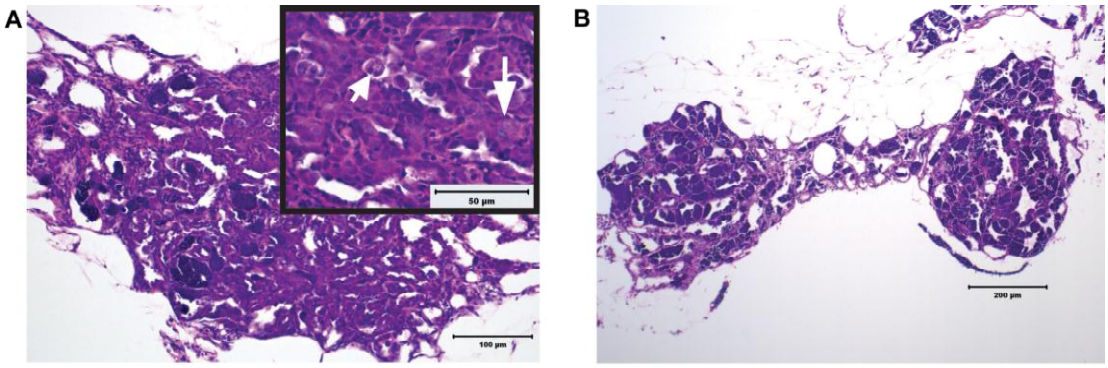

Hyperplastic, dysplastic, and degenerative changes in hematoxylin and eosin sections of testes from adult *brca2*^{Q658X} homozygous zebrafish. (A) Testicular tubules are lined by numerous germ cells that form multicellular layers (inset, long arrow). Multifocally there are dysplastic germ cells with large nuclei, vacuolated chromatin, and prominent nucleoli (inset, short arrow). (B) Testes from *brca2*^{Q658X} homozygotes show segmental degeneration, with loss of spermatocytes in testicular tubules.

brca2 in zebrafish ovarian development, spermatogenesis, and tumorigenesis

Heather R. Shive[a,1], Robert R. West[a], Lisa J. Embree[a], Mizuki Azuma[b], Raman Sood[c], Paul Liu[c], and Dennis D. Hickstein[a]

[a]Experimental Transplantation and Immunology Branch, Center for Cancer Research, National Cancer Institute, National Institutes of Health, Bethesda, MD 20892; [b]Department of Molecular Biosciences, University of Kansas, Lawrence, KS 66045; and [c]Genetics and Molecular Biology Branch, National Human Genome Research Institute, National Institutes of Health, Bethesda, MD 20892

Edited* by Igor B. Dawid, National Institute of Child Health and Human Development, Bethesda, MD, and approved October 4, 2010 (received for review August 9, 2010)

Humans with inherited mutations in *BRCA2* are at increased risk for developing breast and ovarian cancer; however, the relationship between *BRCA2* mutation and these cancers is not understood. Studies of *Brca2* mutation by gene targeting in mice are limited, given that homozygous *Brca2* mutation typically leads to early embryonic lethality. We established a zebrafish line with a nonsense mutation in *brca2* exon 11 (*brca2*^{Q658X}), a mutation similar in location and type to *BRCA2* mutations found in humans with hereditary breast and ovarian cancer. *brca2*^{Q658X} homozygous zebrafish are viable and survive to adulthood; however, juvenile homozygotes fail to develop ovaries during sexual differentiation. Instead, *brca2*^{Q658X} homozygotes develop as infertile males with meiotic arrest in spermatocytes. Germ cell migration to the embryonic gonadal ridge is unimpaired in *brca2*^{Q658X} homozygotes; thus, failure of ovarian development is not due to defects in early establishment of the embryonic gonad. Homozygous *tp53* mutation rescues ovarian development in *brca2*^{Q658X} homozygous zebrafish, reflecting the importance of germ cell apoptosis in gonad morphogenesis. Adult *brca2*^{Q658X} homozygous zebrafish are predisposed to testicular neoplasias. In addition, tumorigenesis in multiple tissues is significantly accelerated in combination with homozygous *tp53* mutation in both *brca2*^{Q658X} homozygous and *brca2*^{Q658X} heterozygous zebrafish. These studies reveal critical roles for *brca2* in ovarian development and tumorigenesis in reproductive tissues.

gonad development | meiosis | sex determination | fancd1

Inherited mutations in the human breast cancer 2 gene (*BRCA2*) are a well-established risk factor for developing ovarian cancer (1, 2). The link between mutations in *BRCA2* and ovarian cancer susceptibility is not understood. Epidemiologic evidence suggests that mutations in the "ovarian cancer cluster region" in *BRCA2* exon 11 are associated with an increased incidence of ovarian cancer relative to breast cancer in affected families (3, 4). Cancer risk occurs in heterozygous carriers of *BRCA2* mutations, but loss of heterozygosity is frequently observed in cancer cells (5).

BRCA2 is a component of the DNA repair machinery and mediates homologous recombination in somatic cells and meiotic recombination in germ cells (6, 7). Mutations in *BRCA2* perturb double-strand DNA break repair, and various chromosomal aberrations are observed in BRCA2-deficient cells (6–8). In vivo studies of *Brca2* mutation in mouse models are limited, given that homozygous loss of *Brca2* by gene targeting leads to decreased cellular proliferation, developmental arrest, and early embryonic lethality in most instances (9, 10).

To investigate the role of *brca2* in development and tumorigenesis, we established a zebrafish line with a nonsense mutation in *brca2* exon 11 (*brca2*^{Q658X}), a mutation similar in location and type to *BRCA2* mutations in humans with hereditary breast and ovarian cancer (11). We report that *brca2* is essential for zebrafish ovarian development. Homozygous *brca2*^{Q658X} mutation leads to an all-male phenotype in zebrafish, which can be abrogated by concomitant loss of *tp53*. *brca2* also functions as a tumor-suppressor gene in zebrafish. Adult *brca2*^{Q658X} homozygotes develop testicular tumors, and tumorigenesis is accelerated in multiple tissues by homozygous *tp53* mutation in both *brca2*^{Q658X} heterozygotes and homozygotes. Thus, *brca2* plays critical roles in both ovarian development and cancer susceptibility.

Results

***brca2* Is Expressed During Embryogenesis and in Adult Gonads.** Zebrafish *brca2* is homologous to human *BRCA2*, with conserved structural organization and a large exon 11 in both species (12). The characteristic BRC repeats located in exon 11 of human *BRCA2* are also found in exon 11 of the zebrafish *brca2* gene (Fig. 1*A* and Fig. S1).

Whole-mount in situ hybridization (WISH) for *brca2* on WT embryos from the two-cell stage through 24 h postfertilization (hpf) showed abundant expression of *brca2* in early cleavage-stage embryos (Fig. S2*A*), corresponding to maternal mRNA produced during oogenesis (13). Thus, maternally provided *brca2* is available for DNA repair before zygotic transcription begins. At 24 hpf, *brca2* expression was highest in the developing brain, eye, and ear (Fig. S2*A*). These findings complement a previous study of *brca2* expression during zebrafish embryogenesis (14). In situ hybridization for *brca2* in adult WT zebrafish ovaries demonstrated *brca2* expression in developing and mature oocytes, with the strongest expression seen in the most mature oocytes (Fig. S2*B*). In adult WT testes, *brca2* was expressed in spermatogonia and developing spermatocytes, but not in mature spermatozoa (Fig. S2*B*).

***brca2* Mutant Zebrafish Are Phenotypically Male and Exhibit Aberrant Spermatogenesis.** To establish a *brca2* mutant zebrafish model, we screened an ethylnitrosourea (ENU)-mutagenized library for mutations in *brca2* exon 11 by resequencing and identified a zebrafish line carrying a C-to-T point mutation that produces a glutamine (Q) to stop codon (X) change (Fig. 1*A*). Multiple incrosses of *brca2*^{Q658X} heterozygotes yielded WT, heterozygous, and homozygous mutant zebrafish in Mendelian ratios, indicating that *brca2*^{Q658X} homozygotes are fully viable (Table S1).

At sexual maturity, all *brca2*^{Q658X} homozygotes were phenotypically male, whereas both the WT and *brca2*^{Q658X} heterozygous cohorts included similar ratios of male and female zebrafish (Fig. 1*B*). *brca2*^{Q658X} homozygotes induced egg laying in fertile WT female zebrafish, but eggs collected from these crosses were unfertilized.

Author contributions: H.R.S., R.R.W., L.J.E., and D.D.H. designed research; H.R.S., R.R.W., L.J.E., and R.S. performed research; R.S. and P.L. contributed new reagents/analytic tools; H.R.S., R.R.W., L.J.E., M.A., and D.D.H. analyzed data; and H.R.S. and D.D.H. wrote the paper.

The authors declare no conflict of interest.

*This Direct Submission article had a prearranged editor.

Freely available online through the PNAS open access option.

[1]To whom correspondence should be addressed. E-mail: shiveh@mail.nih.gov.

This article contains supporting information online at www.pnas.org/lookup/suppl/doi:10.1073/pnas.1011630107/-/DCSupplemental.

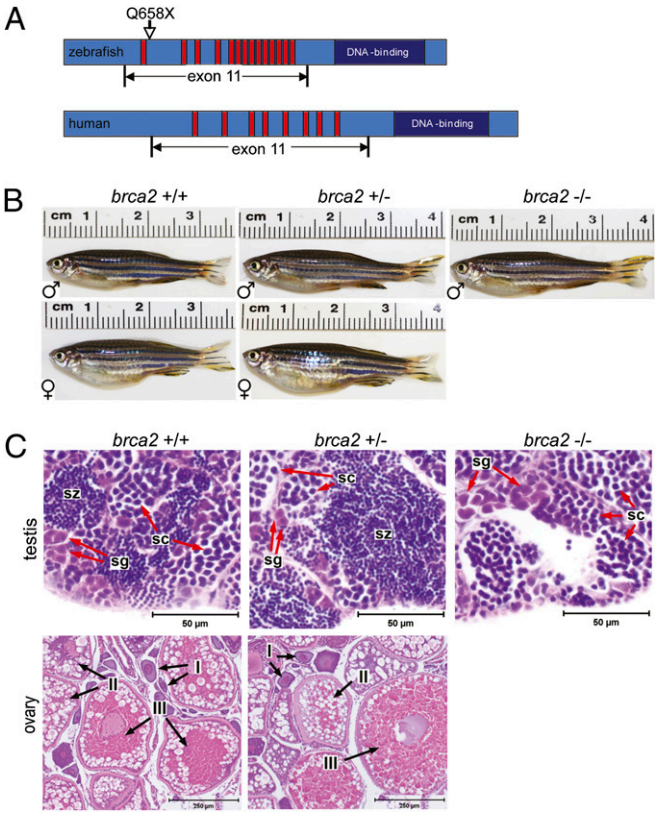

Fig. 1. Zebrafish brca2 structure and zebrafish *brca2*^{Q658X} mutation. (*A*) Schematic of zebrafish brca2 (*Upper*) compared with human BRCA2 (*Lower*). The zebrafish *brca2* gene [National Center for Biotechnology Information (NCBI) sequence NC_007126.4] has 16,583 base pairs with 27 exons and encodes a 2874-aa protein (NCBI sequence NP_001103864). Conserved domains include the Rad51-binding BRC repeats (red bars) and the DNA-binding domain (dark-blue box). The zebrafish *brca2*^{Q658X} mutation (C1971T; Q658X) described herein is shown relative to its position within exon 11. (*B*) WT and *brca2*^{Q658X} heterozygotes exhibit distinctly male or female phenotypes, whereas *brca2*^{Q658X} homozygotes are phenotypically male. (*C*) Gonads from zebrafish of each genotype reflect observed male or female phenotypes in *B*. Spermatogenesis is complete in testes from WT and *brca2*^{Q658X} heterozygotes. Testes from *brca2*^{Q658X} homozygotes contain only spermatogonia and primary spermatocytes. Ovaries from WT and *brca2*^{Q658X} heterozygotes are similar and contain developing and mature oocytes. sg, spermatagonia; sc, spermatocytes; sz, spermatozoa; I, stage I oocyte; II, stage II oocyte; III, stage III oocyte. (Scale bars: 50 μm for sections of testis; 250 μm for sections of ovaries.)

On histological examination of the gonads, adult WT and *brca2*^{Q658X} heterozygotes had either mature ovaries or testes, and gonadal sex was consistent with predicted sex based on physical features and behavior (Fig. 1 *B* and *C*). In contrast, all *brca2*^{Q658X} homozygotes had only testes (Fig. 1*C*). Spermatogenesis was arrested in testes from *brca2*^{Q658X} homozygotes, with only spermatogonia and primary spermatocytes present (Fig. 1*C*). Spermatogenesis was complete in testes from male WT and *brca2*^{Q658X} heterozygotes (Fig. 1*C*). The ovaries from female WT and *brca2*^{Q658X} heterozygotes were morphologically similar, with complete oocyte development and maturation (Fig. 1*C*).

***brca2* Mutant Zebrafish Do Not Develop Juvenile Ovaries.** To determine the stage at which *brca2* mutation affects sexual differentiation, we examined gonads from juvenile zebrafish of each *brca2* genotype by histology at intervals between 21 d and 51 d postfertilization (dpf). During this period, all zebrafish normally develop "juvenile ovaries" that contain gonocytes, early meiotic oocytes, and perinucleolar oocytes (15, 16). With maturation, males undergo oocyte loss and proliferation of spermatogonia and spermatocytes, whereas females continue to experience oocyte proliferation and differentiation (15, 16).

Gonadal development in WT and *brca2*^{Q658X} heterozygotes was similar at all time points. At 21 dpf, the gonads from zebrafish of both genotypes were undifferentiated and contained gonocytes and scant stroma (Fig. 2*A*). At 31 dpf, gonads were classified into four morphologic types: undifferentiated (similar to gonads at 21 dpf), juvenile ovary, presumptive ovary, and presumptive testis (Fig. 2*B*). Juvenile ovaries were distinguished by the presence of perinucleolar oocytes (Fig. 2*B*, short arrows). Presumptive ovaries exhibited maturing oocytes, whereas presumptive testes exhibited developing spermatogonial cysts with reduction or loss of perinucleolar oocytes (Fig. 2*B*). By 41 and 51 dpf, definitive ovarian or testicular differentiation was apparent in WT and *brca2*^{Q658X} heterozygotes (Fig. 2 *C* and *D*).

In contrast, oocyte differentiation was not observed in gonads from *brca2*^{Q658X} homozygotes at any time point. At 21 dpf, gonads from *brca2*^{Q658X} homozygotes were similar to gonads from WT and *brca2*^{Q658X} heterozygotes (Fig. 2*A*). At 31 dpf, gonads from *brca2*^{Q658X} homozygotes were classified as undifferentiated or presumptive testes (Fig. 2*B*). The presumptive testes contained germ cells and clusters of round cells encircled by somatic cells, consistent with developing spermatogonial cysts. Gonads from some *brca2*^{Q658X} homozygotes contained putative premeiotic germ cells (Fig. 2*B*, arrowheads), which were not

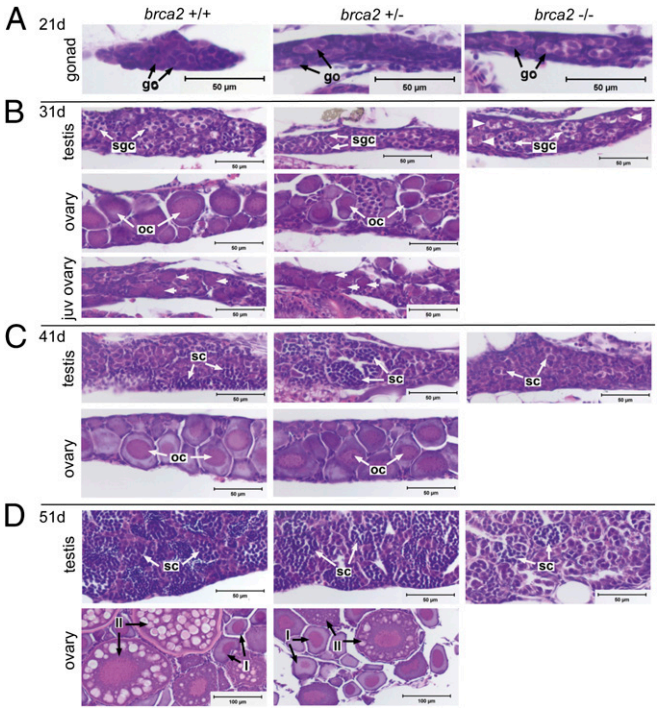

Fig. 2. Failure of ovarian development occurs in *brca2*^{Q658X} homozygotes during gonadal development. (*A*) Gonads from WT, *brca2*^{Q658X} heterozygotes, and *brca2*^{Q658X} homozygotes are indistinguishable at 21 dpf. (*B*) At 31 dpf, WT and *brca2*^{Q658X} heterozygotes exhibit juvenile ovaries, early testicular differentiation, or early ovarian differentiation, whereas *brca2*^{Q658X} homozygotes exhibit only early testicular differentiation. Perinucleolar oocytes in juvenile ovaries are indicated by short arrows; putative premeiotic germ cells are indicated by arrowheads. (*C* and *D*) At 41 and 51 dpf, WT and *brca2*^{Q658X} heterozygotes exhibit continued maturation of testes or ovaries, whereas *brca2*^{Q658X} homozygotes exhibit only testicular development. go, gonocyte; sgc, spermatogonial cyst; oc, oocyte; sc, spermatocyst; I, stage I oocyte; II, stage II oocyte. (Scale bars: 50 μm; 100 μm in 51 dpf ovaries.)

observed in gonads from WT or *brca2*^{Q658X} heterozygotes. Few spermatocysts were observed in developing testes at 41 dpf in *brca2*^{Q658X} homozygotes compared with WT and *brca2*^{Q658X} heterozygotes (Fig. 2*C*). By 51 dpf, *brca2*^{Q658X} homozygous testes contained only spermatogonia and primary spermatocytes, with fewer spermatocysts compared with WT and *brca2*^{Q658X} heterozygotes (Fig. 2*D*). No perinucleolar oocytes were observed in developing gonads from *brca2*^{Q658X} homozygotes at any time point.

Germ Cell Designation, Development, and Survival in *brca2* Mutant Zebrafish. Development of all-male populations has been described in zebrafish with embryonic loss of primordial germ cells (PGCs) or failure of PGCs to migrate to the embryonic gonadal ridge (17, 18). Thus, we evaluated embryos from incrosses of *brca2*^{Q658X} heterozygous zebrafish for the presence and appropriate localization of PGCs at 24 hpf by WISH for the germ cell marker *vasa* (Fig. 3*A*). Expression of *vasa* in 24-hpf embryos indicated no apparent difference in PGC numbers or localization in WT, *brca2*^{Q658X} heterozygotes, or *brca2*^{Q658X} homozygotes (Fig. 3*A*). Similar results were observed at 4 dpf (Fig. S3).

Although *brca2*^{Q658X} mutation did not appear to affect embryonic PGC designation, meiotic progression in germ cells was arrested in *brca2*^{Q658X} homozygotes. Testes from adult *brca2*^{Q658X} homozygotes showed increased numbers of spermatocysts containing spermatocytes with meiotic nuclear morphology (Fig. 3*B*). The numbers of spermatocysts containing spermatocytes in meiosis were statistically significantly higher in testes from adult *brca2*^{Q658X} homozygotes compared with testes from WT (P = 0.0026) and *brca2*^{Q658X} heterozygotes (P = 0.0009) (Table S2).

Meiotic arrest in testes from adult *brca2*^{Q658X} homozygotes was accompanied by extensive spermatocyte apoptosis; in contrast, apoptotic cells were rare in testes from adult WT and *brca2*^{Q658X} heterozygotes. TUNEL assay (Fig. 3*C*) and immunohistochemistry for cleaved caspase-3 (Fig. S4) demonstrated multiple apoptotic spermatocytes in adult *brca2*^{Q658X} homozygotes testes, with apoptotic spermatocytes often forming distinct cell clusters (Fig. 3*C*, *Inset*).

Homozygous Loss of *tp53* Rescues Ovarian Development in *brca2* Mutant Zebrafish. To examine how germ cell apoptosis might impact gonad development in *brca2* mutant zebrafish, we crossed *brca2*^{Q658X} heterozygotes with *tp53*^{M214K} homozygotes (19). We subsequently incrossed *brca2*^{Q658X} heterozygous;*tp53*^{M214K} heterozygous zebrafish, and raised the progeny to adulthood.

Histological examination of the gonads from seven adult *brca2*^{Q658X} homozygous;*tp53*^{M214K} homozygous zebrafish revealed that two zebrafish had developed ovaries (Fig. 3*D*). Oogenesis appeared to be complete in the female *brca2*^{Q658X} homozygous;*tp53*^{M214K} homozygous zebrafish; however, the ovaries contained multiple binucleate oocytes (Fig. 3*D*, *Inset*), which were not seen in female *brca2*^{Q658X} heterozygotes or WT zebrafish.

***brca2* Mutant Zebrafish Are Predisposed to Testicular Neoplasia.** Because *BRCA2* mutations in humans are associated predominantly with cancer development in reproductive tissues, we histologically evaluated the testes from aged adult *brca2*^{Q658X} homozygotes for tumor development. At 10–16 mo of age, 4 out of 13 (31%) *brca2*^{Q658X} homozygotes developed testicular neoplasia (Fig. 4). Testicular tumors were of both somatic cell and germ cell origin and included undifferentiated stromal cell tumors (Fig. 4 *A* and *B*), a papillary cystadenoma (Fig. 4*C*), and a seminoma (Fig. 4*D*). Other changes in testes from aged adult *brca2*^{Q658X} homozygotes included germ cell hyperplasia and dysplasia, as well as segmental testicular degeneration (Fig. S5).

In contrast, no testicular tumors were observed in age-matched cohorts of WT (n = 12) and *brca2*^{Q658X} heterozygotes

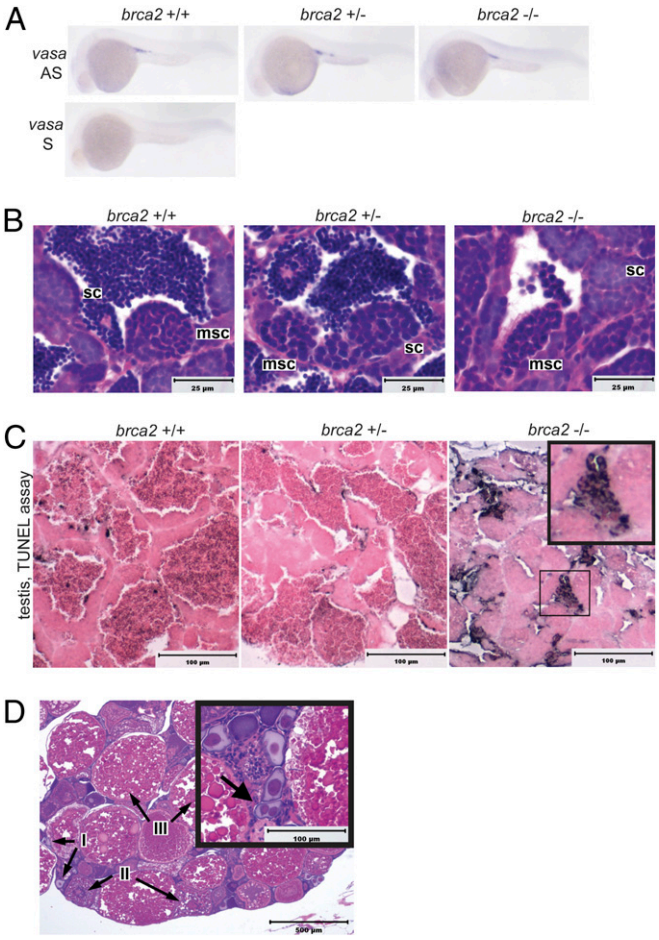

Fig. 3. Germ cell specification, development, and survival in embryonic and adult *brca2*^{Q658X} homozygotes. (*A*) WISH with antisense (AS) and sense (S) RNA probes for *vasa* indicates appropriate migration and colonization of the gonadal ridge in WT, *brca2*^{Q658X} heterozygous, and *brca2*^{Q658X} homozygous embryos. (*B*) Testes from WT, *brca2*^{Q658X} heterozygotes, and *brca2*^{Q658X} homozygotes show spermatocysts containing meiotic spermatocytes. (*C*) TUNEL staining of testes from WT, *brca2*^{Q658X} heterozygotes, and *brca2*^{Q658X} homozygotes. Multiple clusters of apoptotic spermatocytes are present in testes from *brca2*^{Q658X} homozygotes (*Inset*). (*D*) Homozygous *tp53*^{M214K} mutation rescues ovarian development in *brca2*^{Q658X} homozygotes, but female *brca2*^{Q658X} homozygous; *tp53*^{M214K} homozygous zebrafish develop binucleate oocytes (*Inset*). sc, spermatocyst; msc, meiotic spermatocyst; I, type I oocyte; II, type II oocyte; III, type III oocyte. (Scale bars: 25 μm in *B*, 100 μm in *C*, and 500 μm in *D*.)

(n = 12). The hyperplastic, dysplastic, and degenerative changes observed in testes from *brca2*^{Q658X} homozygotes were not seen in testes from WT and *brca2*^{Q658X} heterozygotes.

Collaborative Effects of *tp53* and *brca2* Mutations on Tumorigenesis. Analysis of tumorigenesis in zebrafish from an incross of *brca2*^{Q658X} heterozygous;*tp53*^{M214K} heterozygous zebrafish revealed that combined mutations in *brca2* and *tp53* accelerated the onset of tumor development (Fig. 4*E* and Table S3). The mean age at tumor onset was statistically significantly lower in both *brca2*^{Q658X} homozygous; *tp53*^{M214K} homozygous zebrafish and *brca2*^{Q658X} heterozygous; *tp53*^{M214K} homozygous zebrafish compared with the *tp53*^{M214K} homozygous parent line (Table S3). Of all tumor-bearing zebrafish collected from the *brca2*^{Q658X} heterozygous;*tp53*^{M214K} heterozygous zebrafish incross, only two were *brca2*^{Q658X} WT;*tp53*^{M214K} homozygous zebrafish, and their ages at tumor onset were similar to those observed in the *tp53*^{M214K} homozygous parent line (Table S4).

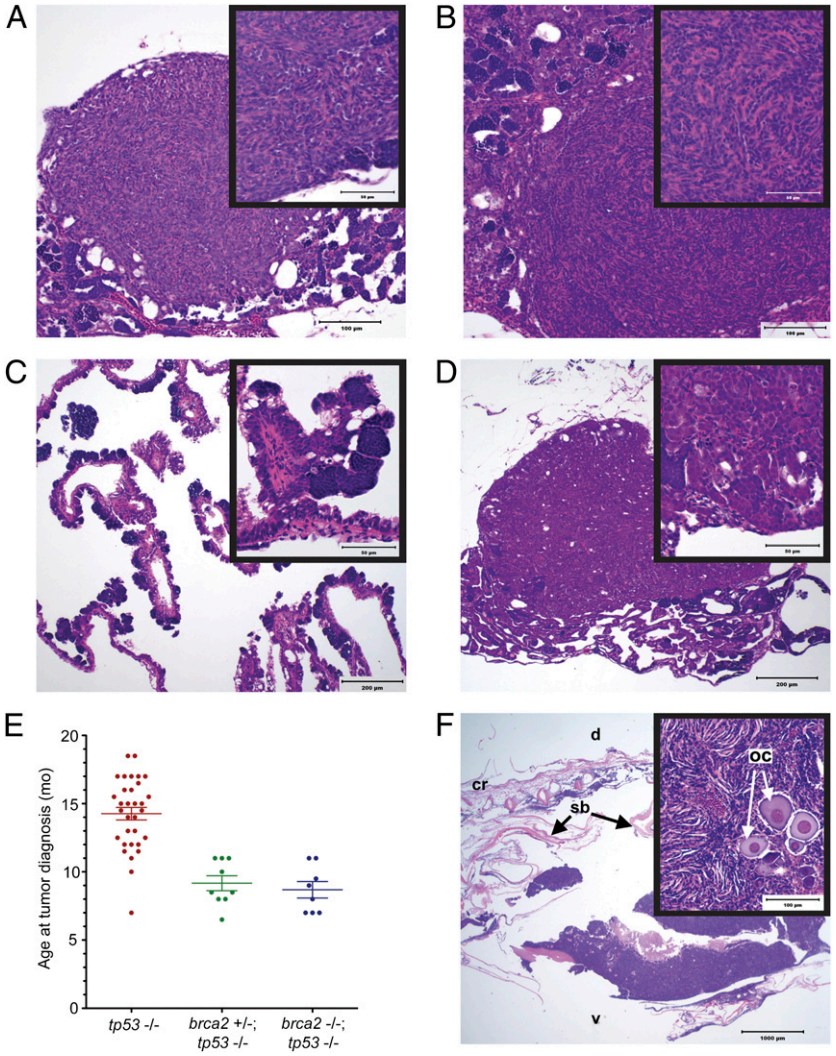

Fig. 4. *brca2*^{Q658X} homozygotes are predisposed to testicular neoplasias, and *brca2*^{Q658X} and *tp53*^{M214K} mutations have collaborative effects on tumorigenesis. (*A*) Undifferentiated stromal cell tumor from a *brca2*^{Q658X} homozygote. (*B*) Undifferentiated stromal cell tumor from a *brca2*^{Q658X} homozygote with irregular bundles around poorly defined small tubular structures (*Inset*). (*C*) Papillary cystadenoma from a *brca2*^{Q658X} homozygote. (*D*) Seminoma from a *brca2*^{Q658X} homozygote. (*E*) Age at tumor onset is significantly lower in both *brca2*^{Q658X} homozygous;*tp53*^{M214K} homozygous zebrafish and *brca2*^{Q658X} heterozygous;*tp53*^{M214K} homozygous zebrafish compared with the *tp53*^{M214K} homozygous zebrafish parent line. (*F*) The ovary is a primary site for tumor development in *brca2*^{Q658X} heterozygous;*tp53*^{M214K} homozygous zebrafish, with oocyte entrapment (*Inset*). oc, oocyte; cr, cranial; d, dorsal; v, ventral; sb, swim bladder. (Scale bars: 100 μm in *A* and *B*; 200 μm in *C* and *D;* 1,000 μm in *F*; 50 μm in the *Insets* in *A*, *B*, *C*, and *D*; 100 μm in the *Inset* in *F*.)

The majority of tumors observed in both *brca2*^{Q658X} heterozygous;*tp53*^{M214K} homozygous zebrafish and *brca2*^{Q658X} homozygous;*tp53*^{M214K} homozygous zebrafish were malignant peripheral nerve sheath tumors (Table S4). Interestingly, in three out of seven female *brca2*^{Q658X} heterozygous;*tp53*^{M214K} homozygous zebrafish, the ovaries appeared to be the primary site of tumor development (Fig. 4*F*). Tumor development in one of two female *brca2*^{Q658X} homozygous;*tp53*^{M214K} homozygous zebrafish also appeared to mainly involve the ovary (Table S4). Primary tumorigenesis in the gonads was not typical of a subset of *tp53*^{M214K} homozygous zebrafish evaluated histologically (Table S4) and was not reported in characterization of the *tp53*^{M214K} zebrafish line (19). In multiple instances, zebrafish developed tumors in more than one anatomic location and/or developed more than one type of tumor (Table S4).

Discussion

Previous studies of *Brca2* mutation in murine models have been limited due to the preponderance of early embryonic lethality associated with homozygous loss of *Brca2* (10). In zebrafish, we find that homozygous loss of *brca2* does not affect embryonic survival. This difference may reflect the relatively late onset of zygotic gene transcription in zebrafish embryos, which begins in cleavage cycle 10 (20). Given that maternal *brca2* is abundant in early-stage zebrafish embryos, it is likely that maternal RNA sustains *brca2*^{Q658X} homozygotes during early development.

BRCA2 is required in germ cells for the repair of double-strand DNA breaks generated during prophase of meiosis I, with loss of *BRCA2* resulting in meiotic arrest (21, 22). Our analyses of *brca2*^{Q658X} homozygous zebrafish demonstrate a conserved role for *brca2* in zebrafish germ cell development and spermatogenesis. Histological analyses of more than 90 zebrafish of each genotype derived from 17 different clutches confirmed that the testicular phenotype described herein was correlated with homozygous *brca2*^{Q658X} mutation in all cases, and was maintained after three outcrosses to WT zebrafish. The patterns of TUNEL staining and cleaved caspase-3 immunoreactivity in *brca2*^{Q658X} homozygous testes appear to reflect apoptosis of spermatocyte

clones, because zebrafish spermatocytes are clonally derived from a single germ cell and organized into discrete groups known as spermatocysts (23).

These studies also reveal an important role for *brca2* in ovarian development, raising questions about the participation of *brca2* in PGC–stromal cell signaling in the immature gonad. *BRCA2*, also known as *FANC-D1*, is a member of the Fanconi anemia (FA) family of proteins that regulate DNA damage response and repair (24). Interestingly, gonadal dysmorphogenesis and hypogonadism are observed in some patients with mutations in various FA genes (25). Hypogonadism and failure of germ cell maturation also have been reported in mouse models with mutations in several FA genes, including a *Brca2*-deficient mouse model that was rescued with human *BRCA2* (22, 26).

brca2 mutation in zebrafish did not affect PGC specification or gonadal colonization in embryos. However, the finding that homozygous *tp53* mutation rescued ovarian development in a small number of *brca2*^{Q658X} homozygotes indicates that germ cell apoptosis is an important contributor to the failure of ovarian development observed in *brca2*^{Q658X} homozygotes. PGCs can significantly affect zebrafish gonad development and sex determination. Germ cell apoptosis is an important feature of male gonad development (27), and germ cell depletion by gene mutation or knockdown generates predominantly male zebrafish populations with structurally and functionally male gonads (17, 18).

Gonad development in *brca2*^{Q658X} homozygotes also may be influenced by disrupted meiosis in germ cells, because meiotic progression is required in developing female gonads. In WT animals, including starfish, sea limpets, and *Xenopus* species, female germ cells initiate meiosis during embryogenesis, whereas male germ cells remain quiescent until sexual maturity (28, 29); thus, the temporal requirements for BRCA2 may differ in female versus male gonads. Given that germ cells from *brca2*^{Q658X} homozygous embryos are likely to be meiotically incompetent, failure of meiotic progression in *brca2*-deficient germ cells during embryogenesis might influence stromal differentiation toward testicular development. Thus, the combined effects of germ cell apoptosis and meiotic failure might be the underlying mechanisms that prevent ovarian development in *brca2*^{Q658X} homozygotes.

Interestingly, multiple binucleate oocytes were present in the rescued *brca2*^{Q658X} homozygous;*tp53*^{M214K} homozygous ovaries. A role for *BRCA2* in cytokinesis has been suggested, with *BRCA2* knockdown or loss resulting in abnormal cell division (30). Although this issue remains controversial (31), our findings support an association between *BRCA2* mutation and aberrant cytokinesis.

The impact of *BRCA2* mutation on cancer susceptibility, particularly in reproductive tissues, is also conserved in zebrafish. Adult *brca2*^{Q658X} homozygotes were predisposed to testicular tumors, which were predominantly of somatic cell origin and were not observed in age-matched male siblings. These types of testicular tumors have not been reported previously in zebrafish. Concomitant homozygous *tp53*^{M214K} mutation accelerates tumorigenesis in multiple tissues in both *brca2*^{Q658X} heterozygotes and *brca2*^{Q658X} homozygotes. The majority of zebrafish developed malignant peripheral nerve sheath tumors, similar to those described previously in *tp53*^{M214K} homozygotes (19); however, a tendency for primary tumor development in the ovary was noted in female *brca2*^{Q658X} heterozygous;*tp53*^{M214K} homozygous and *brca2*^{Q658X} homozygous;*tp53*^{M214K} homozygous zebrafish. These observations, although limited in number, suggest a specific role for *brca2* mutation in gonad tumorigenesis and imply collaborative effects of *tp53* and *brca2* mutations on tumorigenesis.

Zebrafish with a homozygous mutation of *fancl*, another member of the FA family, develop as fertile males with some phenotypic similarities to *brca2*^{Q658X} homozygotes (32). Male zebrafish with a homozygous mutation of the mismatch repair gene *mlh1* share some of these characteristics as well (33). Both of these genes are involved in DNA repair; FANCL participates in the FA DNA damage response pathway (34), whereas MLH1 mediates crossover during prophase I (35). Interestingly, an *mlh1* mutation in zebrafish does not prevent ovarian development (33), possibly because some germ cells are able to complete meiosis in male and female homozygotes (33, 36). These previous studies, along with the data presented herein, imply that germ cell survival and completion of meiosis are critical factors in zebrafish gonad morphogenesis. Importantly, mutations in *fancl* and *mlh1* are not associated with reproductive tumorigenesis or aberrant ovarian morphology in zebrafish (32, 33). Thus, *brca2* mutation uniquely impacts gonadal pathophysiology in zebrafish.

Our findings indicate that *brca2* is required for ovarian development in zebrafish and plays an essential role in zebrafish spermatogenesis. They also show that the propensity for tumorigenesis in reproductive tissues in association with *BRCA2* mutation appears to be conserved in zebrafish. In humans, the role for *BRCA2* in ovarian development and the effects of *BRCA2* mutation on intercellular signaling in the gonad remain unknown. Mammalian germ cells appear to play a significant role in both ovarian development and maintenance of the ovarian phenotype (37). Our studies suggest that *BRCA2* might be of importance in intercellular interactions in both developing and mature gonads. The implications for *BRCA2*-associated ovarian cancer are not yet clear; however, these observations provide important insights into how germ cell–stromal cell interactions in the ovary might be related to cancer susceptibility.

Materials and Methods

Zebrafish Maintenance. All of the experiments with zebrafish were approved by the National Cancer Institute's Animal Care and Use Committee.

WISH of Zebrafish Embryos. Embryos from incrosses of AB* zebrafish were used for analyses of WT *brca2* expression. Embryos from incrosses of *brca2*^{Q658X} heterozygous zebrafish were used for analyses of *vasa* expression. Embryos were processed routinely for WISH experiments (see *SI Materials and Methods*).

In Situ Hybridization of Adult Zebrafish Gonads. Adult AB* zebrafish were processed routinely for analysis of WT *brca2* expression by in situ hybridization (see *SI Materials and Methods*).

Identification and Establishment of *brca2*^{Q658X} Mutant Zebrafish Line. A previously established ENU-mutagenized library (38) was screened by PCR and sequencing with overlapping primer pairs spanning zebrafish *brca2* exon 11. The zebrafish *brca2*^{Q658X} mutant line was identified by analysis of the sequence data using PolyPhred and recovered by in vitro fertilization as described previously (38). In the Zebrafish Model Organism Database (ZFIN), the mutant allele designation for this zebrafish line is *brca2*^{hg5}.

Histological Analyses. Zebrafish were euthanized with tricaine methanesulfonate and fixed in 4% paraformaldehyde at 4 °C for a minimum of 24 h before being transferred to 70% ethanol. Specimens were processed routinely for paraffin embedding and preparation of 5-μm H&E-stained sections (Histoserv).

Histological Analyses of Zebrafish Testes by TUNEL Assay. Testes from 10 adult males (5.5 mo of age) of each genotype were dissected and grouped by genotype for fixation as described above. Sections were processed routinely for TUNEL labeling (see *SI Materials and Methods*).

Histological Analyses of Zebrafish Testes by Immunohistochemistry for Cleaved Caspase-3. Testes from 10 adult males (5.5 mo of age) of each genotype were dissected and grouped by genotype for fixation as described above. Sections were processed routinely for immunohistochemistry (see *SI Materials and Methods*).

Introduction of *tp53*^{M214K} Mutation. Zebrafish embryos homozygous for the *tp53*^{M214K} mutation were acquired from the Zebrafish International Resource Center. Adult *tp53*^{M214K} homozygotes were crossed with *brca2*^{Q658X} heterozygotes to establish a cohort of *brca2*^{Q658X} heterozygous;*tp53*^{M214K} heterozygous zebrafish, which were subsequently incrossed.

ACKNOWLEDGMENTS. We thank the sequencing team at Beijing Genomics Institute for help with PCR analyses and sequencing of the ENU-mutagenized library, Kevin Bishop for help with recovery of the mutant line, and Jennifer Edwards for assistance with immunohistochemistry. This research was supported by the National Institutes of Health's Intramural Research Program, the National Cancer Institute, the Center for Cancer Research, and the National Human Genome Research Institute.

1. Wooster R, et al. (1994) Localization of a breast cancer susceptibility gene, *BRCA2*, to chromosome 13q12-13. *Science* 265:2088–2090.
2. King MC, Marks JH, Mandell JB; New York Breast Cancer Study Group (2003) Breast and ovarian cancer risks due to inherited mutations in *BRCA1* and *BRCA2*. *Science* 302: 643–646.
3. Thompson D, Easton D, Breast Cancer Linkage Consortium (2001) Variation in cancer risks, by mutation position, in *BRCA2* mutation carriers. *Am J Hum Genet* 68:410–419.
4. Gayther SA, et al. (1997) Variation of risks of breast and ovarian cancer associated with different germline mutations of the *BRCA2* gene. *Nat Genet* 15:103–105.
5. Gudmundsson J, et al. (1995) Different tumor types from *BRCA2* carriers show wild-type chromosome deletions on 13q12-q13. *Cancer Res* 55:4830–4832.
6. Thorslund T, West SC (2007) BRCA2: A universal recombinase regulator. *Oncogene* 26: 7720–7730.
7. Venkitaraman AR (2001) Functions of BRCA1 and BRCA2 in the biological response to DNA damage. *J Cell Sci* 114:3591–3598.
8. Yu VP, et al. (2000) Gross chromosomal rearrangements and genetic exchange between nonhomologous chromosomes following BRCA2 inactivation. *Genes Dev* 14: 1400–1406.
9. Suzuki A, et al. (1997) *Brca2* is required for embryonic cellular proliferation in the mouse. *Genes Dev* 11:1242–1252.
10. Evers B, Jonkers J (2006) Mouse models of BRCA1 and BRCA2 deficiency: Past lessons, current understanding and future prospects. *Oncogene* 25:5885–5897.
11. Ramus SJ, et al. (2007) Contribution of *BRCA1* and *BRCA2* mutations to inherited ovarian cancer. *Hum Mutat* 28:1207–1215.
12. Titus TA, et al. (2006) The Fanconi anemia gene network is conserved from zebrafish to human. *Gene* 371:211–223.
13. Pelegri F (2003) Maternal factors in zebrafish development. *Dev Dyn* 228:535–554.
14. Titus TA, et al. (2009) The Fanconi anemia/BRCA gene network in zebrafish: Embryonic expression and comparative genomics. *Mutat Res* 668:117–132.
15. Maack G, Segner H (2003) Morphological development of the gonads in zebrafish. *J Fish Biol* 62:895–906.
16. Takahashi H (1977) Juvenile hermaphroditism in the zebrafish, *Brachydanio rerio*. *Bull Fac Fish Hokkaido Univ* 28:57–65.
17. Weidinger G, et al. (2003) *dead end*, a novel vertebrate germ plasm component, is required for zebrafish primordial germ cell migration and survival. *Curr Biol* 13: 1429–1434.
18. Siegfried KR, Nüsslein-Volhard C (2008) Germ line control of female sex determination in zebrafish. *Dev Biol* 324:277–287.
19. Berghmans S, et al. (2005) *tp53* mutant zebrafish develop malignant peripheral nerve sheath tumors. *Proc Natl Acad Sci USA* 102:407–412.
20. Kane DA, Kimmel CB (1993) The zebrafish midblastula transition. *Development* 119: 447–456.
21. Marcon E, Moens PB (2005) The evolution of meiosis: Recruitment and modification of somatic DNA-repair proteins. *Bioessays* 27:795–808.
22. Sharan SK, et al. (2004) BRCA2 deficiency in mice leads to meiotic impairment and infertility. *Development* 131:131–142.
23. Schulz RW, et al. (2010) Spermatogenesis in fish. *Gen Comp Endocrinol* 165:390–411.
24. Howlett NG, et al. (2002) Biallelic inactivation of *BRCA2* in Fanconi anemia. *Science* 297:606–609.
25. Giri N, Batista DL, Alter BP, Stratakis CA (2007) Endocrine abnormalities in patients with Fanconi anemia. *J Clin Endocrinol Metab* 92:2624–2631.
26. Wong JC, et al. (2003) Targeted disruption of exons 1 to 6 of the Fanconi anemia group A gene leads to growth retardation, strain-specific microphthalmia, meiotic defects and primordial germ cell hypoplasia. *Hum Mol Genet* 12:2063–2076.
27. Uchida D, Yamashita M, Kitano T, Iguchi T (2002) Oocyte apoptosis during the transition from ovary-like tissue to testes during sex differentiation of juvenile zebrafish. *J Exp Biol* 205:711–718.
28. McLaren A, Southee D (1997) Entry of mouse embryonic germ cells into meiosis. *Dev Biol* 187:107–113.
29. Page AW, Orr-Weaver TL (1997) Stopping and starting the meiotic cell cycle. *Curr Opin Genet Dev* 7:23–31.
30. Daniels MJ, Wang Y, Lee M, Venkitaraman AR (2004) Abnormal cytokinesis in cells deficient in the breast cancer susceptibility protein BRCA2. *Science* 306:876–879.
31. Lekomtsev S, Guizetti J, Pozniakovsky A, Gerlich DW, Petronczki M (2010) Evidence that the tumor-suppressor protein BRCA2 does not regulate cytokinesis in human cells. *J Cell Sci* 123:1395–1400.
32. Rodríguez-Marí A, et al. (2010) Sex reversal in zebrafish *fancl* mutants is caused by Tp53-mediated germ cell apoptosis. *PLoS Genet* 6:e1001034.
33. Feitsma H, Leal MC, Moens PB, Cuppen E, Schulz RW (2007) Mlh1 deficiency in zebrafish results in male sterility and aneuploid as well as triploid progeny in females. *Genetics* 175:1561–1569.
34. Meetei AR, et al. (2003) A novel ubiquitin ligase is deficient in Fanconi anemia. *Nat Genet* 35:165–170.
35. Baker SM, et al. (1996) Involvement of mouse Mlh1 in DNA mismatch repair and meiotic crossing over. *Nat Genet* 13:336–342.
36. Leal MC, Feitsma H, Cuppen E, França LR, Schulz RW (2008) Completion of meiosis in male zebrafish (*Danio rerio*) despite lack of DNA mismatch repair gene *mlh1*. *Cell Tissue Res* 332:133–139.
37. Guigon CJ, Magre S (2006) Contribution of germ cells to the differentiation and maturation of the ovary: Insights from models of germ cell depletion. *Biol Reprod* 74: 450–458.
38. Sood R, et al. (2006) Methods for reverse genetic screening in zebrafish by resequencing and TILLING. *Methods* 39:220–227.

Supporting Information

Shive et al. 10.1073/pnas.1011630107

SI Materials and Methods

Histological Staging of Zebrafish Specimens. Staging of zebrafish embryos, ovaries, and testes was performed as described previously (1–3).

WISH of Zebrafish Embryos. The *brca2* probe contained a 3.2-kb portion of the 3′ end of the cDNA, and the *vasa* probe contained the 3′ 549 bases of the cDNA. WISH experiments were performed as described previously (4, 5), with modifications (see below). Embryos used for genotyping after WISH were prepared as described previously (6), with minor modifications. Approximately 50 embryos were analyzed per developmental stage from three independent experiments. For *vasa* expression, 25–35 embryos from two independent experiments were imaged individually and then genotyped for the *brca2*^{Q658X} mutation.

Modifications to the WISH Protocol. The following modifications were made to the WISH protocol: (*i*) Tween 20 was eliminated from prehybridization washes; (*ii*) the hybridization buffer included 0.1% CHAPS and 0.5 mM EDTA; (*iii*) hybridization reactions were incubated at 60 °C or 65 °C; (*iv*) posthybridization washes included 0.3% CHAPS in 2× SSC; and (*v*) proteinase K digestion, acetic anhydride treatment, and RNase treatment were eliminated.

In Situ Hybridization of Adult Zebrafish Gonads. The *brca2* probe contained the 3′ 330 bases of the cDNA. Unstained sections were processed for in situ hybridization as described previously (7), with the following modifications: (*i*) Zebrafish were fixed in 4% paraformaldehyde at 4 °C for 24 h, transferred to 70% ethanol, and embedded in paraffin, and 5-μm unstained sections were prepared; (*ii*) sections were treated with proteinase K (5 μg/mL or 10 μg/mL) at 37 °C; (*iii*) the hybridization buffer contained 0.2 mg/mL Sonicated Salmon Sperm DNA (Stratagene); (*iv*) hybridization reactions were conducted at 50 °C or 60 °C; (v) 5× In Situ Hybridization Blocking Solution (Vector Laboratories) was used for blocking; (*vi*) the BCIP/NBT Alkaline Phosphate Substrate Kit IV (Vector Laboratories) was used for detection; and (*vii*) slides were briefly dehydrated in ethanol grades before coverslipping.

Genotyping. Tail amputation and DNA extraction for genotyping were performed as described previously (5), with minor modifications. Tissue was digested in 100 μL of DNA extraction buffer [10 mM Tris-HCl (pH 8.0), 2 mM EDTA, 0.2% Triton X-100] with 0.2 mg/mL of proteinase K (Fermentas) at 50–55 °C for a minimum of 2 h, followed by 10 min at 95 °C. A *brca2* fragment was amplified by PCR with primers designed to create an *Alu*I restriction site based on the presence of the *brca2*^{Q658X} point mutation. PCR products were incubated with *Alu*I digestion buffer (0.07 U/μL *Alu*I in 1× Tango buffer; Fermentas) at 37 °C for a minimum of 2 h.

Histological Analysis of Gonadal Development. Juvenile zebrafish were collected at 21, 31, 41, and 51 dpf and euthanized, genotyped, and individually fixed as described above. Specimens were grouped in tissue cassettes by genotype. The 21-dpf juveniles were embedded in 2% agarose before being placed in tissue cassettes. Ten sections were screened per group; specimens were assessed for the presence of gonadal tissue, presence of identifiable perinucleolar oocytes in gonads (signifying juvenile ovary formation), presence of spermatogonia in spermatogonial cysts (signifying testicular differentiation), and proliferation and differentiation of oocytes (signifying ovarian differentiation).

Histological Analyses of Meiosis in Spermatocytes. Testes from 10 adult males (age 5.5 mo) of each genotype were dissected and grouped by genotype for fixation as described above. To determine the total percentage of spermatocysts containing cells in meiosis, five tubules were randomly selected from each of 10 testis sections, for a total of 50 tubules. Tubules in which the tubular lumen and margins could not be reasonably ascertained were disregarded, and sections without at least five well-defined tubules in a cross-section were not included. For each tubule, the total number of spermatocysts was counted, and the number of spermatocysts containing spermatocytes with meiotic figures was recorded (Table S2). The numbers of spermatocysts per tubule from testes of each *brca2* genotype were compared using an unpaired *t* test (Table S2). The numbers of meiotic spermatocysts per tubule from testes of each *brca2* genotype were compared using an unpaired *t* test with Welch's correction (Table S2).

TUNEL Assay on Zebrafish Testes. TUNEL labeling was performed on 5-μm unstained sections with a commercially available kit (In Situ Cell Death Detection Kit, AP; Roche Diagnostics). After TUNEL labeling, sections were counterstained with Nuclear Fast Red Solution (Sigma-Aldrich) and mounted with Clear-Mount (Electron Microscopy Services). TUNEL assays were performed with each sample set in three independent experiments.

Immunohistochemistry for Cleaved Caspase-3. Sections were deparaffinized in xylene, rehydrated through a series of ethanol grades, and incubated in 3% H_2O_2/70% methanol to block endogenous peroxidase activity. For antigen retrieval, sections were incubated in 1× Target Retrieval Solution (DAKO) with steam. Protein block (DAKO) and normal goat serum were used for blocking, and the Vector Avidin/Biotin Blocking Kit (Vector Laboratories) was used to block endogenous biotin. Detection of cleaved caspase-3 was done using a rabbit polyclonal anti–cleaved caspase-3 antibody (1:200 dilution; Cell Signaling) with a goat anti-rabbit biotinylated secondary antibody (1:400 dilution; DAKO). Detection was achieved by incubating sections with a preformed avidin–biotinylated enzyme complex (Vectastain ABC Kit; Vector Laboratories), followed by application of 3,3′-diaminobenzidine tetrahydrochloride (DAB-Plus Substrate Kit; Invitrogen). After detection, sections were counterstained with Mayer's hematoxylin solution (Sigma-Aldrich), dehydrated, and coverslipped.

Evaluation of Tumor Incidence in Adult Zebrafish. Adult zebrafish were regularly monitored for evidence of morbidity or overt tumor development. Tumor development in the *tp53*^{M214K} homozygous zebrafish parent line was defined by observation of macroscopically identifiable tumors, and a subset was also screened by histology to confirm diagnosis. Progeny from an incross of *brca2*^{Q658X} heterozygous;*tp53*^{M214K} heterozygous zebrafish were evaluated for macroscopic tumor development and by histology. The ages at tumor onset in each genotype of zebrafish were compared using an unpaired *t* test (Table S3).

Image Acquisition. Embryos were imaged with a Leica MZ16 stereomicroscope and Leica DFC420 camera with Leica Imaging Suite. Histological sections were imaged with an Olympus BX41

and Diagnostic Instruments 14.2 color mosaic camera with SPOT version 4.6.4.3 imaging software (SPOT Imaging Solutions).

Primer Sequences for *brca2*^{Q658X} Genotyping by PCR and Restriction Digest.

Forward primer (mismatched bases in italics): TCCTGCAC-CAAGACCCCCTGTA*A*GC
Reverse primer: CTGTCAAAGTGCCATTTTCTTCAAG

Primer Sequences for *brca2*^{Q658X} Genotyping by Sequencing.

Forward primer: TGAGGCTATAGTAAAGGCAAAGGC
Reverse primer: GTCTTGGAAGCATCACTAACACTCAC

Primer Sequences for *tp53*^{M214K} Genotyping by Sequencing.

Forward primer: CATATTCACAGACCACCAGCCC
Reverse primer: TCACACTAAAAGCATACCTCGCC

1. Kimmel CB, Ballard WW, Kimmel SR, Ullmann B, Schilling TF (1995) Stages of embryonic development of the zebrafish. *Dev Dyn* 203:253–310.
2. Selman K, Wallace RA, Sarka A, Qi X (1993) Stages of oocyte development in the zebrafish, *Brachydanio rerio*. *J Morphol* 218:203–224.
3. Schulz RW, et al. (2010) Spermatogenesis in fish. *Gen Comp Endocrinol* 165:390–411.
4. Strähle U, Blader P, Henrique D, Ingham PW (1993) *Axial*, a zebrafish gene expressed along the developing body axis, shows altered expression in cyclops mutant embryos. *Genes Dev* 7(7B):1436–1446.
5. Streisinger G (1993) *The Zebrafish Book* (Univ Oregon Press, Eugene, OR).
6. Draper BW, McCallum CM, Moens CB (2007) *nanos1* is required to maintain oocyte production in adult zebrafish. *Dev Biol* 305:589–598.
7. Braat AK, et al. (1999) Cloning and expression of the zebrafish germ cell nuclear factor. *Mol Reprod Dev* 53:369–375.
8. Zdobnov EM, Apweiler R (2001) InterProScan: An integration platform for the signature-recognition methods in InterPro. *Bioinformatics* 17:847–848.
9. Oliver AW, Swift S, Lord CJ, Ashworth A, Pearl LH (2009) Structural basis for recruitment of BRCA2 by PALB2. *EMBO Rep* 10:990–996.
10. Bork P, Blomberg N, Nilges M (1996) Internal repeats in the BRCA2 protein sequence. *Nat Genet* 13:22–23.
11. Davies OR, Pellegrini L (2007) Interaction with the BRCA2 C terminus protects RAD51-DNA filaments from disassembly by BRC repeats. *Nat Struct Mol Biol* 14:475–483.
12. Esashi F, et al. (2005) CDK-dependent phosphorylation of BRCA2 as a regulatory mechanism for recombinational repair. *Nature* 434:598–604.

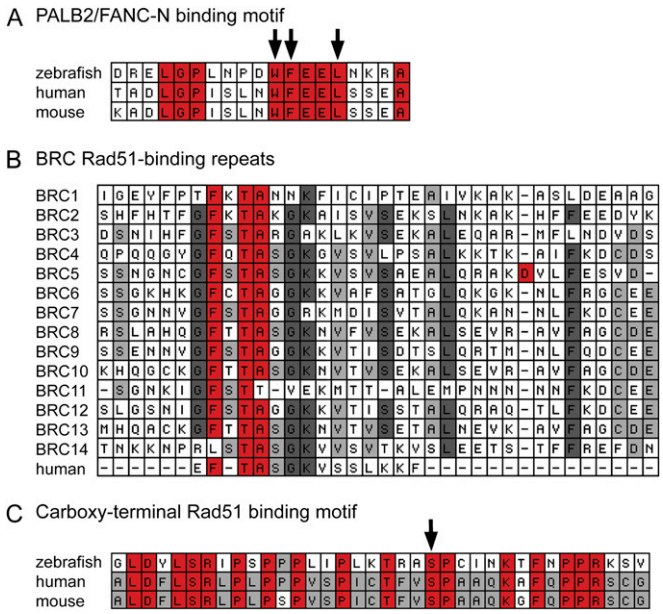

Fig. S1. Amino acid sequence motifs found in zebrafish brca2. The zebrafish (accession no. NP_001103864), mouse (accession no. NP_001074470), and human BRCA2 (accession no. NP_000050.2) were compared using MacVector (MacVector), and sequence motifs were identified using InterProScan (8). The amino acid positions for each motif are given in parentheses. (*A*) Alignment of the 10-residue minimal PALB2-binding motif from human (21–39), mouse (21–39), and zebrafish (10–28) BRCA2. Identical residues are boxed in red. The arrows indicate the core interacting residues Trp31, Phe32, and Leu35 (9). (*B*) Alignment of the zebrafish brca2 BRC Rad51-binding repeat motifs to a consensus sequence from the eight human BRCA2 BRC repeats (10). The positions of the zebrafish BRC repeats are as follows: 1, 586–620; 2, 896–928; 3, 1003–1037; 4, 1129–1163; 5, 1238–1272; 6, 1295–1329; 7, 1361–1395; 8, 1401–1435; 9, 1445–1479; 10, 1488–1522; 11, 1533–1564; 12, 1573–1607; 13, 1617–1651; 14, 1685–1719. Residues found in >90% of the sequences are boxed in red, those found in >70% are boxed in dark gray, and those found in >50% are boxed in light gray. The dashes indicate gaps in the alignment or no defined consensus. (*C*) Alignment of the BRCA2 carboxyl-terminal Rad51-binding domain (11) from zebrafish (2796–2831), human (3270–3305), and mouse (3193–3228). Identical residues are boxed in red, and residues common in two sequences are boxed in gray. The arrow indicates the conserved CDK phosphorylation site (12).

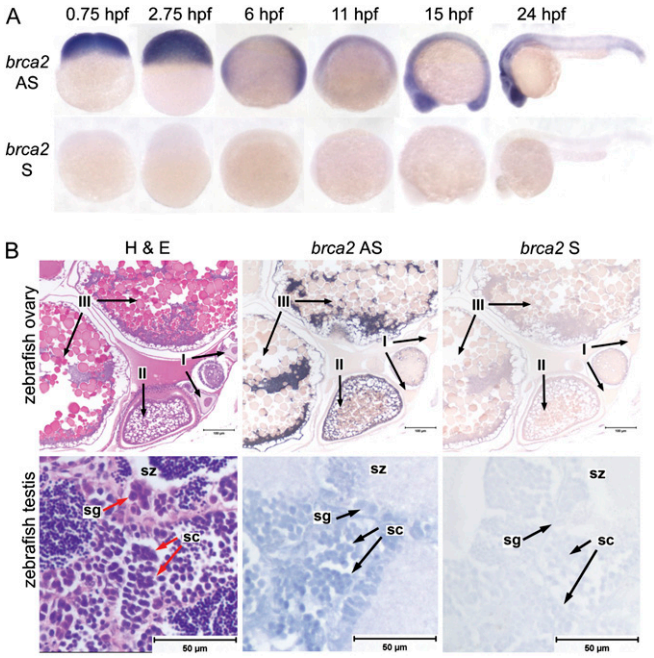

Fig. S2. *brca2* expression in WT embryonic and adult zebrafish. (*A*) WISH for *brca2* expression in zebrafish embryos with antisense (AS; *Upper*) and sense (S; *Lower*) probes at the indicated stages demonstrates expression of *brca2* throughout embryogenesis. (*B*) In situ hybridization for *brca2* expression in sections of adult zebrafish ovary and testis with AS (*Middle*) and S probes (*Right*) indicates that *brca2* is expressed in oocytes, spermatogonia, and spermatocytes (arrows). H&E-stained sections of ovary (*Left*, *Upper*) and testis (*Left*, *Lower*) are provided for anatomic reference. I, stage I oocyte; II, stage II oocyte; III, stage III oocyte; sg, spermatogonia; sc, spermatocytes; sz, spermatozoa. (Scale bars: 100 µm for ovary; 50 µm for testis.)

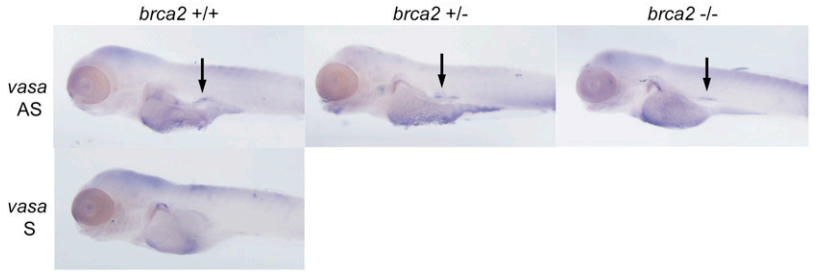

Fig. S3. Germ cell specification and localization at 4 dpf. WISH for the germ cell marker *vasa* indicates similar numbers and localization of PGCs at 4 dpf in zebrafish embryos of each *brca2* genotype. Arrows indicate *vasa*-expressing PGCs. AS, antisense RNA probe; S, sense RNA probe.

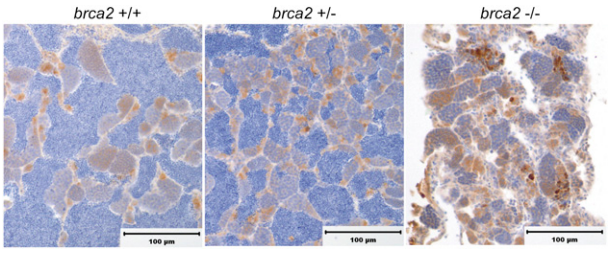

Fig. S4. Immunohistochemistry for cleaved caspase-3 in testes from WT, *brca2*^{Q658X} heterozygous, and *brca2*^{Q658X} homozygous zebrafish. Multiple clusters of apoptotic spermatocytes are present in testes from *brca2*^{Q658X} homozygotes, whereas few individual apoptotic cells are present in testes from WT and *brca2*^{Q658X} heterozygotes. (Scale bars: 100 µm.)

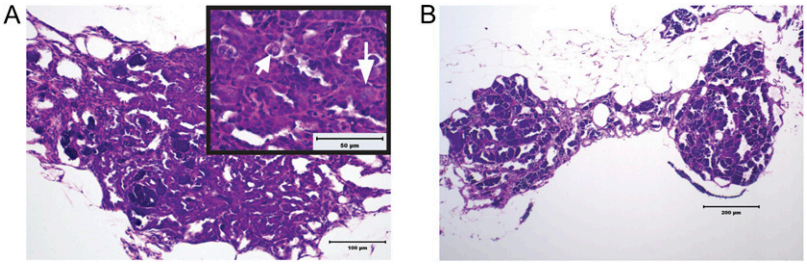

Fig. S5. Hyperplastic, dysplastic, and degenerative changes in H&E-stained sections of testes from adult *brca2*^{Q658X} homozygous zebrafish. (*A*) Testicular tubules are lined by numerous germ cells that form multicellular layers (*Inset*, long arrow). Multifocally, dysplastic germ cells with large nuclei, vacuolated chromatin, and prominent nucleoli are seen (*Inset*, short arrow). (*B*) Testes from *brca2*^{Q658X} homozygotes show segmental degeneration, with loss of spermatocytes in testicular tubules. (Scale bars: 100 μm in *A*; 200 μm in *B*; 50 μm in the *Inset* in *A*.)

Table S1. Genotypes of progeny from incrosses of *brca2*^{Q658X} heterozygotes conform to Mendelian ratios

	WT	*brca2*^{Q658X} heterozygotes	*brca2*^{Q658X} homozygotes
n	221	402	213
Actual	26.4%	48.1%	25.5%
Expected	25%	50%	25%

Zebrafish were genotyped as juveniles or adults, and data were collected on zebrafish derived from 12 different incrosses of *brca2*^{Q658X} heterozygous zebrafish. The percentages of actual genotypes were not statistically significantly different from expected genotypes (χ^2 = 1.378; *P* = 0.504).

Table S2. Quantitative analysis of meiotic spermatocysts in zebrafish testes

Brca2 genotype	Spermatocysts per 50 tubules	Meiotic spermatocysts per 50 tubules	% of meiotic spermatocysts
WT zebrafish	338	15	4%
Brca2^{Q658X} heterozygous zebrafish	364	14	4%
Brca2^{Q658X} homozygous zebrafish	351	38	11%
Comparisons	*P* value	*P* value	
WT and *brca2*^{Q658X} heterozygous zebrafish	0.2867	0.8422	
WT and *brca2*^{Q658X} homozygous zebrafish	0.5074	0.0026	
Brca2^{Q658X} heterozygous and *brca2*^{Q658X}homozygous zebrafish	0.6423	0.0009	

The numbers of meiotic spermatocysts were quantitated as the percentage of the total number of spermatocysts in 50 tubules from 10 zebrafish of each *brca2* genotype. The numbers of spermatocysts per 50 tubules were compared between *brca2* genotypes by the unpaired *t* test (GraphPad Software, www.graphpad.com/quickcalcs/ttest1.cfm). The numbers of meiotic spermatocysts were compared between *brca2* genotypes using the unpaired *t* test with Welch's correction (GraphPad Prism version 5.0).

Table S3. Analysis of age at tumor onset in *brca2*^{Q658X} homozygous;*tp53*^{M214K} homozygous zebrafish, *brca2*^{Q658X} heterozygous;*tp53*^{M214K} homozygous zebrafish, and the parent line of *tp53*^{M214K} homozygous zebrafish

	brca2$^{Q658X-/-}$;*tp53*$^{M214K-/-}$	*brca2*$^{Q658X+/-}$;*tp53*$^{M214K-/-}$	*tp53*$^{M214K-/-}$
Age at tumor onset, mo	7.0	6.5	7.0
	7.0	8.0	10.0
	8.0	8.0	11.0
	7.0	8.5	11.5
	9.0	8.5	11.5
	9.5	10.0	12.0
	11.0	11.0	12.0
	11.0	11.0	12.0
		11.0	12.5
			12.5
			13.0
			13.0
			14.0
			14.0
			14.5
			14.5
			15.0
			15.0
			15.0
			15.0
			15.5
			15.5
			16.0
			16.0
			16.5
			17.0
			17.0
			17.0
			17.0
			17.0
			18.5
			18.5
Total	8	9	32
Mean age, mo	8.7	9.2	14.3

	brca2$^{Q658X-/-}$;*tp53*$^{M214K-/-}$	*brca2*$^{Q658X+/-}$;*tp53*$^{M214K-/-}$
tp53 $^{M214K-/-}$	$P < 0.0001$	$P < 0.0001$
brca2$^{Q658X+/-}$;*tp53*$^{M214K-/-}$	$P = 0.5643$	

Data sets were compared using the unpaired *t* test (GraphPad Prism version 5.0).

Table S4. Analysis of tumors in zebrafish from an incross of *brca2*^{Q658X} heterozygous;*tp53*^{M214K} heterozygous zebrafish and in a subset of zebrafish from the parent line of *tp53*^{M214K} homozygous zebrafish

Specimen	Age, mo	Sex	Diagnosis	Primary site(s)
brca2$^{Q658X-/-}$;*tp53*$^{M214K-/-}$				
1	7.0	M	MPNST	Coelom
			MPNST	Eye
2	7.0	F	MPNST	Ovary
3	7.0	M	MPNST	Coelom
			MPNST	Eye
4*	8.0	ND	Eye mass with proptosis	Eye
5	9.0	M	MPNST	Coelom
6	9.5	ND	MPNST	Coelom
			MPNST	Subpharyngeal
			Cutaneous hemangiosarcoma	Tail
7	11.0	M	Seminoma	Testis
8	11.0	F	Rhabdomyosarcoma	Head
brca2$^{Q658X+/-}$;*tp53*$^{M214K-/-}$				
9	6.5	F	MPNST	Coelom
10	8.0	F	MPNST	Ovary
11	8.0	F	MPNST	Ovary
12	8.5	F	MPNST	Coelom
			MPNST	Eye
13	8.5	M	Sarcoma	Coelom
14	10.0	F	Sarcoma	Ovary
15	11.0	M	MPNST	Coelom
			MPNST	Eye
16	11.0	F	MPNST	Coelom
17	11.0	F	Intestinal adenocarcinoma	Intestine
			Cutaneous hemangioma	Body wall
brca2$^{Q658X+/+}$;*tp53*$^{M214K-/-}$				
18	10.0	F	Primitive neuroectodermal tumor	Coelom
19	11.0	F	MPNST	Body wall
tp53$^{M214K-/-}$ parent line				
20	7.0	F	MPNST	Liver
21	10.0	F	MPNST	Caudal coelom/ovary
22	11.0	F	MPNST	Caudal coelom/ovary
23	11.5	M	Rhabdomyosarcoma	Tail
24	11.5	F	MPNST	Coelom
25	12.0	M	MPNST	Eye
			Rhabdomyosarcoma	Tail

MPNST, malignant peripheral nerve sheath tumor; ND, not determined.
*Specimen 4 was not available for histological analysis.

Bibliography

1. Edwards BK *et al.* (2010) Annual report to the nation on the status of cancer, 1975-2006, featuring colorectal cancer trends and impact of interventions (risk factors, screening, and treatment) to reduce future rates. *Cancer* 116(3):544-573.
2. Altekruse SF KC, Krapcho M, Neyman N, Aminou R, Waldron W, Ruhl J, Howlader N, Tatalovich Z, Cho H, Mariotto A, Eisner MP, Lewis DR, Cronin K, Chen HS, Feuer EJ, Stinchcomb DG, Edwards BK (eds) (2010) SEER Cancer Statistics Review, 1975-2007. (National Cancer Institute, Bethesda).
3. Jacobs IJ *et al.* eds (2002) *Ovarian cancer* (Oxford University Press, New York).
4. Leung PCK & E.Y. A eds (2004) *The ovary* (Elsevier Academic Press, San Diego), 2nd edition Ed.
5. Edson MA, Nagaraja AK, & Matzuk MM (2009) The mammalian ovary from genesis to revelation. *Endocr Rev* 30(6):624-712.
6. Ries LAG *et al.* (2008) SEER Cancer Statistics Review, 1975-2005. (National Cancer Institute, Bethesda).
7. Cho KR & Shih Ie M (2009) Ovarian cancer. *Annu Rev Pathol* 4:287-313.
8. Auersperg N *et al.* (2001) Ovarian surface epithelium: Biology, endocrinology, and pathology. *Endocrine Reviews* 22(2):255-288.
9. Bell DA (2005) Origins and molecular pathology of ovarian cancer. *Mod Pathol* 18 Suppl 2:S19-32.
10. Crum CP (2009) Intercepting pelvic cancer in the distal fallopian tube: theories and realities. *Mol Oncol* 3(2):165-170.
11. Piek JM *et al.* (2001) Dysplastic changes in prophylactically removed Fallopian tubes of women predisposed to developing ovarian cancer. *J Pathol* 195(4):451-456.
12. Landen CN, Jr., Birrer MJ, & Sood AK (2008) Early events in the pathogenesis of epithelial ovarian cancer. *J Clin Oncol* 26(6):995-1005.
13. Shih Ie M & Kurman RJ (2004) Ovarian tumorigenesis: a proposed model based on morphological and molecular genetic analysis. *Am J Pathol* 164(5):1511-1518.
14. Willner J *et al.* (2007) Alternate molecular genetic pathways in ovarian carcinomas of common histological types. *Hum Pathol* 38(4):607-613.
15. Prat J, Ribe A, & Gallardo A (2005) Hereditary ovarian cancer. *Hum Pathol* 36(8):861-870.
16. Gayther SA *et al.* (1997) Variation of risks of breast and ovarian cancer associated with different germline mutations of the BRCA2 gene. *Nat Genet* 15(1):103-105.
17. Ramus SJ *et al.* (2007) Contribution of BRCA1 and BRCA2 mutations to inherited ovarian cancer. *Hum Mutat* 28(12):1207-1215.
18. Morrison PJ, Hodgson SV, & Haites NE eds (2002) *Familial breast and ovarian cancer: genetics, screening, and management* (Cambridge University Press, Cambridge).

19. Lakhani SR *et al.* (2004) Pathology of ovarian cancers in BRCA1 and BRCA2 carriers. *Clin Cancer Res* 10(7):2473-2481.
20. Norquist BM *et al.* (2010) The molecular pathogenesis of hereditary ovarian carcinoma: alterations in the tubal epithelium of women with BRCA1 and BRCA2 mutations. *Cancer*.
21. Gudmundsson J *et al.* (1995) Different tumor types from BRCA2 carriers show wild-type chromosome deletions on 13q12-q13. *Cancer Res* 55(21):4830-4832.
22. King MC, Marks JH, & Mandell JB (2003) Breast and ovarian cancer risks due to inherited mutations in BRCA1 and BRCA2. *Science* 302(5645):643-646.
23. Antoniou A *et al.* (2003) Average risks of breast and ovarian cancer associated with BRCA1 or BRCA2 mutations detected in case Series unselected for family history: a combined analysis of 22 studies. *Am J Hum Genet* 72(5):1117-1130.
24. Mohamad HB & Apffelstaedt JP (2008) Counseling for male BRCA mutation carriers: a review. *Breast* 17(5):441-450.
25. Levy-Lahad E & Friedman E (2007) Cancer risks among BRCA1 and BRCA2 mutation carriers. *Br J Cancer* 96(1):11-15.
26. Lubinski J *et al.* (2004) Cancer variation associated with the position of the mutation in the BRCA2 gene. *Fam Cancer* 3(1):1-10.
27. Ramus SJ & Gayther SA (2009) The contribution of BRCA1 and BRCA2 to ovarian cancer. *Mol Oncol* 3(2):138-150.
28. Wooster R *et al.* (1994) Localization of a breast cancer susceptibility gene, BRCA2, to chromosome 13q12-13. *Science* 265(5181):2088-2090.
29. Thompson D & Easton D (2001) Variation in cancer risks, by mutation position, in BRCA2 mutation carriers. *Am J Hum Genet* 68(2):410-419.
30. Venkitaraman AR (2001) Functions of BRCA1 and BRCA2 in the biological response to DNA damage. *Journal of Cell Science* 114(20):3591-3598.
31. Yu VP *et al.* (2000) Gross chromosomal rearrangements and genetic exchange between nonhomologous chromosomes following BRCA2 inactivation. *Genes Dev* 14(11):1400-1406.
32. Moynahan ME, Pierce AJ, & Jasin M (2001) BRCA2 is required for homology-directed repair of chromosomal breaks. *Mol Cell* 7(2):263-272.
33. Shivji MK & Venkitaraman AR (2004) DNA recombination, chromosomal stability and carcinogenesis: insights into the role of BRCA2. *DNA Repair (Amst)* 3(8-9):835-843.
34. Thorslund T & West SC (2007) BRCA2: a universal recombinase regulator. *Oncogene* 26(56):7720-7730.
35. Gudmundsdottir K & Ashworth A (2006) The roles of BRCA1 and BRCA2 and associated proteins in the maintenance of genomic stability. *Oncogene* 25(43):5864-5874.
36. Chen J *et al.* (1998) Stable interaction between the products of the BRCA1 and BRCA2 tumor suppressor genes in mitotic and meiotic cells. *Mol Cell* 2(3):317-328.

37. Abaji C, Cousineau I, & Belmaaza A (2005) BRCA2 regulates homologous recombination in response to DNA damage: implications for genome stability and carcinogenesis. *Cancer Res* 65(10):4117-4125.
38. Sakai W *et al.* (2008) Secondary mutations as a mechanism of cisplatin resistance in BRCA2-mutated cancers. *Nature* 451(7182):1116-1120.
39. Ashworth A (2008) A synthetic lethal therapeutic approach: poly(ADP) ribose polymerase inhibitors for the treatment of cancers deficient in DNA double-strand break repair. *J Clin Oncol* 26(22):3785-3790.
40. Edwards SL *et al.* (2008) Resistance to therapy caused by intragenic deletion in BRCA2. *Nature* 451(7182):1111-1115.
41. D'Andrea AD & Grompe M (2003) The Fanconi anaemia/BRCA pathway. *Nat Rev Cancer* 3(1):23-34.
42. Kennedy RD & D'Andrea AD (2005) The Fanconi Anemia/BRCA pathway: new faces in the crowd. *Genes Dev* 19(24):2925-2940.
43. Howlett NG *et al.* (2002) Biallelic inactivation of BRCA2 in Fanconi anemia. *Science* 297(5581):606-609.
44. Alter BP, Rosenberg PS, & Brody LC (2007) Clinical and molecular features associated with biallelic mutations in FANCD1/BRCA2. *J Med Genet* 44(1):1-9.
45. Vanderhyden BC, Shaw TJ, & Ethier JF (2003) Animal models of ovarian cancer. *Reproductive Biology and Endocrinology* 1.
46. Garson K *et al.* (2005) Models of ovarian cancer--are we there yet? *Mol Cell Endocrinol* 239(1-2):15-26.
47. Stakleff KD & Von Gruenigen VE (2003) Rodent models for ovarian cancer research. *Int J Gynecol Cancer* 13(4):405-412.
48. Connolly DC *et al.* (2003) Female mice chimeric for expression of the simian virus 40 TAg under control of the MISIIR promoter develop epithelial ovarian cancer. *Cancer Res* 63(6):1389-1397.
49. Suzuki A *et al.* (1997) Brca2 is required for embryonic cellular proliferation in the mouse. *Genes Dev* 11(10):1242-1252.
50. Sharan SK *et al.* (1997) Embryonic lethality and radiation hypersensitivity mediated by Rad51 in mice lacking Brca2. *Nature* 386(6627):804-810.
51. Ludwig T, Chapman DL, Papaioannou VE, & Efstratiadis A (1997) Targeted mutations of breast cancer susceptibility gene homologs in mice: lethal phenotypes of Brca1, Brca2, Brca1/Brca2, Brca1/p53, and Brca2/p53 nullizygous embryos. *Genes Dev* 11(10):1226-1241.
52. Donoho G *et al.* (2003) Deletion of Brca2 exon 27 causes hypersensitivity to DNA crosslinks, chromosomal instability, and reduced life span in mice. *Genes Chromosomes Cancer* 36(4):317-331.
53. Jonkers J *et al.* (2001) Synergistic tumor suppressor activity of BRCA2 and p53 in a conditional mouse model for breast cancer. *Nat Genet* 29(4):418-425.
54. Connor F *et al.* (1997) Tumorigenesis and a DNA repair defect in mice with a truncating Brca2 mutation. *Nat Genet* 17(4):423-430.
55. Friedman LS *et al.* (1998) Thymic lymphomas in mice with a truncating mutation in Brca2. *Cancer Res* 58(7):1338-1343.

56. McAllister KA *et al.* (2002) Cancer susceptibility of mice with a homozygous deletion in the COOH-terminal domain of the Brca2 gene. *Cancer Res* 62(4):990-994.
57. McAllister KA *et al.* (2006) Spontaneous and irradiation-induced tumor susceptibility in BRCA2 germline mutant mice and cooperative effects with a p53 germline mutation. *Toxicol Pathol* 34(2):187-198.
58. Sharan SK *et al.* (2004) BRCA2 deficiency in mice leads to meiotic impairment and infertility. *Development* 131(1):131-142.
59. Cotroneo MS *et al.* (2007) Characterizing a rat Brca2 knockout model. *Oncogene* 26(11):1626-1635.
60. Park PG & Lee H (2008) Development of thymic lymphomas in mice disrupted of Brca2 allele in the thymus. *Exp Mol Med* 40(3):339-344.
61. Moynahan ME (2002) The cancer connection: BRCA1 and BRCA2 tumor suppression in mice and humans. *Oncogene* 21(58):8994-9007.
62. Evers B & Jonkers J (2006) Mouse models of BRCA1 and BRCA2 deficiency: past lessons, current understanding and future prospects. *Oncogene* 25(43):5885-5897.
63. Lieschke GJ & Currie PD (2007) Animal models of human disease: Zebrafish swim into view. *Nature Reviews Genetics* 8(5):353-367.
64. Stern HM & Zon LI (2003) Cancer genetics and drug discovery in the zebrafish. *Nature Reviews Cancer* 3(7):533-539.
65. Knapik EW (2000) ENU mutagenesis in zebrafish - From genes to complex diseases. *Mammalian Genome* 11(7):511-519.
66. Amsterdam A & Hopkins N (2006) Mutagenesis strategies in zebrafish for identifying genes involved in development and disease. *Trends Genet* 22(9):473-478.
67. Detrich HW, Westerfield M, & Zon LI eds (2004) *The Zebrafish: genetics, genomics, and informatics* (Elsevier Academic Press, San Diego), Vol 77.
68. Sood R *et al.* (2006) Methods for reverse genetic screening in zebrafish by resequencing and TILLING. *Methods* 39(3):220-227.
69. Wienholds E, Schulte-Merker S, Walderich B, & Plasterk RH (2002) Target-selected inactivation of the zebrafish rag1 gene. *Science* 297(5578):99-102.
70. Berghmans S *et al.* (2005) tp53 mutant zebrafish develop malignant peripheral nerve sheath tumors. *Proc Natl Acad Sci U S A* 102(2):407-412.
71. Haramis AP *et al.* (2006) Adenomatous polyposis coli-deficient zebrafish are susceptible to digestive tract neoplasia. *EMBO Rep* 7(4):444-449.
72. Titus TA *et al.* (2006) The Fanconi anemia gene network is conserved from zebrafish to human. *Gene* 371(2):211-223.
73. Selman K, Wallace, R.A., Sarka, A., Qi, X. (1993) Stages of oocyte development in the zebrafish, Brachydanio rerio. *Journal of Morphology* 218:203-224.
74. Ge W (2005) Intrafollicular paracrine communication in the zebrafish ovary: the state of the art of an emerging model for the study of vertebrate folliculogenesis. *Mol Cell Endocrinol* 237(1-2):1-10.
75. Schulz RW *et al.* (2009) Spermatogenesis in fish. *Gen Comp Endocrinol* 165(3):390-411.

76. Leal MC *et al.* (2009) Histological and stereological evaluation of zebrafish (Danio rerio) spermatogenesis with an emphasis on spermatogonial generations. *Biol Reprod* 81(1):177-187.
77. Takahashi H (1977) Juvenile Hermaphroditism in the Zebrafish, Brachydanio rerio. *Bulletin of the Faculty of Fisheries Hokkaido University* 28(2):57-65.
78. Maack G, Segner, H. (2003) Morphological development of the gonads in zebrafish. *Journal of Fish Biology* 62:895-906.
79. Wang XG, Bartfai, R., Sleptsova-Friedrich, I., Orban, L. (2007) The timing and extent of 'juvenile ovary' phase are highly variable during zebrafish testis differentiation. *Journal of Fish Biology* 70:33-44.
80. Uchida D, Yamashita M, Kitano T, & Iguchi T (2002) Oocyte apoptosis during the transition from ovary-like tissue to testes during sex differentiation of juvenile zebrafish. *J Exp Biol* 205(Pt 6):711-718.
81. Driever W, Stemple D, Schier A, & Solnica-Krezel L (1994) Zebrafish: genetic tools for studying vertebrate development. *Trends Genet* 10(5):152-159.
82. Knaut H, Werz C, Geisler R, & Nusslein-Volhard C (2003) A zebrafish homologue of the chemokine receptor Cxcr4 is a germ-cell guidance receptor. *Nature* 421(6920):279-282.
83. Slanchev K, Stebler J, de la Cueva-Mendez G, & Raz E (2005) Development without germ cells: the role of the germ line in zebrafish sex differentiation. *Proc Natl Acad Sci U S A* 102(11):4074-4079.
84. Weidinger G *et al.* (2003) dead end, a novel vertebrate germ plasm component, is required for zebrafish primordial germ cell migration and survival. *Curr Biol* 13(16):1429-1434.
85. Siegfried KR & Nusslein-Volhard C (2008) Germ line control of female sex determination in zebrafish. *Dev Biol* 324(2):277-287.
86. Draper BW, McCallum CM, & Moens CB (2007) nanos1 is required to maintain oocyte production in adult zebrafish. *Dev Biol* 305(2):589-598.
87. Houwing S, Berezikov E, & Ketting RF (2008) Zili is required for germ cell differentiation and meiosis in zebrafish. *EMBO J* 27(20):2702-2711.
88. Houwing S *et al.* (2007) A role for Piwi and piRNAs in germ cell maintenance and transposon silencing in Zebrafish. *Cell* 129(1):69-82.
89. Devlin R.H. N, Y. (2002) Sex determination and sex differentiation in fish: an overview of genetic, physiological, and environmental influences. *Aquaculture* 208:191-364.
90. Siegfried KR (2010) In search of determinants: gene expression during gonadal sex differentiation. *J Fish Biol* 76(8):1879-1902.
91. Orban L, Sreenivasan R, & Olsson PE (2009) Long and winding roads: testis differentiation in zebrafish. *Mol Cell Endocrinol* 312(1-2):35-41.
92. Schreeb KH, Groth G, Sachsse W, & Freundt KJ (1993) The karyotype of the zebrafish (Brachydanio rerio). *J Exp Anim Sci* 36(1):27-31.
93. Pijnacker LP & Ferwerda MA (1995) Zebrafish chromosome banding. *Genome* 38(5):1052-1055.
94. McLaren A *et al.* (1984) Male sexual differentiation in mice lacking H-Y antigen. *Nature* 312(5994):552-555.

95. Sreenivasan R *et al.* (2008) Transcriptomic analyses reveal novel genes with sexually dimorphic expression in the zebrafish gonad and brain. *PLoS One* 3(3):e1791.
96. Santos EM *et al.* (2007) Molecular basis of sex and reproductive status in breeding zebrafish. *Physiol Genomics* 30(2):111-122.
97. von Hofsten J & Olsson PE (2005) Zebrafish sex determination and differentiation: involvement of FTZ-F1 genes. *Reprod Biol Endocrinol* 3:63.
98. Shang EH, Yu RM, & Wu RS (2006) Hypoxia affects sex differentiation and development, leading to a male-dominated population in zebrafish (Danio rerio). *Environ Sci Technol* 40(9):3118-3122.
99. Volff JN & Schartl M (2002) Sex determination and sex chromosome evolution in the medaka, Oryzias latipes, and the platyfish, Xiphophorus maculatus. *Cytogenet Genome Res* 99(1-4):170-177.
100. Sekido R *et al.* (2004) SOX9 is up-regulated by the transient expression of SRY specifically in Sertoli cell precursors. *Dev Biol* 274(2):271-279.
101. Swain A & Lovell-Badge R (1997) A molecular approach to sex determination in mammals. *Acta Paediatr Suppl* 423:46-49.
102. De Santa Barbara P *et al.* (1998) Direct interaction of SRY-related protein SOX9 and steroidogenic factor 1 regulates transcription of the human anti-Mullerian hormone gene. *Mol Cell Biol* 18(11):6653-6665.
103. Rouiller-Fabre V *et al.* (1998) Effect of anti-Mullerian hormone on Sertoli and Leydig cell functions in fetal and immature rats. *Endocrinology* 139(3):1213-1220.
104. Bezard J *et al.* (1987) Immunocytochemical study of anti-Mullerian hormone in sheep ovarian follicles during fetal and post-natal development. *J Reprod Fertil* 80(2):509-516.
105. Hillier SG, Zeleznik AJ, Knazek RA, & Ross GT (1980) Hormonal regulation of preovulatory follicle maturation in the rat. *J Reprod Fertil* 60(1):219-229.
106. Munsterberg A & Lovell-Badge R (1991) Expression of the mouse anti-mullerian hormone gene suggests a role in both male and female sexual differentiation. *Development* 113(2):613-624.
107. Chiang EF *et al.* (2001) Two sox9 genes on duplicated zebrafish chromosomes: expression of similar transcription activators in distinct sites. *Dev Biol* 231(1):149-163.
108. Postlethwait JH *et al.* (1998) Vertebrate genome evolution and the zebrafish gene map. *Nat Genet* 18(4):345-349.
109. Chiang EF *et al.* (2001) Two Cyp19 (P450 aromatase) genes on duplicated zebrafish chromosomes are expressed in ovary or brain. *Mol Biol Evol* 18(4):542-550.
110. Rodriguez-Mari A *et al.* (2005) Characterization and expression pattern of zebrafish Anti-Mullerian hormone (Amh) relative to sox9a, sox9b, and cyp19a1a, during gonad development. *Gene Expr Patterns* 5(5):655-667.
111. Josso N *et al.* (1998) The role of anti-Mullerian hormone in gonadal development. *Mol Cell Endocrinol* 145(1-2):3-7.
112. Jorgensen A *et al.* (2008) Expression profiles for six zebrafish genes during gonadal sex differentiation. *Reprod Biol Endocrinol* 6:25.

113. Kimmel CB *et al.* (1995) Stages of embryonic development of the zebrafish. *Dev Dyn* 203(3):253-310.
114. Pelegri F (2003) Maternal factors in zebrafish development. *Dev Dyn* 228(3):535-554.
115. Rajan JV, Marquis ST, Gardner HP, & Chodosh LA (1997) Developmental expression of Brca2 colocalizes with Brca1 and is associated with proliferation and differentiation in multiple tissues. *Dev Biol* 184(2):385-401.
116. Blackshear PE *et al.* (1998) Brca1 and Brca2 expression patterns in mitotic and meiotic cells of mice. *Oncogene* 16(1):61-68.
117. Chodosh LA (1998) Expression of BRCA1 and BRCA2 in normal and neoplastic cells. *J Mammary Gland Biol Neoplasia* 3(4):389-402.
118. Titus TA *et al.* (2009) The Fanconi anemia/BRCA gene network in zebrafish: embryonic expression and comparative genomics. *Mutat Res* 668(1-2):117-132.
119. Kane DA & Kimmel CB (1993) The zebrafish midblastula transition. *Development* 119(2):447-456.
120. Aoki F, Worrad DM, & Schultz RM (1997) Regulation of transcriptional activity during the first and second cell cycles in the preimplantation mouse embryo. *Dev Biol* 181(2):296-307.
121. Sun F *et al.* (2007) Nuclear reprogramming: the zygotic transcription program is established through an "erase-and-rebuild" strategy. *Cell Res* 17(2):117-134.
122. Kobayashi T & Nagahama Y (2009) Molecular aspects of gonadal differentiation in a teleost fish, the Nile tilapia. *Sex Dev* 3(2-3):108-117.
123. Chen PL *et al.* (1998) The BRC repeats in BRCA2 are critical for RAD51 binding and resistance to methyl methanesulfonate treatment. *Proceedings of the National Academy of Sciences of the United States of America* 95(9):5287-5292.
124. Rossteuscher S *et al.* (2008) Background pathology of the ovary in a laboratory population of zebrafish Danio rerio. *Dis Aquat Organ* 79(2):169-172.
125. Rawls JF *et al.* (2003) Coupled mutagenesis screens and genetic mapping in zebrafish. *Genetics* 163(3):997-1009.
126. Neff MM, Turk E, & Kalishman M (2002) Web-based primer design for single nucleotide polymorphism analysis. *Trends Genet* 18(12):613-615.
127. Hagmann M *et al.* (1998) Homologous recombination and DNA-end joining reactions in zygotes and early embryos of zebrafish (Danio rerio) and Drosophila melanogaster. *Biol Chem* 379(6):673-681.
128. Tutt A *et al.* (2001) Mutation in Brca2 stimulates error-prone homology-directed repair of DNA double-strand breaks occurring between repeated sequences. *EMBO J* 20(17):4704-4716.
129. Marcon E & Moens PB (2005) The evolution of meiosis: recruitment and modification of somatic DNA-repair proteins. *Bioessays* 27(8):795-808.
130. Giri N, Batista DL, Alter BP, & Stratakis CA (2007) Endocrine abnormalities in patients with Fanconi anemia. *J Clin Endocrinol Metab* 92(7):2624-2631.

131. Wong JC *et al.* (2003) Targeted disruption of exons 1 to 6 of the Fanconi Anemia group A gene leads to growth retardation, strain-specific microphthalmia, meiotic defects and primordial germ cell hypoplasia. *Hum Mol Genet* 12(16):2063-2076.
132. McLaren A & Southee D (1997) Entry of mouse embryonic germ cells into meiosis. *Dev Biol* 187(1):107-113.
133. Page AW & Orr-Weaver TL (1997) Stopping and starting the meiotic cell cycle. *Curr Opin Genet Dev* 7(1):23-31.
134. Baltus AE *et al.* (2006) In germ cells of mouse embryonic ovaries, the decision to enter meiosis precedes premeiotic DNA replication. *Nat Genet* 38(12):1430-1434.
135. Lin Y, Gill ME, Koubova J, & Page DC (2008) Germ cell-intrinsic and -extrinsic factors govern meiotic initiation in mouse embryos. *Science* 322(5908):1685-1687.
136. Pittman DL *et al.* (1998) Meiotic prophase arrest with failure of chromosome synapsis in mice deficient for Dmc1, a germline-specific RecA homolog. *Mol Cell* 1(5):697-705.
137. Di Giacomo M *et al.* (2005) Distinct DNA-damage-dependent and -independent responses drive the loss of oocytes in recombination-defective mouse mutants. *Proc Natl Acad Sci U S A* 102(3):737-742.
138. Morelli MA & Cohen PE (2005) Not all germ cells are created equal: aspects of sexual dimorphism in mammalian meiosis. *Reproduction* 130(6):761-781.
139. Baker SM *et al.* (1996) Involvement of mouse Mlh1 in DNA mismatch repair and meiotic crossing over. *Nat Genet* 13(3):336-342.
140. Feitsma H, Leal., M.C., Moens, P.B., Cuppen, E., Schulz, R.W. (2007) Mlh1 deficiency in zebrafish results in male sterility and aneuploid as well as triploid progeny in females. *Genetics* 175(4):1561-1569.
141. Leal MC *et al.* (2008) Completion of meiosis in male zebrafish (Danio rerio) despite lack of DNA mismatch repair gene mlh1. *Cell Tissue Res* 332(1):133-139.
142. Rodriguez-Mari A *et al.* (2010) Sex reversal in zebrafish fancl mutants is caused by Tp53-mediated germ cell apoptosis. *PLoS Genet* 6(7):e1001034.
143. Bakker ST *et al.* (2009) Fancm-deficient mice reveal unique features of Fanconi anemia complementation group M. *Hum Mol Genet* 18(18):3484-3495.
144. Thisse C & Thisse B (2008) High-resolution in situ hybridization to whole-mount zebrafish embryos. *Nat Protoc* 3(1):59-69.
145. Koprunner M, Thisse C, Thisse B, & Raz E (2001) A zebrafish nanos-related gene is essential for the development of primordial germ cells. *Genes Dev* 15(21):2877-2885.
146. Gillette-Ferguson I, Ferguson DG, Poss KD, & Moorman SJ (2003) Changes in gravitational force induce alterations in gene expression that can be monitored in the live, developing zebrafish heart. *Adv Space Res* 32(8):1641-1646.

147. Guigon CJ & Magre S (2006) Contribution of germ cells to the differentiation and maturation of the ovary: insights from models of germ cell depletion. *Biol Reprod* 74(3):450-458.
148. Saito T, Goto-Kazeto R, Arai K, & Yamaha E (2008) Xenogenesis in teleost fish through generation of germ-line chimeras by single primordial germ cell transplantation. *Biol Reprod* 78(1):159-166.
149. Daniels MJ, Wang Y, Lee M, & Venkitaraman AR (2004) Abnormal cytokinesis in cells deficient in the breast cancer susceptibility protein BRCA2. *Science* 306(5697):876-879.
150. Jonsdottir AB *et al.* (2009) BRCA2 heterozygosity delays cytokinesis in primary human fibroblasts. *Cell Oncol* 31(3):191-201.
151. Lekomtsev S *et al.* (2010) Evidence that the tumor-suppressor protein BRCA2 does not regulate cytokinesis in human cells. *J Cell Sci* 123(Pt 9):1395-1400.
152. Moore JL *et al.* (2006) Zebrafish genomic instability mutants and cancer susceptibility. *Genetics* 174(2):585-600.
153. Amsterdam A *et al.* (2009) Zebrafish Hagoromo mutants up-regulate fgf8 postembryonically and develop neuroblastoma. *Mol Cancer Res* 7(6):841-850.
154. Neumann JC *et al.* (2009) Identification of a heritable model of testicular germ cell tumor in the zebrafish. *Zebrafish* 6(4):319-327.
155. Saleemuddin A *et al.* (2008) Risk factors for a serous cancer precursor ("p53 signature") in women with inherited BRCA mutations. *Gynecol Oncol* 111(2):226-232.
156. Zweemer RP *et al.* (1999) Accumulation of p53 protein is frequent in ovarian cancers associated with BRCA1 and BRCA2 germline mutations. *J Clin Pathol* 52(5):372-375.
157. Ramus SJ *et al.* (1999) Increased frequency of TP53 mutations in BRCA1 and BRCA2 ovarian tumours. *Genes Chromosomes Cancer* 25(2):91-96.
158. Habu T *et al.* (2004) p53 Protein interacts specifically with the meiosis-specific mammalian RecA-like protein DMC1 in meiosis. *Carcinogenesis* 25(6):889-893.
159. Rajagopalan S, Andreeva A, Rutherford TJ, & Fersht AR (2010) Mapping the physical and functional interactions between the tumor suppressors p53 and BRCA2. *Proc Natl Acad Sci U S A* 107(19):8587-8592.
160. Sussman R (2007) DNA repair capacity of zebrafish. *Proceedings of the National Academy of Sciences of the United States of America* 104(33):13379-13383.
161. Bowles J *et al.* (2006) Retinoid signaling determines germ cell fate in mice. *Science* 312(5773):596-600.
162. Koubova J *et al.* (2006) Retinoic acid regulates sex-specific timing of meiotic initiation in mice. *Proc Natl Acad Sci U S A* 103(8):2474-2479.
163. Zdobnov EM & Apweiler R (2001) InterProScan--an integration platform for the signature-recognition methods in InterPro. *Bioinformatics* 17(9):847-848.
164. Oliver AW *et al.* (2009) Structural basis for recruitment of BRCA2 by PALB2. *EMBO Rep* 10(9):990-996.
165. Bork P, Blomberg N, & Nilges M (1996) Internal repeats in the BRCA2 protein sequence. *Nat Genet* 13(1):22-23.

166. Davies OR & Pellegrini L (2007) Interaction with the BRCA2 C terminus protects RAD51-DNA filaments from disassembly by BRC repeats. *Nat Struct Mol Biol* 14(6):475-483.
167. Esashi F *et al.* (2005) CDK-dependent phosphorylation of BRCA2 as a regulatory mechanism for recombinational repair. *Nature* 434(7033):598-604.